PHOTOPHYSICS OF THE SHORT CHAIN DYAD

A thesis submitted towards partial fulfilment of the requirements for the degree of

Master of Technology in Laser Technology

Course affiliated to Faculty of Engineering and Technology and offered by Faculty Council of Interdisciplinary Studies, Law and Management, Jadavpur University

submitted by

DEBARUN BANERJEE

Examination Roll No. M4LST23009

Registration No. 160426 of 2021-22

Under the guidance of

Prof. Dr. Tapan Ganguly

(THESIS SUPERVISOR)

School of Laser Science and Engineering

Jadavpur University, Kolkata - 700032

School of Laser Science and Engineering

Faculty of Interdisciplinary Studies, Law and Management

Jadavpur University

Kolkata -700032

India

2023

M. Tech in Laser Science & Technology
Course affiliated to
Faculty of Engineering and Technology
and offered by
Faculty Council of Interdisciplinary Studies, Law and Management
Jadavpur University
Kolkata, India- 700032

CERTIFICATE OF RECOMMENDATION

I HEREBY RECOMMEND THAT THE THESIS PREPARED BY **DEBARUN BANERJEE** UNDER MY SUPERVISION ENTITLED **PHOTOPHYSICS OF THE SHORT CHAIN DYAD** BE ACCEPTED IN THE PARTIAL FULFILLMENT OF THE REQUIREMENTS FOR THE DEGREE OF MASTER OF TECHNOLOGY IN LASER TECHNOLOGY DURING THE ACADEMIC SESSION 2022- 2023.

THESIS SUPERVISOR
Prof. Dr. Tapan Ganguly
School of Laser Science and Engineering
Jadavpur University, Kolkata-7000032

Countersigned

Dr. DIPTEN MISRA
Director
School of Laser Science and Engineering
Jadavpur University, Kolkata-700 032

DEAN
Faculty Council of Interdisciplinary Studies, Law and Management
Jadavpur University, Kolkata-700 032

M. Tech in Laser Science & Technology
Course affiliated to
Faculty of Engineering and Technology
and offered by
Faculty Council of Interdisciplinary Studies, Law and Management
Jadavpur University
Kolkata, India-700032

CERTIFICATE OF APPROVAL **

This foregoing thesis is hereby approved as a creditable study of an engineering subject carried out and presented in a manner satisfactory to warrant its acceptance as a prerequisite to the degree for which it has been submitted. It is understood that by this approval the undersigned do not necessarily endorse or approve any statement made, opinion expressed, or conclusion drawn therein but approve the thesis only for the purpose for which it has been submitted.

COMMITTEE OF FINAL EXAMINATION FOR EVALUATION OF THESIS

** Only in case the recommendation is concurred

DECLARATION OF ORIGINALITY AND COMPLIANCE OF ACADEMIC ETHICS

The author hereby declares that this thesis contains original research work by the undersigned candidate, as part of his Master of Technology in Laser Technology studies during academic session 2022-2023.

All information in this document has been obtained and presented in accordance with academic rules and ethical conduct.

The author also declares that as required by these rules and conduct, the author has fully cited and referred all material and results that are not original to this work.

NAME: DEBARUN BANERJEE

EXAMINATION ROLL NUMBER: M4LST23009

THESIS TITLE: PHOTOPHYSICS OF THE SHORT CHAIN DYAD.

SIGNATURE: DATE:

ACKNOWLEDGEMENT

First and foremost, I would like to express my sincere gratitude to my supervisor ***Prof. Dr. Tapan Ganguly***, Emeritus Professor, School of Laser Science and Engineering, Jadavpur University, for his invaluable guidance, whole-hearted support and encouragement for accomplishing the present investigation. His dynamism, fantastic stamina and day-to-day monitoring of every minute detail were a constant source of inspiration to me.

I would also like to express my deep sense of thankfulness to ***Dr. Dipten Misra*** for providing me necessary atmosphere to work on.

I am extremely thankful to my seniors of School of Laser Science and Technology, especially **Dr. Somnath Paul** and **Ms. Ishani Mitra** for their inspiration and encouragement and helping me through the research work.

I record my acknowledgement to ***School of Laser Science and Engineering*** for giving me the opportunity to pursue my research work.

My sincere thanks to Honorable Vice-Chancellor **Dr. Suranjan Das**, Jadavpur University, for the opportunity provided to complete my research work.

Immemorial friendly behavior and constant support of all my friends, seniors and juniors of School of Laser Science and Engineering are highly acknowledged.

All staff members of the School of Laser Science and Technology deserve special thanks for their help in diverse ways during the days of my stay in the department.

No words can convey my sense of gratitude for my family.

Lastly, I will remain grateful to all of them who supported me in any way during my entire time span in research activity.

DEBARUN BANERJEE

Examination Roll No. M4LST23009

Registration No. 160426 of 2021-2022

THIS THESIS WORK IS DEDICATED TO:

MY BELOVED MOTHER **CHANDANA BANERJEE**, FATHER **BARUN KUMAR BANERJEE**

MY SUPERVISOR, FRIENDS, SENIORS

ALMIGHTY

AND

SCIENCE & TECHNOLOGY

Content

Chapter :1

Introduction

- ✓ **Energy**
- ✓ **Photophysical and Photochemical Studies and Processes**
- ✓ **Light Energy Conversion Process by Dyads**
- ✓ **Graphene and Its Derivatives**
  - ❖ **Graphene Quantum Dots**
  - ❖ **Graphene Oxide**
  - ❖ **Reduced Graphene Oxide**
- ✓ **Aim of Thesis**
- ✓ **Literature Review**
- ✓ **References**

1. Energy

Energy is the quantitative property that is transferred to a body or to a physical system, recognizable in the performance of work and in the form of heat and light[1]. If we live better than our primitive ancestors, it is because we use more energy to do work. Energy can exist in various forms. All the energy sources that we use, except geothermal and nuclear energies, are derived initially from solar energy[2]. It is little different because it can be harnessed by using the atomic properties of atoms or molecules. Geothermal energy is different also. Fossil fuel like coal, petroleum, natural gas that we exploit hugely nowadays are derived from several types of organisms which grew over hundreds to millions of years and stored solar energy on planet earth's surface in layers[3]. Renewable energies like biomass, hydro, river water, wind is never ending and are very much needed in today’s world more and more.

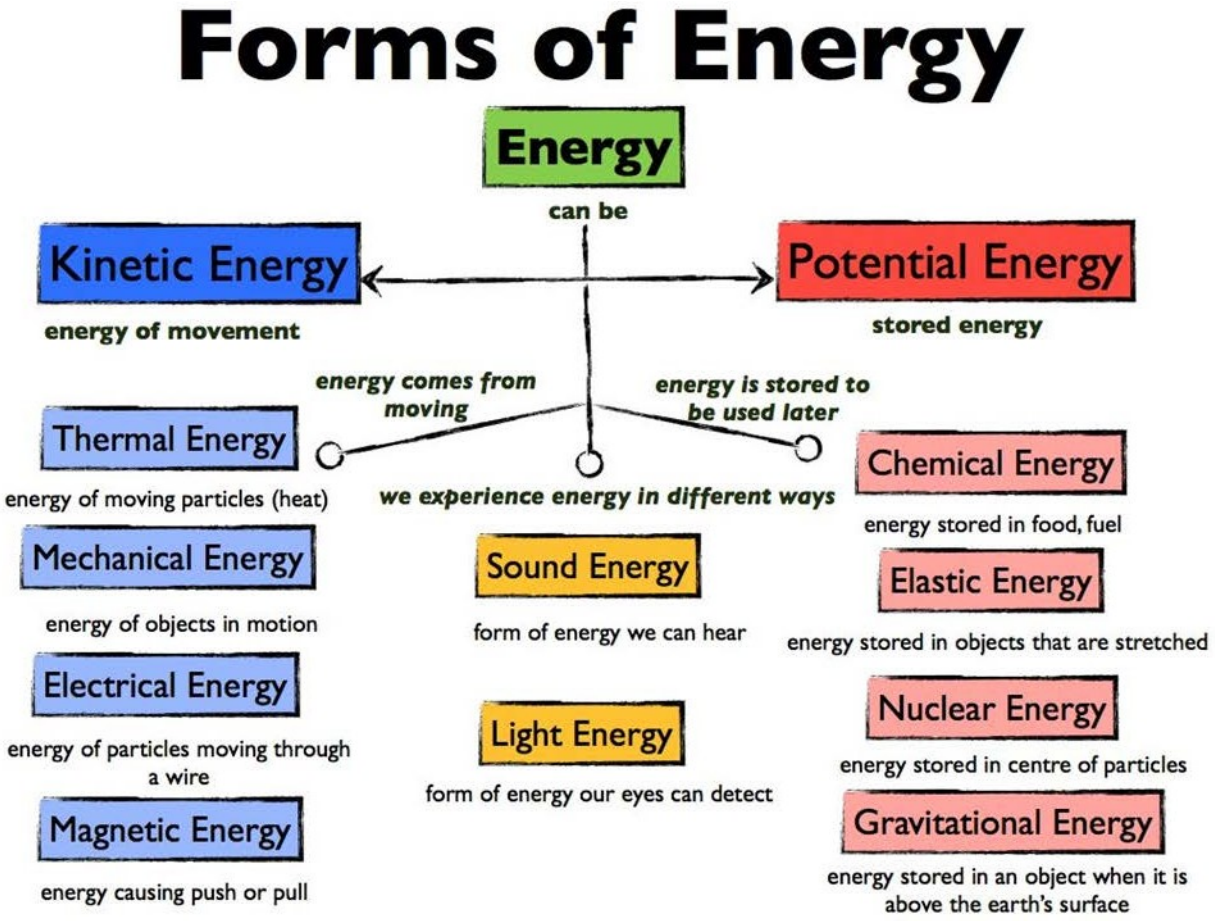

Figure 1.1. Different Forms of Energy[4]

Physical Properties:

- Energy is invisible in nature, but it can manifest itself through light and wind.
- Sun and stars are the ultimate source[5] of energy.
- The universe has a constant and finite amount of energy.
- Primary energy is a form of energy that is available in nature naturally. For Example, Energy released from the muscles of humans and animals.
- Secondary energy is an energy carrier which is converted by humans from. primary energy sources. For Example, electricity is a secondary energy generated from coal, wind and water.
- Energy can vary with the properties such as position, mass, speed, shape, etc.
- In International Systems of Unit (SI), Energy can be measured in Joules (J) which is equal to the work done by one newton force through a one-meter distance[1]. The Dimension of energy is ML^2T^{-2}.

1.1. History and Evolution of Energy Sources

The age of stored photosynthesis has been very brief in historical terms. When coal became widely used due to a lack of wood in the late eighteenth century, it was seen as a poor substitute. Late in the nineteenth century, the era of petroleum fuels began. There are three grounds to believe that the current age is coming to an end: resource constraints, environmental challenges, and societal issues. Pessimists now believe that the peak of world oil production was in the year 2000, and that we are already on the downhill slope, according to a special series of energy reports published in New Scientist lately. There are still optimists who believe it will be another 10 years or more, but there is no significant disagreement on the geological fact that, if it hasn't already occurred, the peak of global oil production will occur in most of our lifetimes. Oil will become scarcer and more. expensive in that near-future planet. So, while current assumptions are that we will have cheap petroleum for a few decades, we will have to shift the basis of our energy use. Two heroic assumptions underpin this belief. The first is that there will be continued stability in the Middle East, as well as a desire to export oil from the region. The second assumption is that most of the world's population will continue to live without the transportation options we take for granted while we waste scarce petroleum resources on such selfish pursuits as car races, jet skis, motorboats, and suburban trips in heavy four-wheel-drive vehicles. As a result, the first and most fundamental argument for shifting away from the current pattern of fuel energy usage is that we are wasting a finite resource, necessitating change.

The use of fossil fuels is causing serious environmental problems at all levels, from local to global[3]. This is the second reason for change. At the local level, urban fuel usage is the primary source of air pollution, which poses major health problems in many large cities (UNEP 2002). In India, Delhi is the city with the most polluted air. The problem of acid precipitation has prompted policy reforms at the regional level to limit Sulphur dioxide production because of fossil fuel consumption (UNEP 2002). The burning of increasing amounts of fossil fuels is the primary source of human-caused climate change on a global scale. Concerns about this situation led to the creation of the Framework Convention on Climate Change and its accompanying Kyoto Protocol, a deal to reduce carbon dioxide and other "greenhouse gas" emissions. According to current scientific consensus, carbon dioxide emissions are around 2.5 times the capacity of natural systems to absorb the gas (IPCC 2001). To put it another way, worldwide fossil fuel consumption needs to be cut by around 40% to bring emissions back into balance with the natural carbon cycle. Climate change, according to recent scientific thought, is speeding up and influencing other planetary cycles, posing a severe threat to human civilization's future[6].

1.2. Energy Statistics in World

China ranked first in energy consumption amongst all the countries in the world. Whether United States of America (USA) just got below China and ranked second in this race[7]. After China and USA, India's total energy consumption ranked third in the world. India is an energy importer that consumes about 3% of the world's total energy. India is the world's third-largest coal-producing country where China is the world's largest in this sector. Oil provides 30% of India's energy demands, and more than 60% of oil is imported and most of them are from middle east[8].

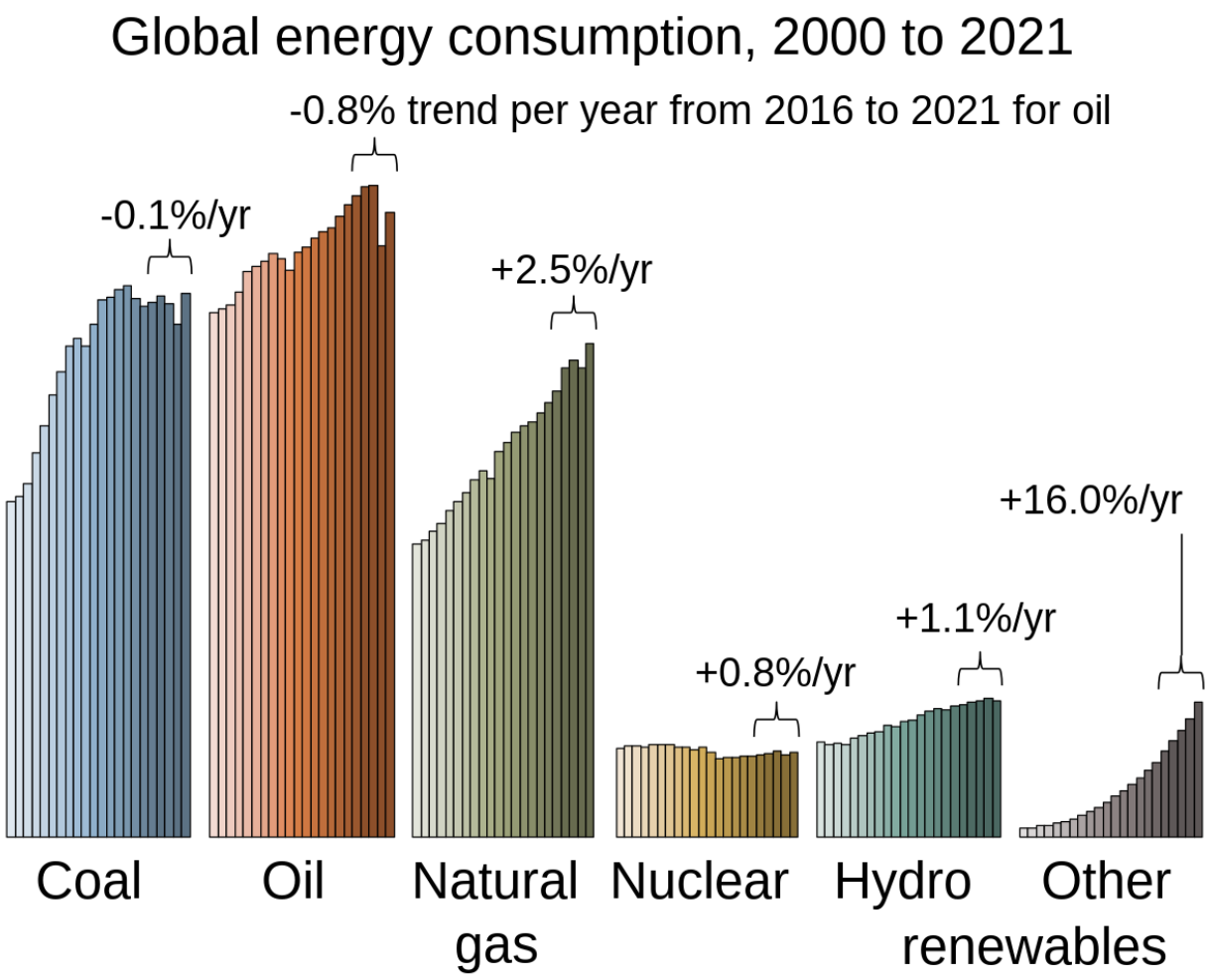

Figure 1.2. Global Change in Energy Consumption[9]. (Percentages represent change in 2000-21)

The transport demand for oil fell during a time of global health crisis. With 1383 TWh of power generation, India is ranked third in the world. According to Ernst & Young's 2021 RECAI (Renewable Energy Country Attractiveness Index) ranked India 3rd. In November 2021, India had a renewable energy capacity of 150 GW consisting of solar (48.55 GW), wind (40.03 GW), small hydro power (4.83 GW), biomass (10.62 GW), large hydro (46.51 GW), and nuclear (6.78 GW). India has made commitment for a goal of 450 GW renewable energy capacity by the year, 2030. The situation must be improved all over the world in terms of energy.

1.3. Energy Consumption of India

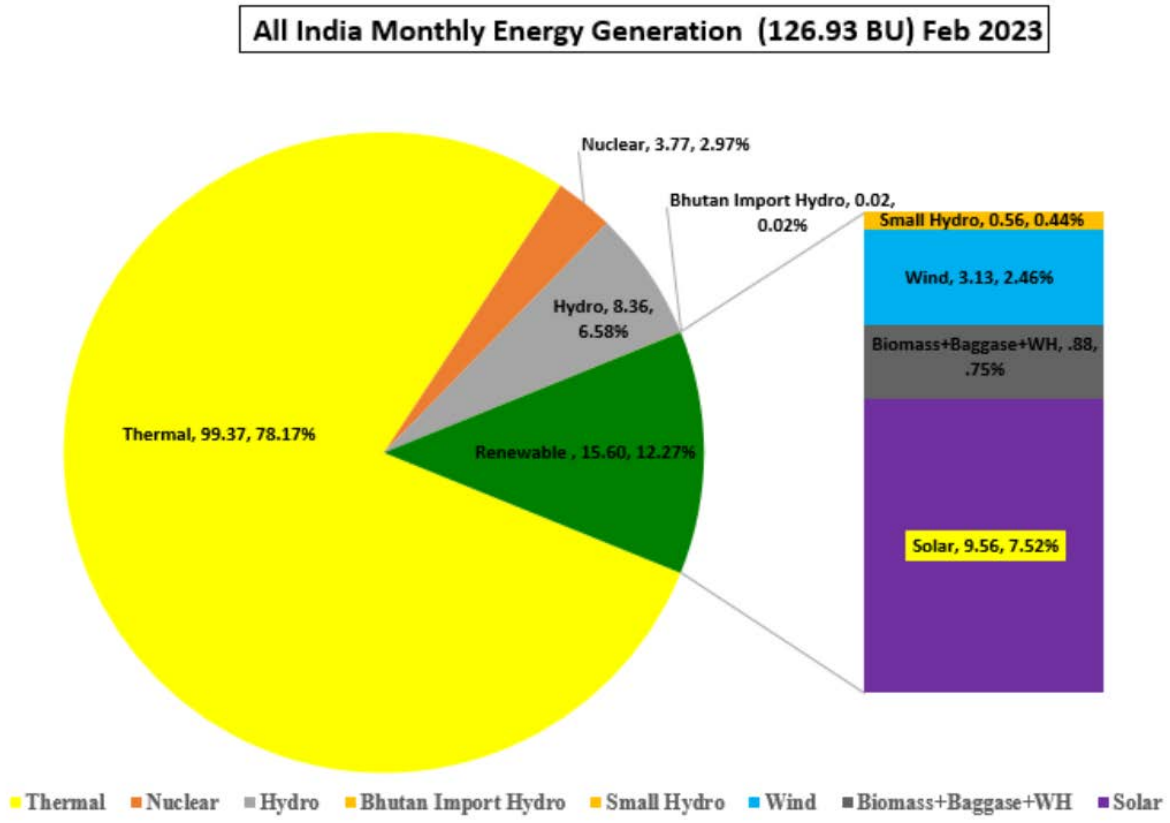

Figure 1.3. Total Energy Generation in India and Share of Renewable Energy in the month of February-2023[10]

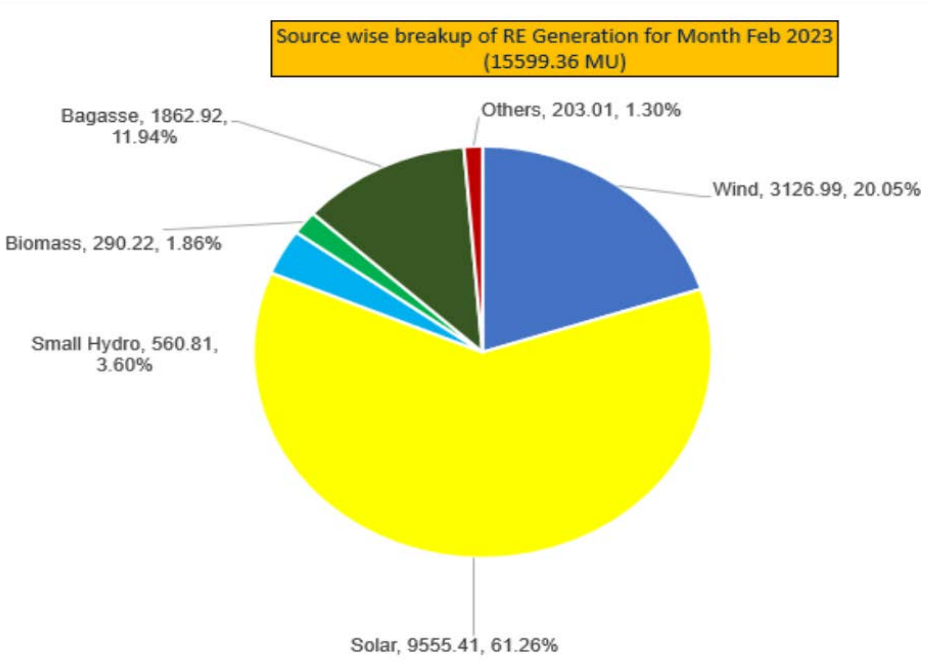

Figure 1.4. Source wise breakup of RE Generation in the month of February-2023[10]

1.4. Energy Crisis

Energy may be transformed between different forms at various efficiencies. All these transformations are bound by the **law of conservation of energy**. It states that energy can be converted in form, but not created or destroyed. The consumption of energy is closely related to the progress of mankind. As the consumption of energy grows, the population depends more and more on fossil fuels such as coal, oil and gas day by day and today's world is mostly dependent on fossil fuel which is a non-renewable energy source. There is a need to secure the energy supply for the future since the prices of gas and oil keep rising with each passing day. It is projected consumption rates natural gas & petroleum will be depleted by the end of the 21st century. This energy crisis of conventional energy resources interferes with economic growth in developed and underdeveloped countries. Petrol, diesel is heavily used in India in transportation sectors and agriculture machinery. Besides that, many production industries and large industriesuse coal, natural gas and petroleum rapidly. So, we assume that we will face an energy crisis very soon. There are two types of energy sources conventional energy sources and non-conventional energy sources/renewable energy sources. Conventional energy sources are used to generation of electricity and various industries for long years. These energy sources are mainly fossil fuels like coal, oil and natural gas. Using fossil fuels for energy has exacted an enormous toll on humanity and the environment—from air and water pollution to global warming. On other hand renewable energy is clean and environmentally friendly and pollution free. These energy sources are solar power, wind energy, hydro power, geothermal energy etc. In the last 20 years electricity generation rapidly changed from conventional to renewable for its advantages and bright future. For less utilization of renewable energy sources and rapid use of fossil fuel for electricity generation we assume that conventional energy will end in few years, and afterthat a huge energy crisis is waiting for us.

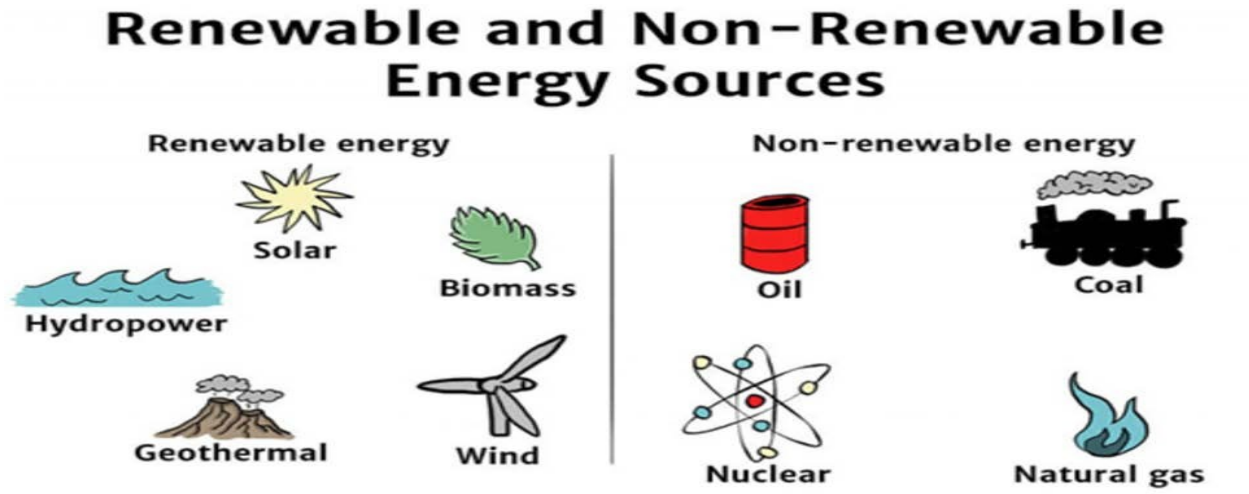

Figure 1.5. Renewable and Non-Renewable Energy[11]

1.5. Solution to Energy Crisis

- Renewable energy is clean, environmentally beneficial, and pollution-free. Solar power, wind power, hydropower, geothermal energy, and other renewable energy sources are among them. Electricity generation has shifted fast from conventional to renewable, owing to the benefits and promising future.
- Photochemistry research focuses on fundamental processes aimed at capturing and converting solar energy to chemical or electrical energy. It involves chemical change caused by the absorption or emission of visible light or ultraviolet radiation[6]. A molecule moves from the ground state to the excited state after absorbing a photon (a particle of light). Light is made up of photochemical reactions. If a molecule loses its chemical identity as a result of electronic photoexcitation, the process is called photochemical; if the molecule retains its chemical identity, the process is called photophysical. Photosynthesis, the technique by which plants obtain energy from the sun, is a well-known photochemical reaction. As a result, different types of artificial photosynthesis are effectively fighting for the right to capture incoming photons and utilize them for the benefit of the community.
- Nanotechnology presents a wide range of solutions to many existing problems and bettering the current situation, e.g., in healthcare, defense system, also in energy crisis. Traditional silicon-based solid state solar cells are one of the few commercially accessible systems for converting solar energy to electricity. Though the performance is not that much, Quantum dots (nanoscale particles) could be used as an alternative. The good thing is these devices can be fabricated in normal atmosphere and room temperature. Efficiency is improving to about 9-11%. The ability to distribute quantum dots in various materials, resulting in “sprinkle on” low-cost and large-area solar cells that may be applied to buildings or vehicles, is perhaps the most interesting aspect of quantum-dot solar cells[10].
- Because hydrogen is clean, versatile & portable, scientists believe it could be an effective way to reduce world’s reliance on non-renewable carbon-formed fossil fuels.
- Photosynthesis is a natural but very advanced method performed by plants. It consists of several chemical reactions and mainly absorbs sunlight for nutrients synthesis. Besides giving us food and every other nutrient all of today’s fossil-fuel-based energy comes from photosynthetic organisms that harvest sunlight. The photosynthesis process is divided into some important parts and factors.
    - Antenna system: Photosynthetic organisms uses its in-built antenna system for light absorption and transfer the required excitation energy to reaction center where the charge separation occurs.
    - Reaction factor: Reaction center builds a stable charge separation system with very less charge wasted back reactions.

- Oxidation: The separation of charge powers oxidation of H_2O molecules[8].

Finally, the product glucose and oxygen are formed.

- Artificial photosynthetic systems would be a significant step forward in energy generation and a vital breakthrough in addressing the growing concerns about environmental degradation caused by use in extreme quantities of fossil fuels[12].

  One appealing technique to solve this crisis is the construction of solar cells. As a result, dye-sensitized solar cells have emerged as a viable alternative to costly solid-state solar cells. Further developments would be going on there and described in this thesis.
- Several other promising approaches to artificial photosynthesis have emerged in recent years, based on the development of organic molecular systems that will provide photosensitized reactions such as PET i.e., photo-induced electron transfer[12]. Some chemical techniques in designing model molecules for artificial photosynthesis have been proposed in preceding years[13,14].
- This photosynthesis phenomenon gives rise to the idea of creating a charge storage and artificial light energy conversion system. Based on the underlying scientific principles of the natural process e.g., Photosynthesis, solar energy is to be captured and converted into useful forms of energy. A novel organic short chain dyad, NNDMBF was synthesized and characterized[15]. The fundamental goal is to construct supercapacitor like storage systems by combining this organic dyad with various noble metals, metal-semiconductor core/shell nanocomposite, and eventually with graphene hybrid materials. The current thesis focuses on a current research question in the field of new solar cell that uses charge electron injection separation in a short chain dyad as a light energy converter.
- UV-vis absorption, steady state, and time resolved spectroscopic investigations were carried out in various environments on this newly synthesized dyad in its pristine form and when combined with graphene quantum dots (GQD), graphene oxide (GO) and reduced graphene oxide (RGO). When the two redox components relate to a short chain, charge separated species arise in both ground and excited states, according to steady state measurements. It is envisaged that by coupling the short chain organic dyad system with GQD, GO and RGO, a highly efficient, stable, and low-cost artificial light energy converter might be constructed that will be safe and biocompatible. To exploit these nanostructures' full potential in the realm of energy storage, we need to fathom how the intricate interplays between the electrical and physical interactions of the active components affect the performance of these devices. This is how our current and future research will be conducted.

2. Photophysical and Photochemical Studies and Processes

Photophysical and Photochemical processes play pivotal role in the development of life on earth and surrounding environment with it. Simple cells became autotrophic, provided the basics of life, stored solar energy in the form of fossil fuels, and still feed us with nearly all our food thanks to a complex set of photochemical and photophysical processes. Photochemistry has an important role in determining the composition of materials in interstellar space and in the creation of pollutants in the atmosphere. Their influence on chemical, physical, biological, and medicinal sciences and technologies, including nanotechnology, is growing at a rapid pace.

Photochemistry deals with chemical reactions[16]. These reactions caused absorption of UV i.e., ultraviolet (wavelength, λ~ 100-400 nm), visible light (λ~ 400-750 nm) or infrared radiation (λ~ 750-2000 nm). Here, photons should have enough energy to raise the atoms from ground to an excited state. In excited state atoms or groups of atoms undergoes chemical reaction more rapidly as compared to ground state.

2.1. Ground States & Excited States

Electronic states i.e., ground states and excited states of a molecule are obtained by considering the properties of all the electrons in the unfilled shells. The electronic structure of states is commonly denoted by their multiplicities, singlet (S) or triplet (T). At natural temperatures and in normal environment most organic molecules' ground states all electrons are paired. Pauli Exclusion formula determines electrons will have opposite spin in a pair. When one of a pair of electrons is promoted to an orbital of higher energy, the two electrons no longer share an orbital, and the promoted electron can have same spin as the former or opposite spin. A quantum state in which two unpaired electrons have the same spin is called a triplet (T), while one in which all spins are paired is called a singlet (S).

A molecule is promoted from its ground state to an electrically excited state by light excitation with a photon of sufficient energy. Each excited state has its own chemical and physical properties as a result of light excitation. Photophysical and photochemical processes are such processes in which the excited species dissociates, rearranges, isomerizes or react with any other molecule.

2.2. Deactivation Process in Excited States

Radiative transitions, in which the excited molecule emits light in the form of fluorescence or phosphorescence and returns to the ground state, and intramolecular non-radiative transitions, in which some or all the energy of the absorbed photon is eventually converted to heat are examples of photophysical processes. The schematic diagram is expressed elegantly by Jablonski Diagram[17].

Physical relaxation processes may be categorized as:

- **Intramolecular:** These processes are
  I. **<u>Radiative transitions:</u>** It emits electromagnetic radiation when an excited molecule happens to go to the ground state. Fluorescence & phosphorescence are collectively known as luminescence.
  II. **<u>Radiation-less transitions:</u>** There is no emission of electromagnetic radiation that occurs during the relaxation process.
- **Intermolecular:** These processes are
  I. **<u>Vibrational Relaxation:</u>** Here the molecules of excited vibrational level which have excess energy undergo rapid collision with one another or with the solvent molecule in the lowest vibrational level of a particular electronic level.
  II. **<u>Electron Transfer:</u>** It involves a photoexcited donor molecule interacting with a ground -state acceptor molecule. An ion pair is formed, which may undergo back electron transfer, resulting in quenching of the excited donor.
  III. **<u>Energy Transfer:</u>** The electronically – excited state of one molecule (the donor) is deactivated to a lower electronic state by transferring energy to another molecule (the acceptor), which is itself promoted to a higher electronic state.

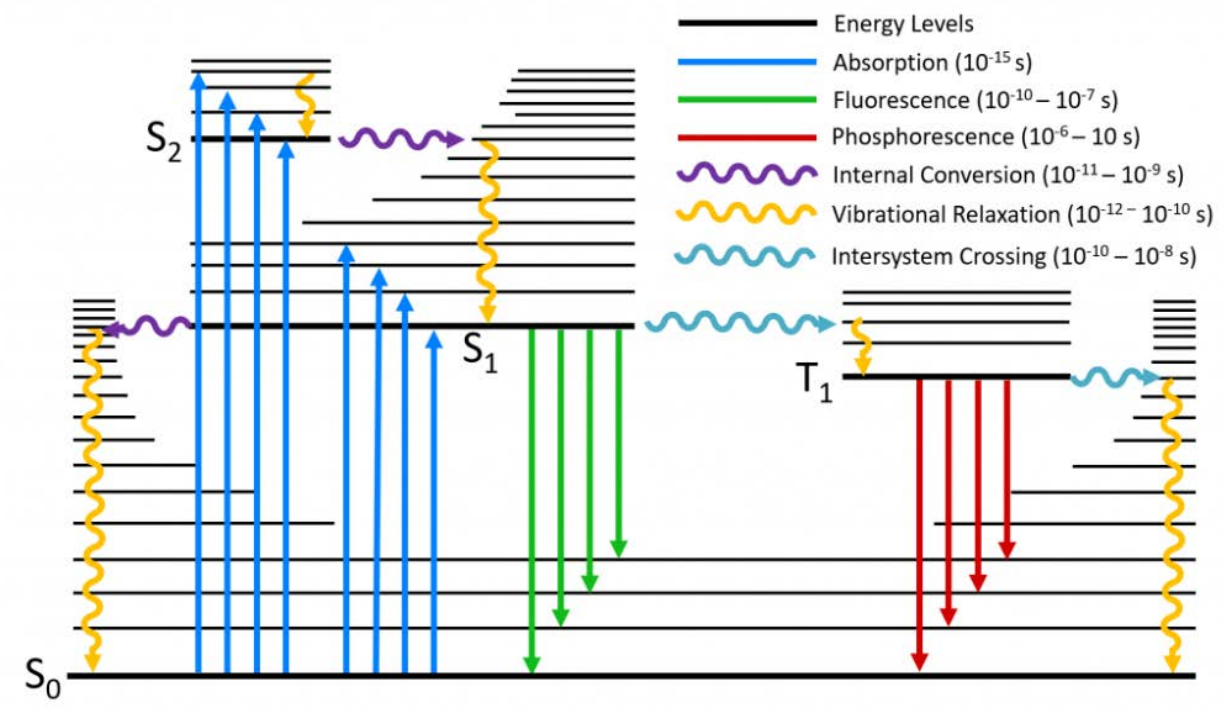

Figure 1.6. A typical Jablonski diagram showing the possible radiative and non-radiative transitions[18]

2.3. Laws of Photochemistry

1. **Absorption:** When an atom in a ground or lower level absorbs a photon with energy, E = hν (frequency ν) and moves to an upper level is called absorption. There are several governing laws regarding absorption of light. They are called laws of photochemistry.

   - **<u>First Law of Photochemistry: Grotthuss-Draper Law:</u>**

     The First Law of Photochemistry states that light must be absorbed for photochemistry to occur. This is a simple concept, but it is the foundation for performing photochemical and photobiological experiments correctly. This law also is known as the Grotthuss-Draper law, states that light must be absorbed by a compound for a photochemical effect to take place. Only the light which is absorbed by a molecule can be effective in producing photochemical changes in the molecule[19].

   - **<u>Second Law of Photochemistry: Stark-Einstein's Law:</u>**

     The Second Law of Photochemistry states that for each photon of light absorbed by a chemical system, only one molecule is activated for a photochemical reaction. This law also is known as, the Stark-Einstein law, states that for each photon of light absorbed by a chemical system, only one molecule is activated for a consequent reaction. It states that for each photon of light absorbed by a chemical system, only one molecule is activated for a photochemical reaction[13].Albert Einstein developed the quantum theory of light and came up with this 'photo-equivalence law'.

   - **<u>Lambert's Law:</u>**

     When a ray of monochromatic light goes through an absorbing material, the intensity of the ray falls exponentially as the absorbing medium's length grows. This is known as Lambert law[13]. Mathematically it can be written as,

$$I = I_0 e^{-kx}$$

     I, I_0 denotes Intensity of transmitted and incident light respectively and 'k' is absorption coefficient.

- **Beer-Lambert Law:**

  Beer–Lambert law, also known as Beer's law, is a relationship between light attenuation and the qualities of the substance through which it travels. The law is extensively used in chemical analysis measurements and in physical optics to understand attenuation for photons, rarefied gases. The modified form of Lambert's law comes from the consideration that decreasing rate in intensity of monochromatic light falls exponentially with the length of the medium as well as concentration (c) of solution.

$$I = I_0 e^{-\varepsilon c x}$$

$\boldsymbol{\varepsilon}$= molar absorption coefficient or molar extinction coefficient.

2. **Spontaneous emission:**

   If the transition between E2 and E1 is radiative, an atom in upper level can be able to decay spontaneously to lower level and release a photon of frequency v. Phase and direction of this photon is arbitrary.

3. **Stimulated emission:**

   An incident radiation causes an upper-level atom to decay into lower level, resulting in the emission of a "stimulated" photon with identical properties as input photon. This term 'stimulated' emphasizes that this type of radiation happens only when an incident photon is present. The amplification occurs because the incident and radiated photons are similar.

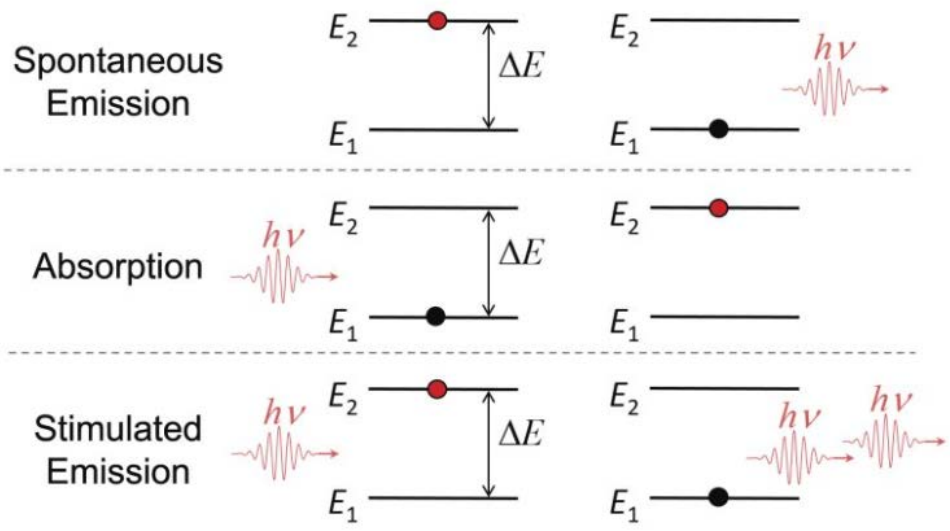

Figure 1.7. Mechanism of the interaction between an atom and a photon[20]

4. Franck Condon Principle:

In spectroscopy and quantum chemistry, the Franck–Condon principle describes the intensity of vibronic transitions. Vibronic transitions are changes in a molecule's electronic and vibrational energy levels that occur simultaneously as a result of the absorption or emission of a photon of sufficient energy. The principle states that if the two vibrational wave functions overlap more considerably during an electronic transition, a change from one vibrational energy level to another is more likely to occur[21].

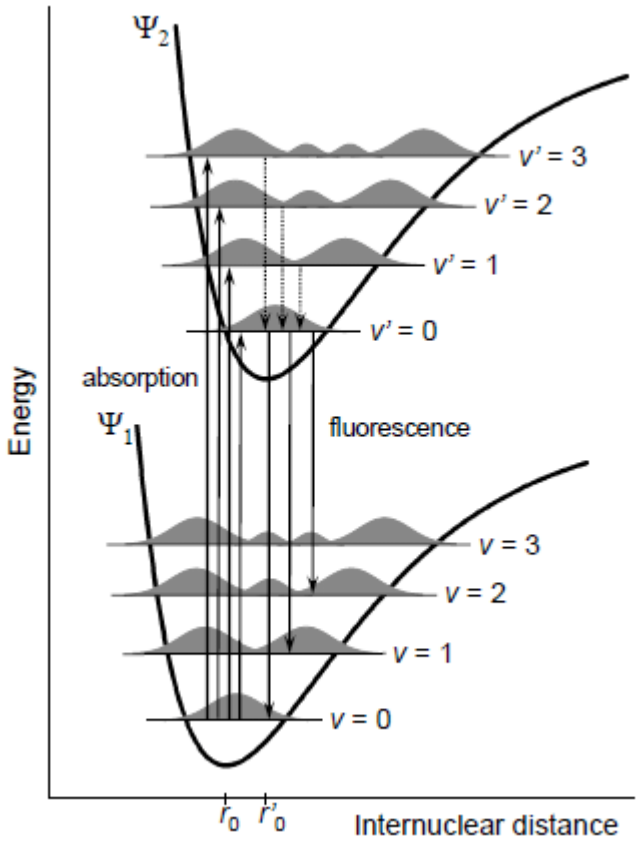

Figure 1.8. Diagram depicting Franck-Condon principle & absorption, fluorescence emission processes[21]

5. Quantum Efficiency:

The term quantum efficiency (QE) commonly refers to incident photon to converted electron ratio. In photochemical reaction it defines the efficiency of that reaction. For this photochemical reaction, QE needs to be unity.

$$\mathbf{QE=\frac{no.\ of\ molecules\ reacted/sec}{no.\ of\ photons\ absorbed/sec}\ (Theoretically)} \quad ; \quad \mathbf{QE=\frac{rate\ of\ chemical\ reaction}{quanta\ absorbed/sec}\ (Experimentally)}$$

3. Light Energy Conversion Process by Dyads

For light harvesting assemblies some doner-acceptor dyads and triads have been synthesized. The basic principle of these dyads and triads is based on photosynthesis. Here the doner-acceptor system containing Chlorophyll and porphyrins can copy the photo induced electron transfer process of natural photosynthesis because they can achieve long lived charge separation state.

Some nanoparticles have ingenious properties to protect the charge separation species involved within various excited short chain dyads system by inhibiting the energy wasting charge recombination process[17].

For constructing light emitting diodes (LEDs), photovoltaic cells, organic solar cells and artificial or model photosynthetic devices, etc. Many model compounds in which electron donors and acceptors are connected by covalent bonds were synthesized. Such types of synthesized compounds in the form of organic dyad systems comprising of electron donor and acceptor moieties linked together by short spacers will lead to the development of several efficient light energy conversion devices. The short-chained dyads are capable of efficient light harvesting, excitation energy transfer, electron transfer, and the formation of long-lived charge-separated states. To build various light energy conversion devices, several techniques were used on model donor–acceptor linked dyads or multichromophoric systems to increase the charge-separation rate[22].

A novel short-chain dyad (NNDMBF) (Figure 1.9) has been synthesized in which electron donor 4(N,N-dimethylamine)benzaldehyde (NNDMB) is linked by a short chain with the acceptor fluorene(F)[23].

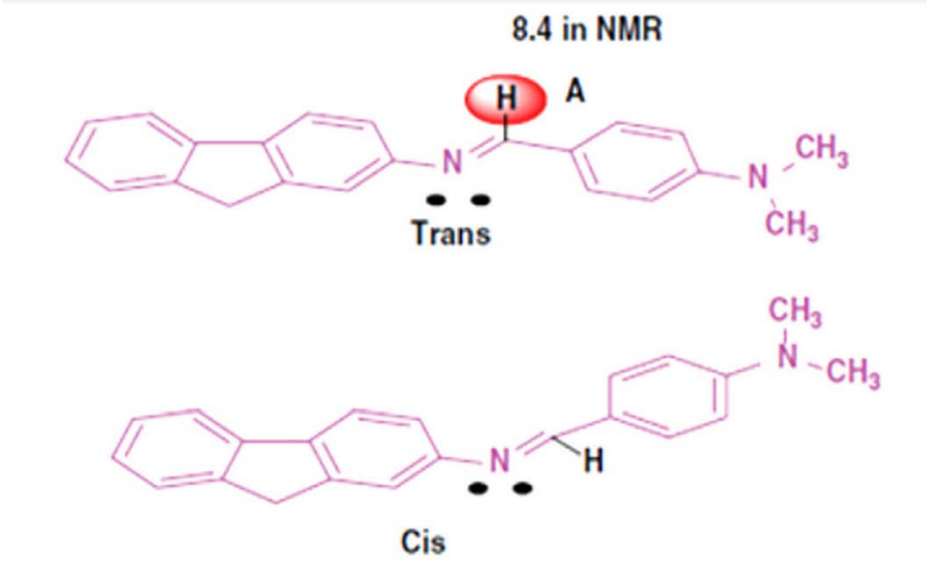

Figure 1.9. Cis and Trans-structure of the Novel short-chain dyad NNDMBF[56]

4. Graphene and Its Derivatives

4.1. Introduction

Graphene is an allotrope of carbon. This name was introduced by Boehm, Setton, and Stumpp in 1994[24] . Graphene is a monolayer of carbon atoms arranged in a hexagonal lattice. It's a two-dimensional substance made up of carbon atoms that have undergone sp^2 hybridization. Its bond length (molecular) is 0.142 nm. It has attracted a lot of attention in recent years due to its unique electrical, optical, magnetic, thermal, and mechanical capabilities, as well as its enormous specific surface area. Because graphene is widely utilized in nanoelectronics, it is critical to generate high-quality graphene. By mechanically cleaving a graphite crystal, Geim and Nosovelov were able to synthesize single layers of graphene in 2004.

Graphite is made up of layers of graphene stacked on top of each other with an interplanar spacing of 0.335 nm. Van der Waals forces the individual layers of graphene in graphite together, which can be overcome during graphene exfoliation. In terms of thermal and electrical conductivity, graphite has a remarkable anisotropic behavior.

Graphene has some unique features that distinguish it from other carbon allotropes. It is around 100 times stronger than the strongest steel in terms of thickness, yet its density is far lower than any steel. This conducts heat and electricity very well and is practically translucent. Graphene has a large and nonlinear diamagnetism, even stronger than graphite, which can be levitated by Nd-Fe-B magnets.

Graphene has extraordinary electronic, chemical, mechanical, thermal, and optical properties, making it a crucial material in the twenty-first century. It is also known as the world's 'thinnest' material. Graphene is now used in a wide range of applications, including energy storage materials, supercapacitors, nanoelectronics, drug delivery systems, polymer composites, liquid crystal devices, biosensors, and many others[25].

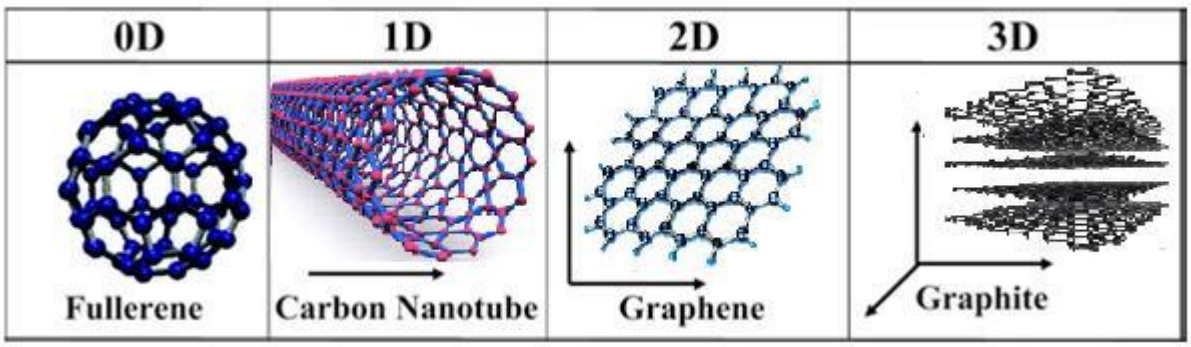

Figure 1.10. Graphene structure[26]

4.2. Graphene Quantum Dots (GQD)

Graphene quantum dots (GQDs) are a type of 0D material formed from small fragments of graphene. Due to quantum confinement and edge effects, GQDs display new phenomena akin to semiconducting QDs. Graphene and similar materials utilized for chemical sensing, such as GO or RGO, offer a lot of potential. This is owing to the 2-dimensional structure, which provides a large sensing surface per unit volume and low noise in comparison to conventional solid-state sensors.

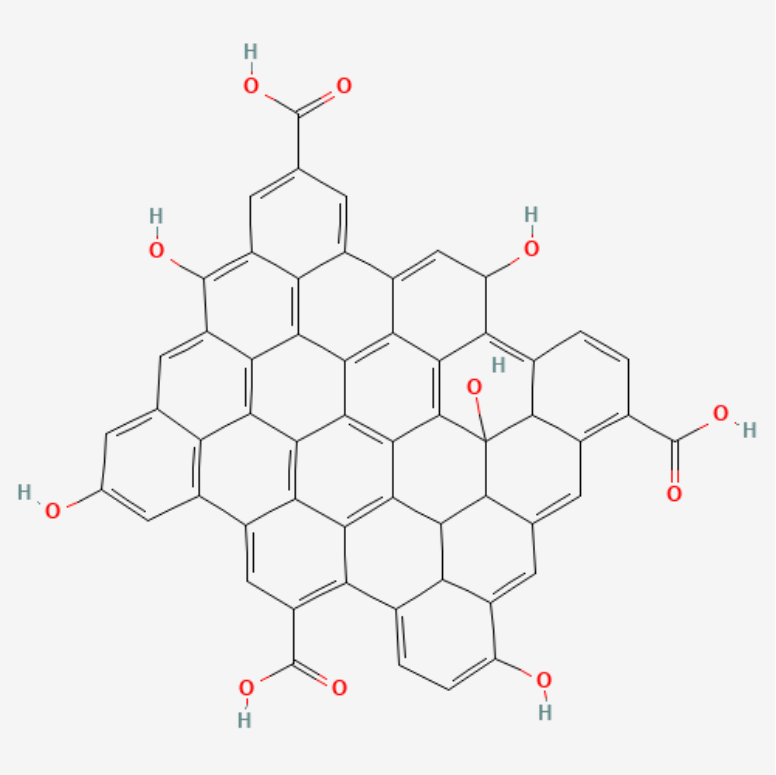

Figure 1.11. Molecular Structure of GQD[27]

Properties:

- GQD consists of one or a few layers of graphene and are smaller than 100 nm in size.
- Less toxicity, having quantum confinement property.
- They are chemically and physically stable.
- GQD has a large surface to mass ratio.
- It can be dispersed in water easily due to functional groups at the edges.
- Fluorescence emission of G-dots has a broad spectral range, including IR, visible & UV.

4.3. GQD Synthesis Method

A variety of approaches have been created to make GQDs[27]. These methods are usually classified as either top down or bottom up. Different techniques, such as graphite, graphene, and carbon nanotubes, were used to turn bulk graphitic materials into GQDs via top-down methodologies. Electron beam lithography, chemical oxidation, graphene oxide (GO) reduction, ultrasonic assisted exfoliation method is some of the more useful ones[28]. Because strong mixed acids are used in top-down methods, substantial purification is frequently required. Bottom-up techniques, on the other hand, construct GQDs from small organic molecules such as citric acid and glucose. The biocompatibility of these GQDs is improved.

Top- Down Method

Hydrothermal Method:

The hydrothermal approach is a simple and quick way to make GQDs. Using a range of macromolecular or tiny molecular compounds as starting ingredients, GQDs can be produced at high temperatures and pressure. To make GQDs, high temperature and high pressure are used to disrupt the bonds between carbon components.

Electrochemical Oxidation:

In this particular process, carbon–carbon graphite bonds, graphene is oxidized and decomposed in high redox voltage circumstance (1.5-3 V) into making GQD.

Chemical Exfoliation:

It is one of the suitable methods for GQD synthesis. In this method c-c bonds of graphene, carbon nanotubes are destroyed by adding acids like H2SO4, HNO3. Then it oxidizes or exfoliates graphene in layers and GQDs are formed.

Bottom-Up Process

Electron-beam lithography:

Electron-beam lithography or EBL is a process of scanning a focused beam of electrons to draw custom shapes on a surface covered with an electron-sensitive film. It requires costly and professional equipment. By this method GQD can be synthesized even at room temperature[28].

Microwave Method:

Because the hydrothermal method's long reaction time is a typical issue, microwave technology has evolved into a quick heating method that is widely employed in the fabrication of nanomaterials. It not only cut the reaction time in half, but it also boosted the yield. GQDs are purified by microwave irradiation utilizing Asp (Aspartic acid), DI water and NH4HCO3. High fluorescence (blue) is observed in produced GQD.

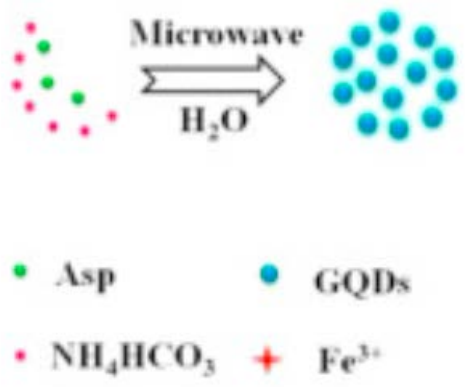

Figure 1.12. Preparation Process of GQD by Microwave Method[29]

4.4. Graphene Oxide (GO)

Graphene oxide (GO) can be considered as a monolayer of graphite oxide. The main difference between graphite oxide and GO is the interplanar spacing between the individual atomic layers of the compounds, which is caused by water intercalation. This increased spacing, caused by the oxidization process, sp^2 also disrupts the bonding network, meaning that both graphite oxide and GO are often described as electrical insulators. GO is a poor conductor but its treatment with light, heat, or chemical reduction can restore most properties of the famed pristine graphene. After fabrication of graphite oxide, GO can be obtained by exfoliating graphite oxide into monolayer sheets through a variety of thermal and mechanical methods[30]. Among these methods thermal exfoliation becomes a popular method of GO exfoliation. During heating, the oxygen-containing functional groups attached to carbon plane decompose into gases such as H_2O, CO_2 and CO, which will diffuse along the lateral direction. This exfoliation occurs only if the decomposition rate of functional groups surpasses the diffusion rate of evolved gases. Here the interlayer pressure existing among adjacent layers is large enough to overcome their van der Waals interactions and pushes the layers separated from each other. Generally, a minimum temperature of 550 °C is necessary for the successful exfoliation at atmospheric pressure[31]. Similarly, the mechanical method of exfoliation can be done by sonicating graphite oxide in water or polar organic media. Especially, sonicating and mechanical stirring can be combined to exfoliate graphite oxide with a better efficiency than using any individual method. But sonication has a great disadvantage that it causes substantial damage to GO platelets. It can reduce them in surface size from microns to nanometers.

4.5. Reduced Graphene Oxide (RGO)

Reducing GO to produce RGO is an extremely vital process because it has a large impact on the quality of the RGO produced; therefore, it will determine how close RGO will come in terms of structure to pristine graphene[32]. There are several ways reduction can be achieved, although they are all methods based on chemical, thermal, or electrochemical means. Some of these techniques can produce very high-quality RGO, like pristine graphene, but they can be complex or time-consuming to perform. RGO produced by chemical reduction has relatively poor yields in terms of surface area and conductivity. Thermally reducing GO at temperatures of 1000^0C or more creates RGO that has been shown to have a very high surface area, close to that of pristine graphene. This thermal process damages the graphene platelet as pressure builds up, produces CO_2 and reduces mechanical strength by creating imperfections, vacancies etc. in its structure. Electrochemical reduction of GO produces high quality RGO, like pristine graphene. The primary benefit of this process is that no hazardous chemical is used, so no toxic waste comes out.

Advantages and Disadvantages of GO and RGO:

The advantage of GO is its easy dispersibility in water and other organic solvents because of the presence of oxygen functionalities. This solubility of GO remains a very important property when it is mixed with other material to improve their conductivity. Though GO is often described as an electrical insulator because of the disruption of its sp^2 bonding networks. To recover the honeycomb hexagonal lattice, and the electrical conductivity, the reduction of GO must be achieved. Functionalization of GO can fundamentally change the properties of GO. The resulting chemically modified graphene's could then potentially become much more adaptable for many applications. For optoelectronics, biodevices, or as a drug-delivery material, it is possible to substitute amines for the organic covalent functionalization of graphene to increase the dispersibility of chemically modified graphene's in organic solvents. It has also been proven that porphyrin-functionalized primary amines and fullerene-functionalized secondary amines could be attached to GO platelets, ultimately increasing nonlinear optical performance. Although the chemical reduction of GO is currently seen as the most suitable method of mass production of graphene, it has been difficult for scientists to complete the task of producing graphene sheets of the same quality as mechanical exfoliation but on a much larger scale.

4.6. Synthesis Methods of GO and RGO

The discovery of GO & RGO brings new method of synthesis in light. Several methods are introduced through ages and in research papers. Synthesis of GO can be divided into two main categories - 1) bottom-up methods where simple carbon molecules are used to construct pristine graphene; 2) top-down methods where

layers of graphene derivatives are extracted graphite or other carbon source. The effective and useful methods are described here below.

Bottom-Up Methods

Chemical Vapor Deposition (CVD):

By this bottom-up method GO can be produced. In this process the substrate is exposed to one or more volatile precursors, which react and/or decompose on the substrate surface to produce the desired thin film deposit. The waste gases pumped out from the reaction chamber. Here temperature is the vital physical quantity which is controllable. Depending, Requirement of precursors and the structure depends on the material quality. There are many various types of CVD processes like thermal, plasma enhanced (PECVD), hot wall etc[33].

Silicon Carbide:

Silicon carbide (SiC) is one of the candidate materials for use in the first wall and blanket component of fusion reactors and is used in nuclear fuel particle coatings for high-temperature gas-cooled reactors[34].

Top-Down Methods

The focus on top-down methods, which first generate GO and/or RGO are more popular for yielding graphene derivatives, for use in nanocomposite materials.

Mechanical Exfoliation:

This is a top-down technique in nanotechnology, by which a longitudinal or transverse stress is created on the surface of the layered structure materials. mechanical method of exfoliation can be done by sonicating graphite oxide in water or polar organic media. Especially, sonicating and mechanical stirring can be combined to exfoliate graphite oxide with a better efficiency than using any individual method. But sonication has a great disadvantage that it causes substantial damage to GO platelets.

Thermal Exfoliation:

During heating, the oxygen-containing functional groups attached to carbon plane decompose into gases such as H2O, CO2 and CO, which will diffuse along the lateral direction. This exfoliation occurs only if the decomposition rate of functional groups surpasses the diffusion rate of evolved gases. Here the interlayer pressure existing among adjacent layers is large enough to overcome their van der Waals interactions and pushes the layers separated from each other. Generally, a minimum temperature of 550 °C is necessary for the successful exfoliation at

atmospheric pressure[66].

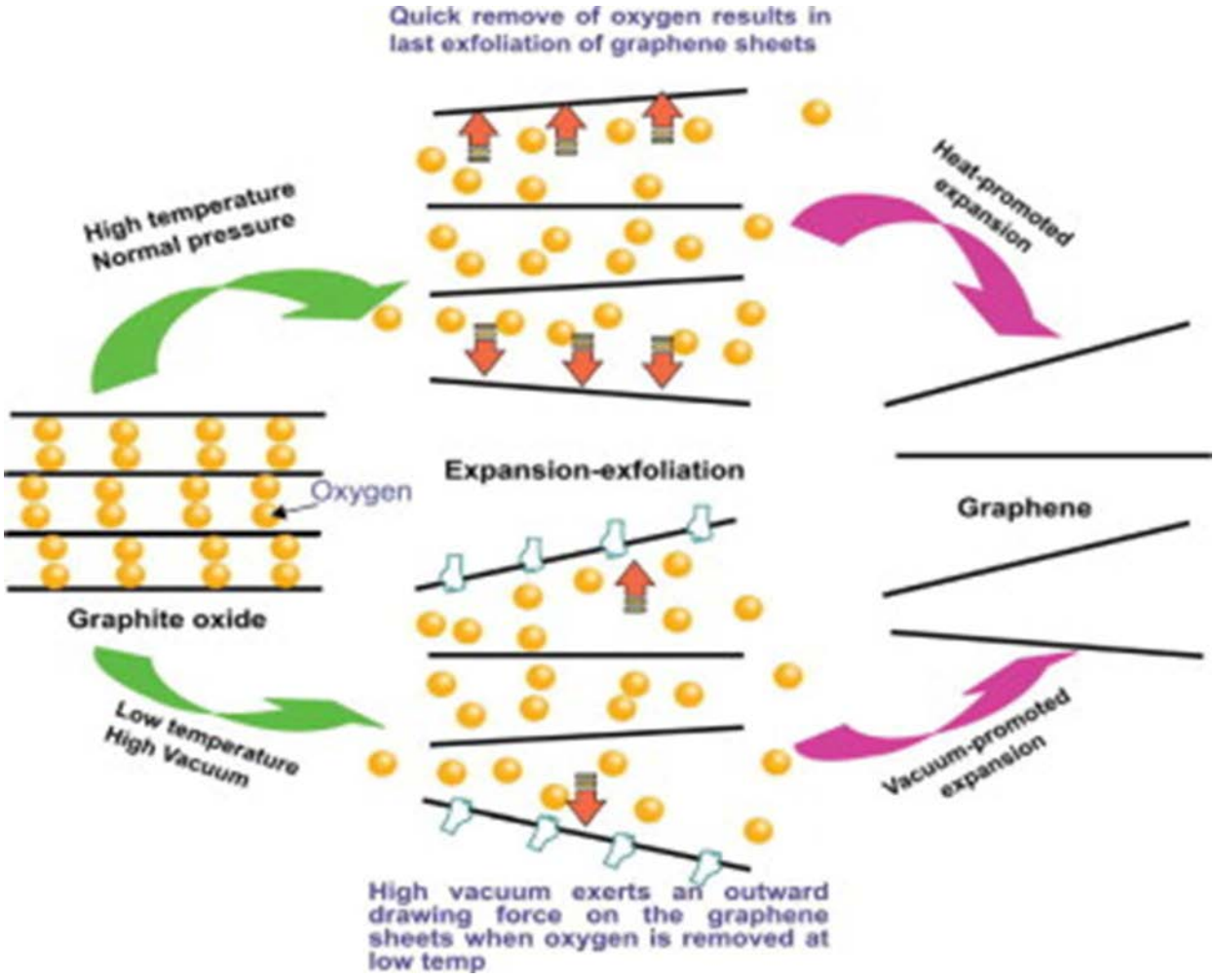

Figure 1.13. Thermal exfoliation of graphite oxide[35]

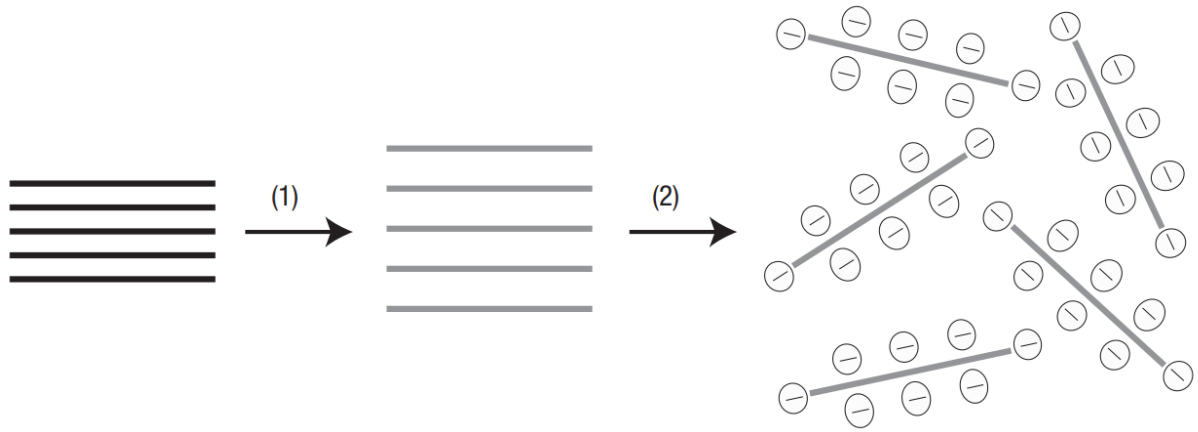

Figure 1.14. Exfoliation of graphite oxide in water by sonication[36] (1) Oxidation of graphite (black blocks) to graphite oxide (lighter colored blocks) with greater interlayer distance. (2) Exfoliation of graphite oxide in water by sonication to obtain GO colloids that are stabilized by electrostatic repulsion

These two methods lack quality and control. Due to that some other methods are introduced.

Modified Hummers Method:

Any method which changes or improves upon the synthesis route proposed by Hummers is regarded ubiquitously as a "modified Hummers method"[37]. In general, a carbon source (often graphite flakes or powders) is put into a protonated solvent (such as sulfuric acid, phosphoric acid, or some mixture of these) and a strong oxidizing agent (usually $KMnO_4$) is introduced. Following a dilution step, it is common to treat the resulting mixture with H_2O_2 to remove any metal ions from the oxidizer; this results in a yellow bubbling and ultimately a yellow-brown liquid. The resulting solids are then separated and treated with dilute hydrochloric acid to further remove any metal species, and the solution is washed and centrifuged several times with water until the pH of the solution is essentially neutral.

Tour Method:

GO (Graphene oxide) is prepared by mixing 90 mL concentrated H_2SO_4 (sulfuric acid) and 10 mL concentrated H_3PO_4 (Hydro-phosphoric acid). GO was reduced by using ascorbic acid as a reducing agent and distilled water. Then it is centrifuged and RGO is formed. This process involves several other similar or a little different step. That is being discussed below.

1) **Oxidation or intercalation:** GTO (graphite oxide) needs to be prepared from graphite powder by mixing H_2SO_4 with potassium permanganate (strong oxidizing agent).
2) **Exfoliation:** Oxidized form of graphite should be dispersed into distilled water to form single-layer graphene oxide (GO). Then heating it with magnetic stirrer, black paste formed collected by filtration and followed centrifugation and drying a day at 60°C .
3) **Reduction:** In order to synthesize reduced graphene oxide (RGO), the GO was dispersed, and ascorbic acid was added as the reducing agent, and the same procedure followed. Last, the black product should be washed with ethanol and distilled water, respectively[38].

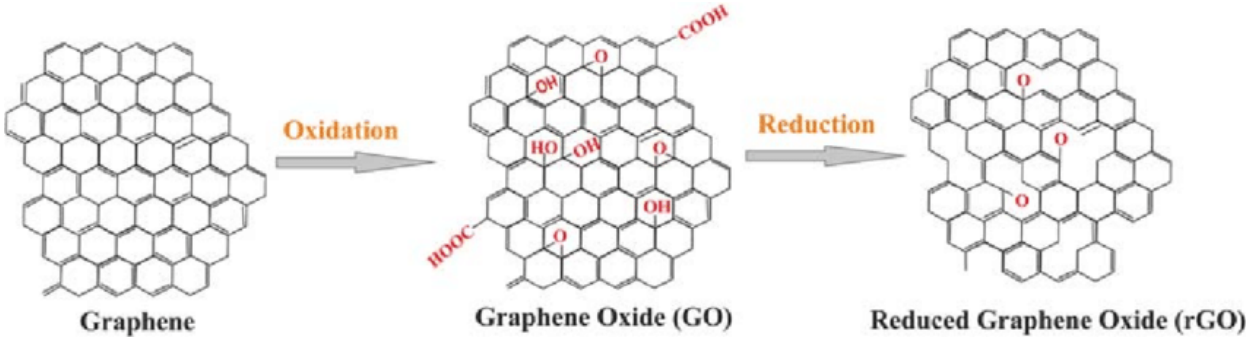

Figure 1.15. The chemical structures of graphene, graphene oxide (GO), the reduced graphene oxide (RGO) and the Conversion of graphene into GO and RGO via oxidation/reduction reactions[39]

4.7. Applications of GQD, GO & RGO

4.7.1. Biomedical Applications

- **Drug Delivery System:** Medicine delivery or drug distribution also possible by GQD, GO & RGO. GQD has a greater chance in biomedical applications than graphene or graphene oxide because of its small size (GO). There are efficient GQDs-based drug delivery systems e.g., EPR-pH delivery-release mode, EPR-Photothermal Delivery-Release mode[40].

- **Bio Imaging**: Bio-imaging and fluorescent bio-imaging using GQD or GO of cells and tissues shows great performance because fluorescent nano materials are biocompatible and bio-toxic less[41].

- **Biosensor**: GQD have some great properties like high solubility in water, flexibility in surface modification, nontoxicity, multicolour emission, excellent biocompatibility, good cell permeability, and high photostability, reason of its being used in biosensors. GQD and GO biosensors are used for visual monitoring of glucose, phosphate, cellular copper, iron and nucleic acid.

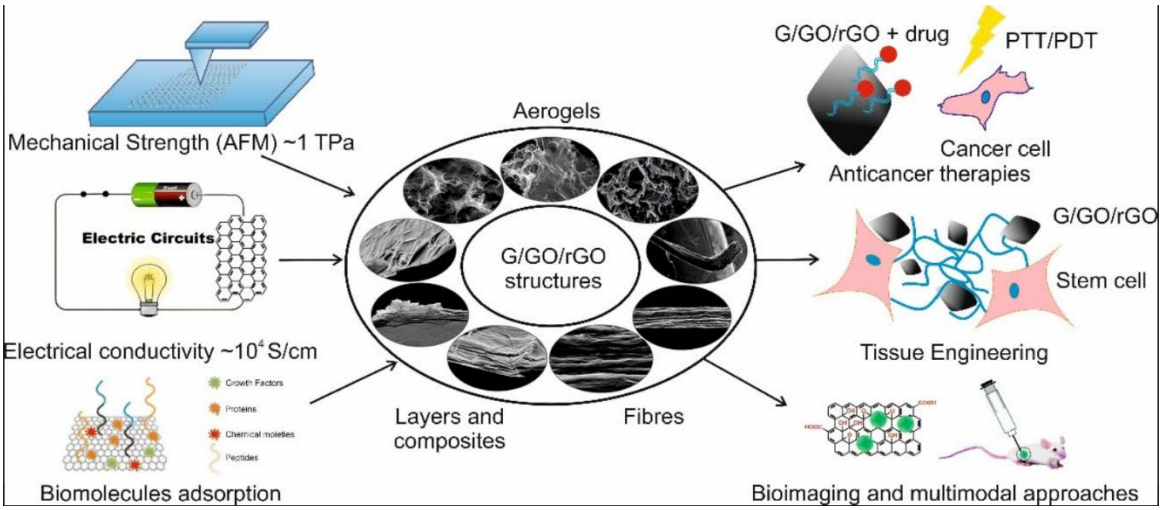

Figure 1.16. Applications of GQD, GO[41]

4.7.2. Optoelectronics Applications

- **LED: Light Emitting Device:** GQD are great material for LEDs due to their stable light emitting, low cost and eco-friendliness. Nitrogen-rich GQD shows broad and bright visible light under UV illumination that would be worth utilizing in phosphor applications.

- **OSC: Organic Solar Cells**: By GQD organic solar cells can be made and this type of solar cell are very light weight, flexible and light harvesting capacity is high because it can absorb near infrared light. It has special optical properties to control efficiently by changing their quantum dot size[41].

- **DSC: Dye-Sensitized Solar Cells**: DSCs are very popular because the making process is very easy and the making cost is also very low. It is an organic dye, and the efficiency is also great. GO or GQD with stable light absorption made from broad and cheap sources show its potential in DSCs[41].

- **Supercapacitor:** GO & GQD can be electrode for supercapacitors. These and some of its hybrid perform electrochemical performance achieved by efficient dispersion of reduced GO. It is useful in charge–discharge process and charge transportation[16].

5. Aim of thesis

Our primary aim of this thesis would be to fabricate a new nanocomposite hybrid by combining organic novel short-chain dyad i.e., NNDMBF with GQD, GO and RGO. At first synthesis and characterization of NNDMBF are to be made. The investigations are being carried out by using steady state and time-resolved spectroscopic techniques on the pristine dyad and its hybrid nanocomposite systems. Some quantum chemical calculations are being carried out by using Gaussian 03 software to support the experimental findings from a theoretical point of view. Both from the theoretical predictions and NMR studies it reveals that in the ground state only elongated (E-type) trans conformation of the pristine dyad exists, whereas on photoexcitation these elongated conformers are converted into folded forms (Z-type) cis conformation. Time resolved fluorescence spectroscopic (fluorescence lifetime by TCSPC method) measurement demonstrates that in acetonitrile medium and in presence of GO and RGO nanoparticles the organic-inorganic hybrid nanocomposite possesses larger number of trans conformers relative to cis one, even in the excited singlet state. This indicates the possibility of slower energy destructive charge recombination rates relative to the rate possesses associated with charge-separation within the dyad. In the present experiment using Ultraviolet-Visible absorption, steady state & time resolved spectroscopic (TCSPC) and Transient Absorption Spectra, investigations have done on the same dyad when combined with graphene quantum dots/ graphene oxide/ reduced graphene oxide to examine the suitability of the nanocomposite form and compare it with its pristine form. Finally, we do analyze the result to know which form of dyad is an effective energy storage candidate. So that in future we can use that as a budget and eco-friendly charge storage device (supercapacitor) way or efficient energy storage device to solve the global energy crisis phenomenon.

6. Literature Review

The suitability of a novel synthesized short-chain dyad **NNDMBF** as a light energy converter has a wide application in optical data storage, light emitting diode (LEDs), optical solar cell, photovoltaic cell etc. The primary aim of this thesis is to develop several nanocomposite devices where the novel synthesized dyad being combined with noble nanomaterial graphene oxide (GO) and reduced graphene oxide (RGO), which behaves as a highly efficient, biocompatible, bio-safe and of low-cost artificial light energy converters compared to its pristine form. From the present time resolved spectroscopic results it could be hinted that relatively stable elongated trans-conformer in the excited state in case of the nanocomposite system of dyad NNDMBF-GO (or RGO or GQD) in comparison to the pristine form may arise from the surface trap effects. In future it may be able to solve the global energy crisis phenomenon[31].

T. Ganguly et al.[42] investigated the photophysical characteristics and the nature of the photoinduced electron transfer (PET) reactions using electrochemical, steady state, and time-resolved spectroscopic methods, in a synthetic anisole (A)-thioindoxyl (T) dyad system (24MBTO). The outcomes show how the charge separation reactions produced the two types of isomeric species, Z- and E- forms. According to thorough investigations, the current thioaurone may function as a flexible photo switchable system.

Wang et al.[43] stated that new photophysical phenomena had been introduced together with the optimization of existing photophysical processes, such as charge separation during light absorption. The use of fundamental concepts for converting solar energy into chemical energy, selective chemical synthesis, e-/h+ excitation of semiconductors and biological system self-replication are also examined. The intensity of the incident light and the higher temperature will both affect how much the nanoparticles' localized temperature increase. This practical method of fusing natural and artificial systems results in very effective and long-lasting solar to chemical energy conversion.

T. Ganguly et al.[44] demonstrates using steady state and fluorescence lifetime measurements that singlet-singlet energy transfer occurs to populate the lowest excited singlet of carbazole as a result of photoexcitation of the benzotriazole (BZ) part of the bichromophore, 9(1-H-benzotriazole-lylmethyl)-9H-carbazole (BHC) (CZ). As a result of this indirect energy transfer process, CZ is indirectly stimulated and conducts a strong charge transfer reaction (CT) with the polar medium acetonitrile (ACN). BHC behaves as a triad system of BZ-CZ-CAN when dissolved in CAN, with BZ serving as an antenna molecule and CZ serving as a reaction centre. It has been suggested that the bichromophoric system BHC may function as a synthetic photosynthesis or solar energy conversion mechanism.

Chakraborty et al.[45] claimed that core-shell nanostructures had typically been discovered to have enhanced qualities, leading to the development of a more effective light energy conversion device using chore-shell nanocomposites rather than just nanoparticles.

T. Asahi et al.[46] used femtosecond laser spectroscopy to investigate photoinduced intramolecular charge separation (CS) and charge recombination (CR) of the product ion pair (IP) state of a number of fixed-distance dyads composed of zinc or free-base porphyrin and quinines in order to ascertain the energy gap and temperature dependences of CS and CR reactions in nonpolar media. The obtained CS and CR rates were in the normal and inverted regions, respectively. They have verified that when the energy gap narrows, the activation barrier for the CS reaction rises. Here, the CS rate constant shows negligible solvent polarity dependence while the CR rate constant exhibits an increase in solvent reorganisation energy with solvent polarity.

T. Ganguly et al.[47] used steady state, time-resolved spectroscopic methods, and fluorescence anisotropy decay to observe the photophysical properties of the synthesised short-chain organic dyad, 1-(4-chlorophenyl)-3-(4-methoxy-naphthalen-1-yl)-propenone (MNCA) in isotropic media and gel (P123) environment. According to NMR and time-resolved spectroscopic studies, the charge-transfer species of the dyad MNCA appear to have only one isomeric form in the ground state, and this conformation persists even after photoexcitation, regardless of the environment's characteristics, such as whether it is an isotropic solution or a micro-heterogeneous medium (gel phase of P123).

T. Ganguly et al.[48] studied the nature of charge separation as well as the energy-wasting charge recombination processes within a short-chained organic dyad 1-(4-bromo-phenyl)-3-(2-methoxynapthalen-1-yl)-propenone (MNBA) have been revealed by using electrochemical, steady state and time resolved fluorescence (by TCSPC), nanosecond laser flash photolysis methods. On photoexcitation, further conformers probably of the nature of folded type isomeric species (Z-form) were also obvious from time resolved fluorescence studies, even if in the ground state elongated type structure (E-form) is observable from NMR spectra. However, this time-resolved study has revealed a predominance of elongated shape in the excited singlet state. The charge separation rate was found to be much higher than the energy-wasting charge recombination rate, which was calculated from the transient absorption measurement using nanosecond laser flash photolysis technique. This finding suggests that MNBA may be a good candidate for building artificial light energy conversion devices or molecular photovoltaic cell components.

T. Torres et al.[49] looked at the photophysical characteristics of a new dyad molecule made up of a donor Zn-phthalocyanine and a C60 derivative that are covalently bonded (acceptor). They provided experimental proof of charge separation with a long half-life in solid state, which is many orders longer than in solution. The foundation for potential photovoltaic applications is it.

T. Ganguly et al.[50] investigated steady state and time resolved spectroscopic measurements on the organic dyad 1-(4-Chloro-phenyl)-3-(4-methoxy-naphthalen-1-yl)-propenone (MNCA) at ambient temperature. When the surrounding medium is changed from being only chloroform to being a mixture of chloroform and Ag@TiO2 (noble metal-semiconductor) nanocomposites, time resolved fluorescence and absorption measurements show that the rate parameters associated with charge separation within the dyad increase while charge recombination rate reduces significantly. According to the results, a dyad and core-shell nanocomposites may be coupled to create an organic-inorganic nanocomposite system that may be used to create light energy conversion devices.

According to T. Ganguly et al.[51], different photophysical properties could be measured using UV-vis absorption, steady state spectroscopic experiments, and time-resolved spectroscopic experiments. When the results of the silver (Ag)-dyad MNTMA and gold (Au)-MNTMA hybrid nanocomposites systems were examined, a striking difference was found between the two.

T. Ganguly et al.[52] measured various photophysical properties of the silver (Ag)-dyad MNTMA system and compared the results to the gold (Au)-MNTMA hybrid nanomaterials by using UV-vis, steady state, and time resolved spectroscopic techniques, Ag-dyad systems have a significant amplification of the plasmonic absorption band, whereas the other Au-dyad systems do not. In the case of the Ag-dyad hybrid nanocomposite system, the preponderance of folded conformation, which enables charge recombination, was detected even in the excited state from the measured fluorescence lifetime values. According to transient absorption tests using the laser flash photolysis method, the Ag-dyad system's rate of energy destruction is significantly higher than that of the Au-dyad nanocomposite device.

Bhattacharya et al.[53] reported on the nature of the charge separation and recombination processes in an organic dyad with a short spacer. This inquiry shown that an effective light energy conversion device may be created using the 1-(4-Bromo-phenyl)-3-(2-methoxynaphthalen-1-yl)-propenone (MNBA) candidate. Therefore, this technique can be used to create low-cost, effective energy conversion devices in the future.

Bhattacharya et al.[54] looked at the possibility of employing metal-semiconductor nanoparticles to modulate the charge recombination process in light energy conversion devices. It was discovered that a significantly enhanced version of the light energy conversion device was implied by the use of TiO2 nanoparticles. Charge-separated organisms could be protected for a long time under this system.

T. Ganguly et al.[55] looked and studied pure dyads, dyad-spherical gold nanoparticles (GNP), and dyad-star shaped gold nanoparticles using UV-vis absorption, steady state, and time-resolved spectroscopy examinations (GNS). Although the pristine form of the dyad has a trans- (elongated and planar) isomer in the ground state, it was found that during photoexcitation, the trans- transforms into the cis- structure (folded). It's interesting to note that the dyad behaves differently whether it combines with GNP or GNS. Due to the stimulation of the dyad-GNS system, 60% of the trans-species remain unaltered in the excited state. In the current experiment, the dyad-GNS nanocomposite appears to be a better light energy storage device than the dyad-GNP and the pure form of the dyad.

Mitra et al.[56] noticed the impact of short chain dyad carbon quantum dots (CQD) and their capacity for storing energy. The research on the pure short chain dyad €-4-(((9H-fluorene-2- yl)imino)methyl)-N,Ndimethylaniline (NNDMBF) and its nanocomposite forms with CQD or NCQD was done using time resolved

spectroscopic approach. The experiment's findings demonstrate that the ground state dyad's more than 80% trans structure can be maintained in the presence of photoexcitation in the CQD environment and functions as a powerful energy storage system.

Gust et al.[57] claimed that a biomimicry system may lessen the complexity of natural photosynthesis. The liposomal device, a biometric nanoscale machine, converts solar energy into chemical energy. The system has a very high level of efficiency. A photosynthetic bacterium's solar energy conversion method is like how the liposomal system transfers energy overall.

Rozzi et al.[58] noted that the main issue is how effectively light energy can be turned into electrical power or chemical fuels. This conversion is typically believed to occur on extremely fast, femto-to-pico second time scales in artificial photosynthesis and solar devices. They also looked into the primary charge transfer process in a prototypical artificial reaction center called a supramolecular trio.

Sen et al.[59] stated that time-resolved and steady-state spectroscopy has been used to examine the surface energy transfer between confined dye and Au nanoparticles. Analysis shows that the energy transfer from the dye to the Au nanoparticles is a process of surface energy transfer. It may be possible to create novel light harvesting systems using this energy transfer between restricted dye and Au nanoparticles.

Dutta et al.[60] recognized that photoexcitation of a donor molecule followed by electron transfer to an accepter is a typical pathway for energy storage. They confine trisbipyridine ruthenium (II), the light sensitizer donor, in the super cages of zeolite.

Zhang et al.[61] found that a variety of advantages exist for nanostructured materials, including high surface-to-volume ratios, favourable transport characteristics, altered physical properties, and confinement effects brought on by the nanoscale size. Thus, it has a wide range of applications, including solar cells, catalysts, thermoelectric devices, lithium-ion batteries, and super capacitors, among others. Some applications gain from this review, such as increasing electrochemical reaction by increasing surface area, or improving solar cell optical absorption by producing optical effects.

Balaya et al.[62] discussed the cutting-edge idea at the nanoscale for the creation of superior materials that perform effective energy conversion and storage. The use of nanostructured materials in thermoelectric devices for efficient waste heat conversion is highlighted. He claimed that metal oxides of the nanoscale can improve the performance of supercapacitors.

Edward et al.[63] mentioned were fuel cells and hydrogen's usage and applications. Energy storage, distributed heat and power generation, and transportation are all applications for hydrogen and fuel cells. Using fuel cells, electricity is produced by converting hydrogen or a fuel rich in hydrogen into an oxidant. It involves an electrochemical reaction at low temperature. It has a promising future because it is a sustainable energy source with low CO2 emissions.

Brudving et al.[64] ventured that relying on fossil fuels has a number of disadvantages, including concerns about energy security and greenhouse gas emissions. By directly transforming solar energy into fuel, it might be avoided by artificial fuel-producing systems that replicate natural photosynthesis. The three key aspects of photosynthesis—light capture, charge separation, and catalysis—were discussed. Here, we describe the design of dye-sensitized solar cells for fuel production.

Eustis et al.[65] studied the noble metal surface plasmon resonance and its radiative and non-radiative properties of different forms of nanocrystals, as well as its contemporary applications. The characteristics of nanoparticles can change when their size or form is altered. Future applications may be created by implementing them.

T. Ganguly et al.[66] noticed the photo switchable properties of the unique self-synthesised dyad system, i.e. 1-(4-chloro-phenyl)-3-(1-methoxy-3,4-dihydro-naphthalen-2-yl) propene (MNCADH). They claimed to have discovered this dyad's "trans" isomer in its ground state. Both the "cis" and "trans" isomers are present in the excited state, according to steady state and time resolved spectroscopic techniques. The energy barrier for trans-cis interconversion is discovered to be lower in the excited state than in the ground state, and trans-cis conversion is more effective in the excited state.

Mandal et al.[67] reported on the synthesis and technique of 3-(1-Methoxy-3,4-dihydro-naphthalyn-2-yl)-1-p-chlorophenyl propane, a new chemical dyad. By mixing the organic dyad with various noble metals, semiconductor nanoparticles, and noble metal-semiconductor core/shell nanocomposites, they create new hybrid nanocomposites.

Paul et al.[68] discovered that the pristine dyad, dyad-spherical gold nanoparticles (GNP), and dyad-star shaped gold nanoparticles (GNS), underwent UV-vis, steady state, and time resolved spectroscopic investigations. In the ground state, the dyad in its pristine form possesses trans-type isomer, but on photoexcitation trans-form converts into cis-structure. When the dyad combines with GNP or GNS, it behaves differently. The best light energy conversion or storage system available is the dyad-GNS nanocomposite.

Olabi et al.[69] observed that graphene exhibits exceptional performance in the majority of energy storage device applications. Performance can be improved with graphene, and it has excellent durability. This work emphasises the use of graphene in electrochemical, absorbance, and energy storage devices.

Park et al.[70] ventured that in order to fully benefit from the use of graphene in micro-scale devices, it is crucial to include two-dimensional graphene nanosheet into a micro/macro sized structure. In order to do this, a brand-new high temperature organic solvent spray aided self-assembly technique is used to produce a spherically integrated graphene microstructure.

K. Maruyama et al.[71] investigated photoindused intramolecular charge separation (CS) and charge recombination (CR) of the product ion pair (IP) state of a series of fixed-distance dyads consisting of free-base porphyrin or zinc porphyrin and quinines by using femtosecond laser sopectroscopy, to determine energy gap and temperature dependences of CS and CR reactions in nonpolar media. Obtained CS rates were in the normal region and CR rates were in the inverted region. They have confirmed that the activation barrier for the CS reaction increases with a decrease of the energy gap, while the CR process is activationless, indicating the dominant effect of the high-frequency quantum mode in the inverted region. They also examined solvent polarity effect upon the energy gap dependence upon CS rate constant and CR rate constant. Here solvent reorganization energy increases with the solvent polarity, with the CS rate constant but CR rate constant shows little solvent polarity dependence.

S. Fukuzumi et al.[72] observed that the photoindused process in zinc porphyrin-C60 dyad (ZnP-C60) in different organic solvents by fluorescence lifetime measurements and picosecond and nanosecond time-resolved transient absorption spectroscopies. The charge-separated state (ZnP*+-C60*-) is formed via photoinduced electron transfer from the excited singlet state of the porphyrin to the C60 moiety. In nonpolar solvents such as benzene (ε= 2.28), the charge-separated state undergoes charge recombination to yield the C60 singlet excited state, followed by intersystem crossing to the C60 triplet excited state. More polar solvents such as anisole (ε= 4.33) render the energy level of the charge-separated state lower than the C60 singlet excited state, resulting in the direct formation of the C60 triplet excited state (1.50 eV) from the charge-separated state. In polar solvents such as benzonitrile (ε=25.2), where the energy level of the charge-separated state (1.38 eV) is low compared with the C60 triplet excited state, the charge-separated state, produced upon excitation of the both chromophores, decays directly to the ground state. Such solvent dependence of charge recombination processes in ZnP-C60 can be rationalized by small reorganization energies of porphyrins and fullerenes in electron-transfer processes.

S.Fukuzumi et al.[73] examined photoinduced charge separation (CS) and charge recombination (CR) processes in various porphyrin-fullerene linked systems (i.e., dyads and triads) by means of time-resolved transient absorption spectroscopy and fluorescence lifetime measurements. Here lowest lying chargeseparated state of all the investigated systems, namely, that of ferrocenium ion (Fc+) and the C60 radical anion (C60*-) pair in the Fc-ZnP-C60 triad, has been generated with the highest quantum yields. Determination of CS and CR rate constants, together with the one-electron redox potentials of the donor and acceptor moieties in different solvents, has allowed us to examine the driving force dependence of the electron-transfer rate constants. Interestingly, the Marcus plot has provided clear evidence for intramolecular CR located in both the normal and inverted regions of the Marcus parabola.

Ganguly et. al.[74] described the methods of synthesis and characterization of the bichromophores (4MBA and 4MBAS) comprising 4-methoxybenzo[b]thiophene (4MBT) as donor and p-chloroacetophenone (PCA) as acceptor linked together by an olefinic (unsaturated in the former bichromophore and saturated in the case of the latter one) bridge. Here they compared the monomolecular photophysical properties of the bichromophores with the photophysics of the bimolecular systems. Both from the steady-state electronic absorption and fluorescence emission spectra it shows that the bichromophores exhibit charge transfer (CT) complex both in the ground and excited states. In intermolecular interactions it appears that a weak excited singlet (S1) CT complex of contact nature is formed, whereas in intramolecular systems (bichromophores 4MBA and 4MBAS) relatively stronger excited CT complexes of two types: cis (folded) and trans (extended) isomers for 4MBA and two conformers for 4MBAS are formed and transient absorption measurements clearly demonstrate the occurrences of photoinduced intermolecular ET reactions. Transient absorption spectral measurements by laser flash photolysis technique reveal that energy wasting charge recombination process within the bichromophore is largely precluded on changing the nature of the spacer from unsaturated to more flexible saturated one. So, it is necessary to incorporate two spacers (cyclophane type) instead of one to enhance the charge separation rate and to minimize the energy wasting recombination process.

O. Ito et al.[75] investigated intramolecular photoinduced charge-separation and charge-recombination processes in two C60-spacer-TTF dyads, in which C60 and TTF (tetrathiafulvalene) are connected through a flexible spacer of different lengths, have been investigated in polar solvents by time-resolved absorption and fluorescence techniques. Weak interaction between the C60-moiety and TTF-moiety in the ground state was suggested by the steady-state absorption spectra; the dyad with the shorter spacer shows slightly stronger interaction than that with the longer spacer. The observed short fluorescence lifetimes of these dyads, compared with that of their precursor fullerene derivative in THF and benzonitrile indicate that the charge separation takes place via the singlet excited state of the

C60-moiety, producing the ion pairs (C60 - -spacer-TTF+) as shown from the transient absorption spectra in the 800–1100 nm region. In polar benzonitrile solvent, the ion-pair state with the long flexible chain shows longer lifetime than that with the short chain, suggesting that weaker interaction between C60 and TTF moieties is preferred to the long ion-pair lifetime.

Ganguly et al.[76] described the method of synthesis and characterization of a novel organic dyad, 3-(1-Methoxy-3,4-dihydro-naphthalyn-2-yl-)-1-p-chlorophenyl propenone. Here they fabricate new hybrid nanocomposites by combining the organic dyad with different noble metals, semiconductor nanoparticle and noble metal semiconductor core/shell nanocomposites. In this organic dyad, donor part is 1-Methoxy-3, 4-dihydro-naphthalen- 2-carboxaldehyde with the acceptor p-chloroacetophenone. They have carried out steady state and time-resolved spectroscopic measurements on the dyad and its hybrid nanocomposite systems. Both from the theoretical predictions and NMR studies it reveals that in the ground state only extended (E-type or trans-type) conformation of the dyad exists whereas on photoexcitation these elongated conformers are converted into folded forms (Z- or cis-type) of the dyad, showing its photoswitchable character. Time resolved fluorescence spectroscopic (fluorescence lifetime by TCSPC method) measurements demonstrate that in chloroform medium all the organic–inorganic hybrid nanocomposites possess larger amount of extended conformers relative to folded ones, even in the excited singlet state. This indicates the possibility of slower energy destructive charge recombination rates relative to the rate processes associate with charge-separation within the dyad. This indicates the suitability to construct efficient light energy conversion devices especially with the Ag-dyad nanocomposites.

E. Rivera eet al.[77] were synthesized and characterized a series of pyrene-fullerene C60 dyad bearing pyrene units (PyFC12, PyFPy, Py2FC12 and PyFN) and studied their optical properties by absorption and fluorescence spectroscopy. Dyads were designed in this way because the pyrene moieties act as light-harvesting molecules and are able to produce “monomer” (PyFC12) or excimer emission (PyFPy, Py2FC12 and PyFN). The fluorescence spectra of the dyads exhibited a significant decrease in the amount of pyrene monomer and excimer emission, without the appearance of a new emission band due to fullerene C60. The pyrene fluorescence quenching was found to be almost quantitative, ranging between 96%–99% depending on the construct, which is an indication that energy transfer occurred from one of the excited pyrene species to the fullerene C_{60}.

J.H. Kim et al.[78] demonstrated that the photosensitive conjugated polymer with electron donor-acceptor dyad which contains a terthiophene unit, can modulate charge accumulation by photoirradiation resulting in a threshold voltage shift in the polymer field-effect transistors (PFETs) while this effect of the photoinactive polymer containing a thienothiophene unit is negligible. These results suggest that the feasible molecular design strategies can provide an effective platform to

achieve controllable threshold voltage modulation in PFETs.

Schuster et al.[79] investigated that the topological control of intramolecular electron transfer in donor-acceptor systems, a symmetrical parachute-shaped octaethylporphyrin-fullerene dyad has been synthesized. Charge separation in these hybrid systems occurs through space in unsymmetrical conformations, where the centre-to-centre distance between the component π-systems is minimized.

Ma et al.[80] designed and synthesized a cationic cyano-substituted p-phenylenevinylene derivative (PPTA), which can form supramolecular assemblies through electrostatic interaction with a type of polyelectrolyte material anionic guar gum (GP5A). A polyelectrolyte-based artificial light-harvesting system (LHS) was constructed by selecting a fluorescent dye sulforhodamine 101 (SR101) that matched its energy level as an energy acceptor. The energy harvested by the acceptors was used in the aqueous phase cross dehydrogenation coupling (CDC) reaction with a yield of up to 87%. In addition, the general applicability of polyelectrolyte materials to build artificial LHS was demonstrated by three other polyelectrolyte materials sodium polyphenylene sulfonate (RSS), sodium carboxymethyl cellulose (CMC), and sodium polyacrylate (PAAS), in which the CDC reaction was also carried out by these three LHSs and obtained high yields.

He et al.[81] used electrostatic assembly of polyanionic PSS with cationic bolaamphiphile (PRB) containing pyrene to achieve close stacking of pyrene, resulting in significantly enhanced excimer emission. Furthermore, the morphology of the assemblies changed from nanodisks to nanospheres. In particular, the quantum yield of the PRB with PSS increased from 0.5% to 23.1%. In contrast, the amphiphilic molecule containing pyrene with a single hydrophilic head also showed enhanced fluorescence after being co-assembled with PSS. Nevertheless, the fluorescence quantum yield of excimers was much lower than that of the co-assemblies formed with PRB. The assembly formed by PSS and PRB acted as an energy donor. It underwent Forster ¨ resonance energy transfer with Nile red, achieving high energy conversion efficiency (Φ_{ET} = 49.6%) and antenna effect (9.8) at a donor/acceptor molar ratio of 12.5:1.

Dey et al.[82] used a ruthenium-anthraquinone dyad consisting of the bi-imidazole spacer in which one imidazole proton acts as a hydrogen bonding agent to investigate the effects of H-bonding on both photo-induced electron transfer (PET) and proton-coupled electron transfer process (PCET). The present investigation has established that the arrangement of an intramolecular H-bond between the attached AQ and the imidazole proton consequences in a notable increase in the rate of intramolecular electron transfer from Ru(II) to AQ. Further, they have also demonstrated the ultrafast electron transfer and PCET dynamics in presence of water. They have successfully detected the transient absorption photoproduct Ru(III) by which we could determine the time constants of each step which is rare in literature. Most importantly, their study demonstrates electron transfer and

intra-molecular PCET dynamics in the femtosecond time domain. The results of the steady-state and transient absorption spectroscopic studies suggest that bi-imidazole spacer and water molecules have a significant role in both PET and PCET dynamics as a proton source in the excited state. They have demonstrated PCET reaction in ultrafast time scale using Ru-polypyridyl complex, with significant kinetic isotope effect.

Mozdbar et al.[83] investigated the impact of carbon quantum dots (CQDs) on the photocatalytic performance of TiO2 in aqueous medium under UV and visible light. CQDs were synthesized through a solvothermal procedure, and the effect of synthesis conditions on their optical properties were optimized. The CQDs/TiO2 nanocomposites were prepared via a hydrothermal method using CQDs with the extreme band-gaps (i.e. CQDs450 and CQDs550). The physicochemical properties of CQDs and CQDs/TiO2 samples were studied by various characterization techniques. The Diffuse Reflectance Spectroscopy (DRS) analysis revealed that incorporation of CQDs into nanocomposite samples causes a remarkable shift in absorption edge to the visible region, in comparison with pure TiO2. They proposed two different reaction mechanisms to explain the obtained results on CQDs/TiO2 samples, based on possible electron transfer between TiO2 and CQDs nanoparticles under UV and Visible lights.

Sinha et al.[84] used a hybrid approach at electrode and electrolyte systems to fabricate a high-energy density supercapacitor. Hybrid nanocomposite electrodes were fabricated using a facile hydrothermal synthesis. The kinetics were studied by preparing in-situ and ex-situ nanocomposites. The in-situ preparation delivers a homogeneous flower petal-like interconnected porous morphology with an appreciable BET surface area of 97 m2 g− 1 . The actual electrochemical performance was analyzed by accounting for discharge area instead of discharge time to avoid discrepancies related to hybrid energy storage systems. The three-electrode measurement suggests that the electrode delivers an excellent specific capacitance of 3802 F g− 1 at 1 A g− 1 .However, upon adding 0.02 M KI as redox mediators in a traditional electrolyte (6 M KOH), a ~37% increase in specific capacitance is achieved without the degradation in the device stability. The nanocomposite also showed excellent compatibility in a flexible device assembly, delivering a specific capacitance of 192 mF cm− 1 at 1 mA cm− 1 without deteriorating its performance upon different bending angles. Through this study they claimed the design of a low-cost, environmentally benign, and facile approach for developing a high-performance hybrid supercapacitor.

Wang et al.[85] found that the supercapacitor performance of graphene quantum dots (GQDs)at MnO_2 composite is superior to that of pure MnO_2 electrode. The GQDs at MnO_2 composite is obtained by a highly efficient one-step hydrothermal method, in which $KMnO_4$ reacts with graphene oxide to produce MnO_2 nanosheets anchored with GQDs in a short time. The also got the excellent supercapacitor performance of GQDs at MnO2 composite results from its enhanced electrical

conductivity, good wettability and abundant available contact sites for aqueous electrolyte, which are ascribed to the intrinsic high electrical conductivity as well as the quantum confinement and edge effects of GQDs.

Rangaraj et al.[86] used carbon quantum dots (CQDs) in a strategic approach to obtain pristine mesoporous Zn_2SnO_4 (ZTO) and enhanced photodegradation of methylene blue (MB) dye. The Zn_2SnO_4/carbon quantum dots (ZTO/C) were hydrothermally prepared using mineralizer, Na2CO3 and quantified amount of sugarcane juice. The mesoporous nature and high surface area of ZTO and ZTO/C was revealed from Brunauer, Emmett and Teller (BET). The close overlapping of CQD with ZTO was evident from the HRTEM and Raman spectra. The MB dye degradation study employing ZTO and ZTO/C catalyst under direct sunlight irradiation showed 84 % and 95 % degradation in 150 min respectively. The presence of CQDs in ZTO/C nanocomposites enhanced the transportation of photoinduced electrons at the interface between ZTO and CQDs, whereas holes stayed in the valence band of ZTO, suppressing the recombination of photogenerated charge carriers during photocatalysis. This study reveals that ZTO/C is a possible candidate for sunlight-driven photocatalysis and environmental remediation.

Raikwar et al.[87] used carbon quantum dots synthesized by using aloe vera biomass by facile carbonization process. The aqueous solution of carbon quantum dots (CQDs) showed blue light emission upon excitation by 365 nm ultraviolet radiation. The field effect scanning electron microscopy images showed CQDs as spherical quantum dots of the size around 10 nm. The transmission electron microscopy (TEM) bright field images confirmed the size of the CQDs. The CQDs thus prepared can be used for bioimaging of plant cells and as ink for security printing applications. A CQD@LaPO4:Eu^{3+} nanocomposite has been prepared and its photoluminescence property has been studied. The increased photoluminescence intensity of composite attributed to Forster ¨ Resonance Energy Transfer (FRET) from CQDs to Eu^{3+}.

Liu et al.[88] summarized the basic knowledge on CQDs and GQDs before focussing on their application to sensing thus far followed by a discussion of future directions for research into CQDs and GQD-based nanomaterials in sensing are discussed. With regard to the latter, the authors suggested that with the potential of these nanomaterials in sensing more research is needed on understanding their optical properties and why the synthetic methods influence their properties so much, into methods of surface functionalization that provide greater selectivity in sensing and into new sensing concepts that utilise the virtues of these nanomaterials to give us new or better sensors that could not be achieve in other ways.

Hsiao et al.[89] used novel one-step thermal treatment to synthesize N-doped GQD. Citric acid and urea ratios were varied to synthesize N-doped GQD with different

N-doping extents and electrical conductivities. CB and GQD mixtures, GQD and CB are used as conductive agent for fabricating SC electrodes. Activated carbon electrode with CB and GQD mixture showed the highest specific capacitance (CF) of 241.4 F/g at 20 mV/s, while electrodes without conductive agent and with CB conductive agent respectively showed CF of 41.5 and 108.6 F/g, due to more functional groups, defects, hydrophilic sites and electrochemical surface area of the former case. Symmetric SC with CB and GQD showed a maximum energy density of 10.54 Wh/kg at 550 W/kg, and CF retention of 85% and Coulombic efficiency of 80% after 5000 charging/discharging cycles. That provided them a N-doped graphene quantum dot which can be used as conductive agent for carbon-based supercapacitors.

Sikiru et al.[90] examined the advancement of CQDs in energy conversion applications, supercapacitors, solar cell applications, and electrocatalysis with their synthesis approach. Carbon nanomaterials such as carbon quantum Dots (CQDs) and graphene quantum dots (GQDs) have been attracting a great deal of attention recently due to their unique properties in terms of electrical conductivity, thermal stability, mechanical strength, chemical resistance, photoluminescence, low cost, and facile surface functionalization. By virtue of their rapid electron transfer and large surface area, CQDs and GQDs are desirable in these electrochemical applications. Carbon nanomaterials are widely used in various applications, including semiconductors, photovoltaic energy storage, biomedicals, drug delivery, environmental sectors, supercapacitors, electrocatalysis, and energy conversion applications. However, energy storage and conversion techniques are developing rapidly as new promising approaches emerge to solve some of the unprecedented challenges in energy at a low cost and with a low environmental footprint.

References

1. Wikimedia Foundation. 2022. Energy. Wikipedia. https://en.wikipedia.org/wiki/Energy
2. C. Ngo and J. B. Natowitz, "Our energy future – resources, alternative and the environment", Wiley, 1, 2009.
3. Vaclav Smil, "Energy in World History", Routledge, 1994.
4. Learn with Kassia https://mskuksclass.weebly.com/lesson-2-forms-of-energy.html
5. Unacademy, "Energy" https://unacademy.com/content/kerala-psc/study-material/science-technology/energy/
6. N.S. Lewis and D.G. Nocera, "Powering the planet: Chemical challenges in solar energy utilization", Proc.Natl.Acad Sci. U.S.A, 103, 15729, 2006.
7. World Energy Balances. https://www.iea.org/reports/world-energy-balances-overview/world
8. Wikimedia Foundation. 2022. Energy in India. Wikipedia. https://en.wikipedia.org/wiki/Energy_in_India
9. Wikimedia Foundation. 2022. World energy supply and consumption. Wikipedia. https://en.wikipedia.org/wiki/World_energy_supply_and_consumption
10. Central Electricity Authority (CEA) https://powermin.gov.in/en/content/power-sector-glance-all-india
11. ADT Solar " The guide to renewable vs. non-renewable energy sources " https://www.adtsolar.com/renewable-energy/renewable-vs-non-renewable-energy-sources/
12. E.A. Rohlfing, W.J. Stevens, M.E. Gress, "Project of Chemical Sciences, Geosciences and Bio-sciences", 2003.
13. Gopa Dutta Pal, Somnath Paul, Munmun Bardhan, Asish De and Tapan Ganguly. Designing of an artificial light energy converter in the form of short-chain dyad when combined with core-shell gold/silver nanocomposites. Spectrochimica Acta Part A: Molecular and Biomolecular Spectroscopy. (2017). 180:168-174. https://doi.org/10.1016/j.saa.2017.03.015
14. G.M. Whitesides, "The right size in nanobiotechnology", Nat. Biotechnol, 21, 1161, 2003
15. J. Pan, G. Benkö, Y. Xu, T. Pascher, L. Sun, V. Sundström, T. Polivka, "Photoinduced electron transfer between a carotenoid and TiO2 Nanoparticle", J. Am. Chem. Soc, 124, 13949, 2002.
16. V. Balzani, P. Seroni, A. Juris, "Photochemistry and Photophysics: Concepts, Research, Applications", Wiley-VCH, 2014.
17. St. Pius X College. 2022. Photochemistry. http://stpius.ac.in/crm/assets/download/Photochemistry.pdf (Accessed 28.05.2022)
18. EDINBURGH INSTRUMENTS " What is a Jablonski Diagram (Perrin-Jablonski Diagram)? " https://www.edinst.com/in/blog/jablonski-diagram/

19. Wikimedia Foundation. 2022. Photochemistry. Wikipedia. https://en.wikipedia.org/wiki/Photochemistry (Accessed 28.05.2022)
20. Newport " Light-Matter Interactions in Lasers " https://www.newport.com/n/laser-light-matter-interactions
21. Wikimedia Foundation. 2021.Frank-Condon-Principle. Wikipedia. https://en.wikipedia.org/wiki/Frank-Condon_Principle (Accessed 28.05.2022)
22. M. Julliard, M. Chanon, "Photoelectron transfer catalysis: its connection with the thermal and electrochemical analogues", Chem. Rev., 83, 425, 1983.
23. Sudeshna Bhattacharya, MunmunBardhan, Avijit Kumar De, Asish De, Tapan Ganguly. Photoinduced electron transfer within a novel synthesized short-chain dyad. Journal of Luminescence 130 (2010) 1238–1247. doi:10.1016/j.jlumin.2010.02.032
24. H.P. Boehm, R. Setton and E. Stumpp, "Nomenclature and terminology of graphite"
25. Md. Sajibul Alam, Md. Nizam Uddin, Md. Maksudul Islam, Ms. Bipasha & Sayed Shafayat Hossain. Synthesis of graphene. Crossmark. Int Nano Lett 6, 65–83 (2016). DOI 10.1007/s40089-015-0176-1
26. Elham F. Mohamed Nanotechnology: Future of Environmental Air Pollution Control Environmental Management and Sustainable Development ISSN 2164-7682 2017, Vol. 6, No. 2 doi:10.5296/emsd.v6i2.12047
27. PubChem, National Library of Medicine. https://pubchem.ncbi.nlm.nih.gov/compound/Graphene-quantum-dot
28. Graphene Quantum Dot. https://en.m.wikipedia.org/wiki/Graphene_quantum_dot
29. Chunfang Zhang, Yanyan Cui, Li Song, Xiangfeng Liun , Zhongbo Hun Microwave assisted one-pot synthesis of graphene quantum dots as highly sensitive fluorescent probes for detection of iron ions and pH value Talanta Volume 150, 1 April 2016, Pages 54-60. DOI: https://doi.org/10.1016/j.talanta.2015.12.015
30. H.P. Boehm, R. Setton and E. Stumpp, "Nomenclature and terminology of graphite intercalation compounds", Pure & Appl. Chem., 66, 1893, 1994.
31. M.J. McAllister, J.L. Li, D.H. Adamson, H.C. Schniepp, A.A. Abdala, J.Liu, M.H. Alonso, D.L. Milius, R. Car, R.K. Prud'homme and I.A. Aksay, "Single sheet functionalized graphene by oxidation and thermal expansion of graphite", J. Am. Chem. Soc., 19, 4396, 2007.
32. C.H. Chuang, Y.F. Wang, Y.C. Shao, Y.C.Yeh, D.Y. Wang, C.W. Chen, J.W. Chiou, S.C. Ray, W.F. Pong, L.Zhang, J.F.Jhu and J.H. Guo, "The effect of thermal reduction on the photoluminescence and electronic structures of graphene oxides", Sci. Rep., 4, 4525, 2014.
33. Peter M. Martin, "Handbook of Deposition Technologies for Films and Coatings", 3rd Edition, Elsevier, 2010

34. Advanced Materials ’93, IIA: Biomaterials, Organic and Intelligent Materials. https//doi.org/10.1016/C2013-1-15211-2
35. W. Lv, D.M. Tang, Y.B. He, C.H. You, Z.Q. Shi, X.C. Chen, C.M. Chen, P.X. Hou, C. Liu and Q.H. Yang, “Low-temperature exfoliated graphenes: vacuum-promoted exfoliation and electrochemical energy storage”, ACS Nano., 3, 3730, 2009.
36. D. Li, M.B. Muller, S. Gilje, R.B. Kaner and G.G. Wallace, “Processable aqueous dispersions of graphene nanosheets”, Nat. Nanotechnol., 3, 101, 2008.
37. Alam, S. , Sharma, N. and Kumar, L. (2017) Synthesis of Graphene Oxide (GO) by Modified Hummers Method and Its Thermal Reduction to Obtain Reduced Graphene Oxide (RGO)*. Graphene, 6, 1-18. Doi: 10.4236/graphene.2017.61001.
38. Adere Tarekegne Habte, Delele Worku Ayele, “Synthesis and Characterization of Reduced Graphene Oxide (RGO) Started from Graphene Oxide (GO) Using the Tour Method with Different Parameters”, Advances in Materials Science and Engineering, vol. 2019, Article ID 5058163, 9 pages, 2019. https://doi.org/10.1155/2019/5058163
39. Liu Fenghua, Lifeng Zhang, Lijian Wang, Binyuan Zhao, Weiping Wu Graphene Oxide for Electronics In book: Oxide Electronics (pp.1-19), April 2021, DOI: http://dx.doi.org/10.1002/9781119529538.ch1
40. Zhao, C., Song, X., Liu, Y. et al. Synthesis of graphene quantum dots and their applications in drug delivery. J Nanobiotechnol 18, 142 (2020). https://doi.org/10.1186/s12951-020-00698-z
41. Gity Behbudi, Mini review of Graphene Oxide for medical detection and applications, September 2020. DOI:10.47277/AANBT/1(3)66
42. S. Bhattacharya, T.K. Pradhan, A. De, S.R. Choudhury, A.K. De and T. Ganguly, “Photophysical processes involved within the anisole-thioindoxyl dyad system”, J. Phys. Chem. A, 110, 5665, 2006.
43. Feifan Wang, Qi Li, and Dongsheng Xu. Recent Progress in Semiconductor-Based Nanocomposite Photocatalysts for Solar-to-Chemical Energy Conversion. Advanced Energy Material.(2017), 7, 1700529, DOI: 10.1002/aenm.201700529
44. P. Mondal, T. Misra, A.De, S. Ghosh, S.R. Choudhury, J. Chowdhury and T. Ganguly, “Phtophysical processes involved within the bichromophoric system 9-benzotriazole-1-ylmethyl-9H-carbazole and its role as an artificial photosynthetic device”, Spectrochim Acta Part A, 66, 534, 2007.
45. Amrita Chakraborty, TapanGanguly.Developments of novel nanomaterials by combining shortchain dyad with semiconductor nanoparticles. Optics: Phenomena, Materials, Devices, and Characterization. American Institute of Physics. AIP Conf. Proc. 1391, 31-32 (2011)doi: 10.1063/1.3646772
46. T.Asahi, M. Ohkohchi, R. Matsusaka, N. Mataga, R.P. Zhang, A. Osuka and K. Maruyama, “Intramolecular photoinduced charge separation and charge recombination of the product ion pair states of a series of fixed-distance dyads of porphyrins and quinones: energy gap and temperature

dependences of the rate constants", J. Am. Chem. Soc., 115, 5665, 1993.
47. M. Bardhan, T. Misra, J. Chowdhury and T. Ganguly, "Comparative studies by using spectroscopic tools on the charge transfer (CT) band of a novel synthesized short-chain dyad in isotropic media and in a gel (P123)", Chem. Phys. Lett., 481, 142, 2009.
48. S. Bhattacharya, J. Chowdhury and T. Ganguly, "Nature of charge separation and recombination processes within an organic dyad having short spacer", J. Lumin., 130, 1924, 2010
49. M.A. Loi, P. Denk, H. Hoppe, H. Neugebauer, C. Winder, D. Meissner, C. Brabee, N.S. Sariciftci, A. Gouloumis, P. Vazquez and T. Torres,"Long lived photoindused charge separation for solar cell applications in phthalocyanine-fulleropyrrolidine dyad thin films", J. Mater. Chem., 13, 700, 2003.
50. G. Mondal, S. Bhattacharya, S. Das and T. Ganguly, "The rates of charge separation and energy destructive charge recombination processes within an organic dyad in presence of metal-semiconductor core shell nanocomposites", J. Nanosci Nanotechnol., 12, 187, 2012.
51. Gopa Dutta (Pal), Abhijit Paul, Somnath Yadav, MunmunBardhan, Asish De, Joydeep Chowdhury, Aindrila Jana, and TapanGanguly. Time Resolved Spectroscopic Studies on a Novel Synthesized Photo-Switchable Organic Dyad and Its Nanocomposite Form in Order to Develop Light Energy Conversion Devices. Journal of Nanoscience and Nanotechnology Vol. 15, 5775–5784, (2015). doi:10.1166/jnn.2015.10290
52. G. Dutta, P. Chakraborty, S. Yadav, A De, M. Bardhan, P. Kumbhakar, S. Biswas, H.S. DeSarkar and T. Ganguly, "Time resolved spectroscopic investigations to compare the photophysical properties of a short-chain dyad when combined with silver and gold nanoparticles to form nanocomposite systems", J. Nanosci Nanotechnol., 16, 7411, 2016.
53. Sudeshna Bhattacharya, Joydeep Chowdhury, Tapan Ganguly. Nature of charge separation and recombination processes within an organic dyad having short spacer. Journal of Luminescence 130 (2010) 1924–1934. doi: 10.1016/j.jlumin.2010.05.007
54. Sudeshna Bhattacharya, Gopa Mandal, Mrinal Dutta, Durga Basak, and Tapan Ganguly. Is Dye Mixture More Suitable Rather Than Single Dye to Fabricate Dye Sensitized Solar Cell?. Journal of Nanoscience and Nanotechnology Vol. 11, 1–9, (2011). doi:10.1166/jnn.2011.5115
55. Somnath Paul, Ishani Mitra, Rituparna Dutta, MunmunBardhan, Mridul Bose, Subrata Das, MithuSaha, and Tapan Ganguly. Comparative Analysis to Explore the Suitability of a Short Chain Dyad in Its Pristine and Nanocomposite Forms for Designing Artificial Light Energy Conversion Device. Journal of Nanoscience and Nanotechnology Vol. 18, 1–9, (2018). doi:10.1166/jnn.2018.15533
56. I. Mitra , S. Paulb, M. Bardhanc, S. Dasd, M. Sahae, A. Sahaf, T. Ganguly. Effects of carbon quantum dots (CQD) on the energy storage capacity of a novel synthesized short- chain dyad. Chemical Physics Letters 726 (2019)

1–6. https://doi.org/10.1016/j.cplett.2019.04.025
57. DEVENS GUST, THOMAS A. MOORE, AND ANA L. MOORE. Mimicking Photosynthetic Solar Energy Transduction. Acc. Chem. Res. (2001), 34, 40-48
58. Carlo Andrea Rozzi, Sarah Maria Falke, Nicola Spallanzani, Angel Rubio, Elisa Molinari, Daniele Brida, Margherita Maiuri, Giulio Cerullo, Heiko Schramm, Jens Christoffers& Christoph Lienau. Quantum coherence controls the charge separation in a prototypical artificial light-harvesting system. NATURE COMMUNICATIONS. (2013). 4:1602. DOI: 10.1038/ncomms2603
59. Tapasi Sen, Sreyashi Jana, SubratanathKoner and Amitava Patra. Energy Transfer between Confined Dye and Surface Attached Au Nanoparticles of Mesoporous Silica. J. Phys. Chem. C 2010, 114, 707–714
60. Marlon Bhorja& Prabir K. Dutta. Storage of light energy by photoelectron transfer acress a sensitized zeolite-solution interface. Letters to nature. Vol 362 (1993)
61. Qifeng Zhang, Evan Uchaker, Stephanie L. Candelariaz and Guozhong Cao. Nanomaterials for energy conversion and storage. Chem. Soc. Rev., (2013), 42, 3127—3171. DOI: 10.1039/c3cs00009e
62. Palani Balaya. Size effects and nanostructured materials for energy applications. Energy Environ. Sci., (2008), 1, 645–654. DOI: 10.1039/b809078p
63. P.P. Edwards, V.L. Kuznetsov, W.I.F. David, N.P. Brandon. Hydrogen and fuel cells: Towards a sustainable energy future. Energy Policy 36 (2008) 4356–4362.
64. Iain McConnell, Gonghu Li, and Gary W. Brudvig. Energy Conversion in Natural and Artificial Photosynthesis. Chemistry & Biology 17, May 28, (2010). DOI 10.1016/j.chembiol.2010.05.005
65. Susie Eustis and Mostafa A. El-Sayed. Why gold nanoparticles are more precious than pretty gold: Noble metal surface plasmon resonance and its enhancement of the radiative and nonradiative properties of nanocrystals of different shapes. Chem. Soc. Rev., (2006), 35, 209–217. DOI: 10.1039/b514191e
66. A Chakraborty, S Chakraborty and T Ganguly. Photoisomerization within a novel synthesized photoswitchable dyad: experimental and theoretical approaches. Indian J Phys (2013). DOI 10.1007/s12648-013-0344-y
67. Gopa Mandal, Amrita Chakraborty, Ujjal Kumar Sur, BalaprasadAnkamwar, Asish De and TapanGanguly. Synthesis, Characterization, Photophysical Properties of a Novel Organic Photoswitchable Dyad in Its Pristine and Hybrid Nanocomposite Forms. J. Nanosci. Nanotechnol. (2012), Vol. 12, No. 6
68. Somnath Paul, Ishani Mitra, Rituparna Dutta, MunmunBardhan, Mridul Bose, Subrata Das, MithuSaha and TapanGanguly. Comparative Analysis to Explore the Suitability of a Short Chain Dyad in Its Pristine and Nanocomposite Forms for Designing Artificial Light Energy Conversion

Device. J. Nanosci. Nanotechnol. (2018), Vol. 18, No. 11
69. A.G. Olabi, Mohammad Ali Abdelkareem, Tabbi Wilberforce, Enas Taha Sayed. Application of graphene in energy storage device – A review. Renewable and Sustainable Energy Reviews 135 (2021) 110026
70. Park, S.-H., Kim, H.-K., Yoon, S.-B., Lee, C.-W., Ahn, D., Lee, S.-I., … Kim, K.-B.(2015). Spray-Assisted Deep-Frying Process for the In Situ Spherical Assembly of Graphene for Energy-Storage Devices. Chemistry of Materials, 27(2), 457–465. doi:10.1021/cm50342
71. T.Asahi, M. Ohkohchi, R. Matsusaka, N. Mataga, R.P. Zhang, A. Osuka and K. Maruyama, "Intramolecular photoinduced charge separation and charge recombination of the product ion pair states of a series of fixed-distance dyads of porphyrins and quinones: energy gap and temperature dependences of the rate constants", J. Am. Chem. Soc., 115, 5665, 1993.
72. H. Imahori, H.E. El-Khouly, M. Fujitsuka, O. Ito, Y. Sakata and S. Fukuzumi, "Solvent dependence of charge separation and charge recombination rates in porphyrin-fullerene dyad", J. Phys. Chem. A, 105, 325, 2001.
73. H. Imahori, K. Tamaki, D.M. Guldi, C. Luo, M. Fujitsuka, O. Ito, Y. Sakata and S. Fukuzumi, "Modulating charge separation and charge recombination dynamics in porphyrin-fullerene linked dyads and triads: marcus-normal versus inverted region", J. Am. Chem. Soc., 123, 2607, 2001.
74. M Maiti, T Misra, T Bhattacharya, C Basu (nee Deb), A De, S K Sarkar,T Ganguly, "Comparative studies on inter- and intramolecular electron transfer processes within 4-methoxybenzo[b]thiophene (4MBT) and p-chloroacetophenone (PCA) reacting systems by using steady-state and laser flash photolysis techniques ", J. Photochem. Photobiol. A: Chem., 152, 41, 2002.
75. E. Allard, J. Cousseau, J. Orduna, J. Garin, H. Luo, Y. Araki and O. Ito, "Photoinduced electron-transfer processes in C60 tetrathiafulvalene dyads containing a short or long flexible spacer", Phys. Chem. Chem. Phys., 4, 5944, 2002.
76. G. Mondal, A. Chakraborty, U.K. Sur, B. Ankamwar, A. De and T. Ganguly, "Synthesis, characterization, photophysical properties of a novel organic photoswitchable dyad in its pristine and hybrid nanocomposite forms", J. Nanosci Nanotechnol., 12, 4591, 2012.
77. G.Z. Galan, J.O. Palacios, B.X. Valderrama, A.A.C. Davila, D.C. Flores, V.H.R. Sanchez and E. Rivera, "Pyrene-fullerene C60 dyads as light-harvesting antennas", Molecules, 19, 352, 2014.
78. J. Kim, J.E. Kwom, A.A. Boampong, J.H. Lee, M.H. Kim, S.Y. Park, T.D. Kim and J.H. Kim, "Threshold voltage modulation of polymer transistors by photoinduced charge–transfer between donor–acceptor dyads", Dyes Pigm., 142, 387, 2017.
79. David I. Schuster, Peng Cheng, Peter D. Jarowski, Dirk M. Guldi, Chuping Luo, Luis Echegoyen, SoomiPyo, Alfred R. Holzwarth, Silvia E. Braslavsky, Rene´ M. Williams and Gudrun Klihm. Design, Synthesis, and

Photophysical Studies of a Porphyrin-Fullerene Dyad with Parachute Topology; Charge Recombination in the Marcus Inverted Region. J. AM. CHEM. SOC. (2004), 126, 7257-7270

80. Chao-Qun Ma , Ning Han , Rong-Zhen Zhang, Ying Wang, Rui-Zhi Dong, Hui Liu, Rong-Zhou Wang, Shengsheng Yua , Yue-Bo Wang, Ling-Bao Xing Construction of artificial light-harvesting systems based on a variety of polyelectrolyte materials and application in photocatalysis Journal of Colloid and Interface Science Volume 634, 15 March 2023, Pages 54-62. DOI: https://doi.org/10.1016/j.jcis.2022.11.156
81. Xiongfei He, Shensong Zhang, Shuang Qi, Pan Xu, Bin Dong, Bo Song Enhanced excimer fluorescence emission of pyrene derivatives: Applications in artificial light-harvesting systems Dyes and Pigments Volume 209, Part B, February 2023, 110933. DOI: https://doi.org/10.1016/j.dyepig.2022.110933
82. Ananta Dey, Nandan Ghorai, Amitava Das, Hirendra N. Ghosh Effects of hydrogen bonding on intramolecular/intermolecular proton-coupled electron transfer using a Ruthenium-anthraquinone dyad in ultrafast time domain Journal of Photochemistry & Photobiology A: Chemistry, Volume 441, 1 July 2023, 114709. DOI: https://doi.org/10.1016/j.jphotochem.2023.114709
83. Afsaneh Mozdbar, Amideddin Nouralishahi, Shohreh Fatemi, Fatemeh Sadat Talatori The impact of Carbon Quantum Dots (CQDs) on the photocatalytic activity of TiO2 under UV and visible light Journal of Water Process Engineering, Volume 51, February 2023, 103465. DOI: https://doi.org/10.1016/j.jwpe.2022.103465
84. Prerna Sinha, Kamal K. Kar Enhanced performance with ionic and organic redox-couple electrolytes on MTMO anchored CQD nanocomposites and renewable carbon-based asymmetric flexible supercapacitor Applied Materials Today, Volume 32, June 2023, 101806. DOI: https://doi.org/10.1016/j.apmt.2023.101806
85. Yangjun Zhu, Zijie Huang, Xinyue Huang, Yipei Li, Huiqin Li, Binghua Zhou, Jian Liu, Keng Xu, Mingxi Wang, Hironori Ogata, Gan Jet Hong Melvin, Josue Ortiz-Medina, Wei Gong, Zubiao Wen, Mauricio Terronesj, Morinobu Endo, Zhipeng Wang One-step hydrothermal synthesis of manganese oxide nanosheets with graphene quantum dots for high-performance supercapacitors Journal of Energy Storage, Volume 62, June 2023, 106948. DOI: https://doi.org/10.1016/j.est.2023.106948
86. Preethi G, R. Pillai, Balan Ramdas, S. Ramamoorthy, Balu Patil, I.C. Lekshmi, P. Mohan Kumar, Lingappa Rangaraj Diamond and Related Materials, Volume 131, January 2023, 109554. DOI: https://doi.org/10.1016/j.diamond.2022.109554
87. V.R. Raikwar Synthesis and study of carbon quantum dots (CQDs) for enhancement of luminescence intensity of CQD@LaPO4:Eu^{3+} nanocomposite Materials Chemistry and Physics, Volume 275, 1 January 2022, 125277. DOI: https://doi.org/10.1016/j.matchemphys.2021.125277
88. Meixiu Li, Tao Chen, John Justin Gooding, Jingquan Liu A Review of

Carbon and Graphene Quantum Dots for Sensing ACS SENSORS, 03 Jul 2019. DOI: 10.1021/acssensors.9b00514
89. Yu-Cheng Hsiao, Jau-Lian Hung, Subbiramaniyan Kubendhiran, Sibidou Yougbare, Lu-Yin Lin, Yung-Fu Wu Novel synthesis of N-doped graphene quantum dot as conductive agent for carbon based supercapacitors Journal of Energy Storage, Volume 56, Part A, 1 December 2022, 105902. DOI: https://doi.org/10.1016/j.est.2022.105902
90. Surajudeen Sikiru, Temidayo Lekan Oladosu, Sanusi Yekinni Kolawole, Lawal Adeyemi Mubarak, Hassan Soleimani, Lukmon Owolabi Afolabi, Afolabi-Owolabi Oluwafunke Toyin Advance and prospect of carbon quantum dots synthesis for energy conversion and storage application: A comprehensive review Journal of Energy Storage, Volume 60, April 2023, 106556. DOI: https://doi.org/10.1016/j.est.2022.106556

Chapter: 2

Materials and Experimental Methodology

- ✓ **Materials**
- ✓ **Experimental Methodology**
  - ❖ **HRTEM**
  - ❖ **UV-Vis Spectroscopy**
  - ❖ **Fluorescence Spectroscopy**
  - ❖ **NMR Spectroscopy**
  - ❖ **TCSPC**
  - ❖ **Transient Absorption Spectral Analysis**
- ✓ **References**

1. Materials

The solvents acetonitrile (ACN) (SRL) and cyclohexane (CH) of spectroscopic grade (purchased from Sigma-Aldrich) are purified following the standard procedures and tested before use for the absence of any impurity emission in the concerned wavelength region. Water is deionized using a Millipore Milli-Q system. The primary experimental solutions were made by dissolving the necessary amount of dyad, ACN, and CH.

1.1. Synthesis and Characterization of the Novel short-chain dyad (NNDMBF)

Figure 2.1. depicts the investigated dyad synthesis technique. 2-amino fluorene was produced during the method. In a round bottle flask, 7 mL of anhydrous ethanol was added to a combination of 1.5 mmol 2- aminofluorene and 1.5 mmol 4-(dimethylamino) benzaldehyde. The reaction mixture was stirred for 2 hours at room temperature. The solvent was removed under high vacuum after the reaction was completed (monitored by thin layer chromatography, TLC), and the crude reaction mass was washed several times with hexane to obtain the pure product, which is the dyad €-4-((9H-fluorene-2-yl)imino)methyl)-N,N-dimethylaniline (Compound 5)[1].

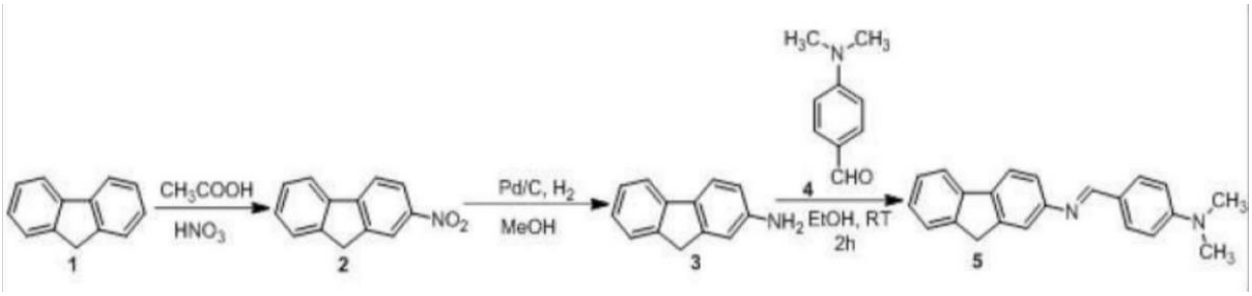

Figure 2.1. Synthesis procedure of NNDMBF dyad[1]

On a Bruker AVIII- 500, 1H and 13C NMR spectra (Figures 2.2.-2.3.) were acquired. Chemical changes were measured in parts per million (ppm). In Hertz, coupling constants (J values) were reported. The chemical shifts of 1H NMR were compared to CDCl3. The chemical shifts of 13C NMR were compared to CDCl3.

Value: 1H NMR (500MHz, CDCl3): δ =2.90 (s, 6H), 3.81 (s, 2H), 6.62 (d, 2H, J = 8.5Hz), 7.13-7.18 (m, 2H), 7.24-7.28 (m, 2H), 7.41 (d, 1H, J = 7.5 Hz), 7.64-7.69 (m, 4H), 8.31 (s, 1H). 13C NMR (125 MHz, CDCl3): δ = 36.9, 40.2, 111.6, 117.5, 119.5, 120.2, 120.3, 124.5, 125.0, 126.2, 126.8, 130.4, 138.9, 141.6, 144.4, 151.9, 152.4, 159.6[1].

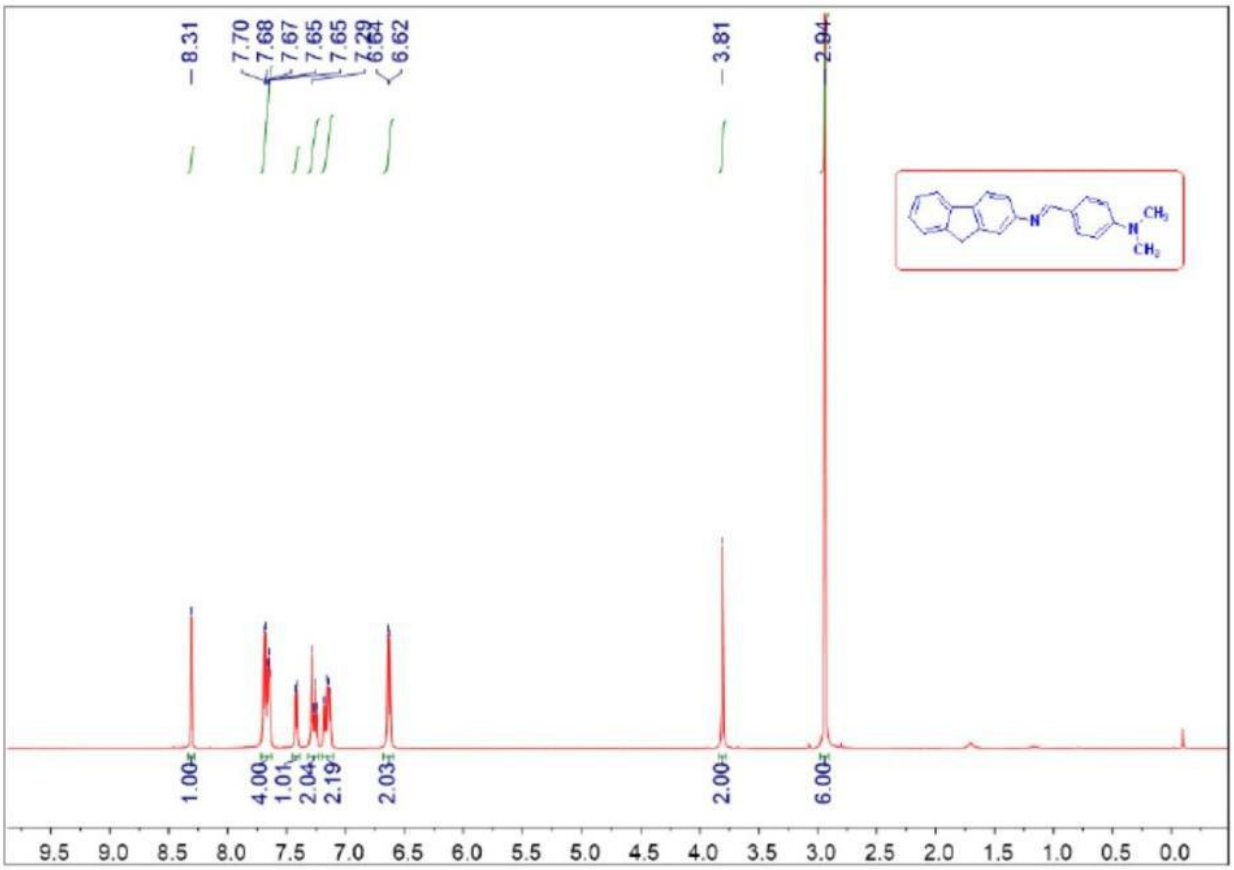

Figure 2.2. 1H NMR of (E)-4-(((9H-fluorene-2-yl)imino)methyl)-N,N-dimethylaniline[1]

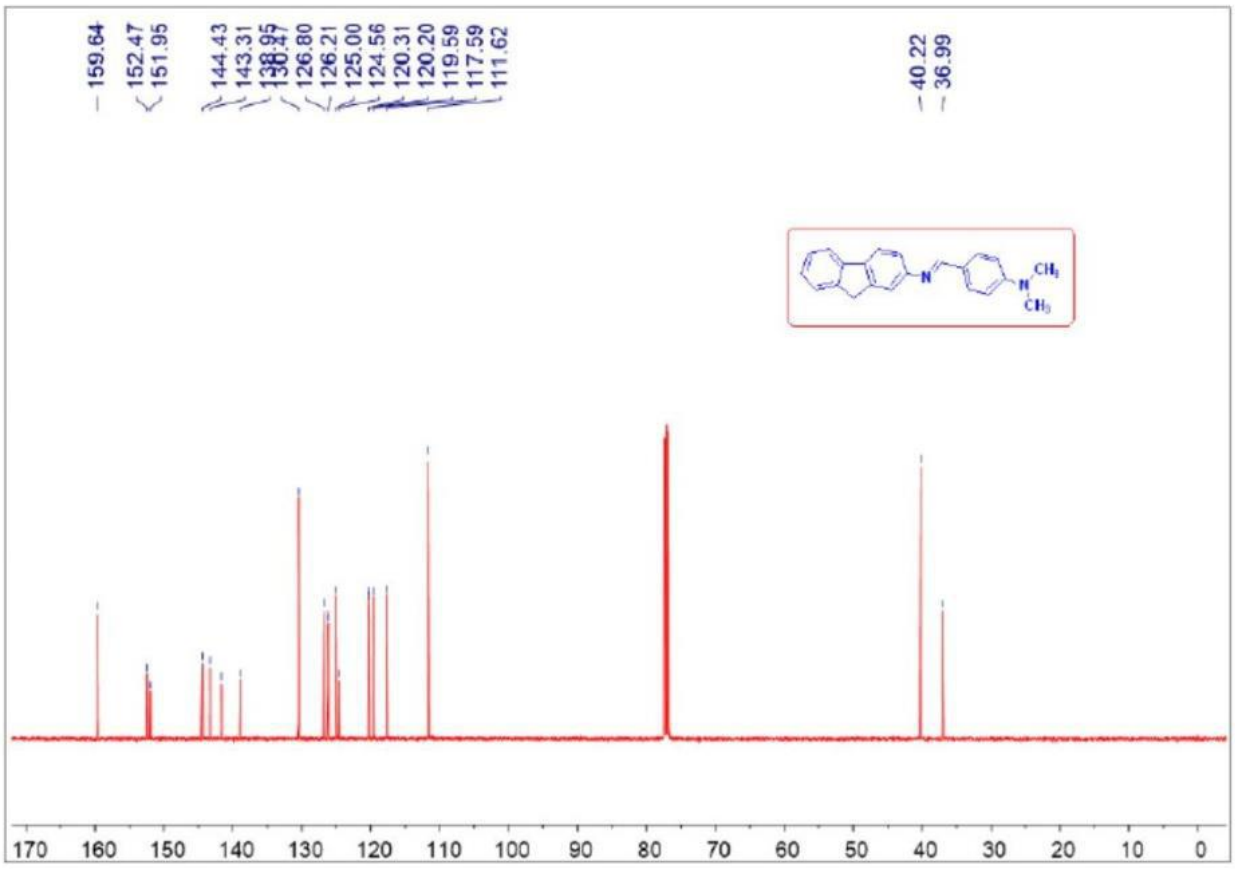

Figure 2.3. 13C NMR of (E)-4-(((9H-fluorene-2-yl)imino)methyl)-N,N-dimethylaniline[1]

The astounding possibility of two conformers: Trans and Cis (Figure 2.4.) of our dyad can be inferred from the molecular structure of the dyad. Because the N atom has no proton, coupling constant values from NMR cannot be used to forecast the dyad's potential ground state conformation. Theoretical simulations on the ground state optimal geometry of the dyad NNDMBF utilizing the BL-LYP/6- 311g (d,p) level of theory on HOMO–LUMO surfaces reveal that there may be two types of conformers, Cis- and Trans-, with the latter being more stable in the ground state. As a result of the preceding theoretical expectations, both cis and trans forms of the dyad exist in the ground state, with the latter predominating[1].

Figure 2.4. Trans & Cis conformers of dyad[1]

The electron donor 4(N,N-dimethylamine)benzaldehyde (NNDMB) is coupled to the acceptor fluorene(F)[1] by a short chain in a novel short-chain dyad (NNDMBF) (Figure 2.5.).

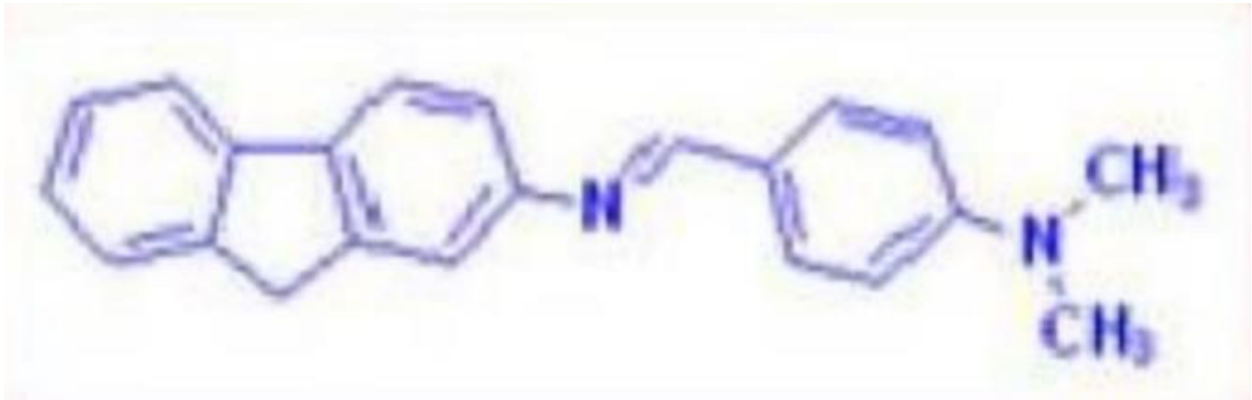

Figure 2.5. Novel short-chain dyad (NNDMBF)[1]

1.2. Graphene Quantum Dots (GQD) Synthesis

Citric acid is pyrolyzed to make graphene quantum dots (GQD). After heating and melting five grammes of citric acid, it turned a dark orange color in 25–30 minutes. At room temperature, a 1.5 M solution of NaOH was added dropwise to a melting thick solution of citric acid[2].

1.3. Graphene Oxide (GO) Synthesis

GO Synthesis: GO can be produced using a modified Hummer's method[3]. In this process, 2 gm of graphite powder was combined with 1 gm of $NaNO_3$ in an ice bath. Now, 130 mL of concentrated H_2SO_4 was added to the mixture while swirling it. 6 gm of $KMnO_4$ was gently added under vigorous stirring conditions, keeping the reaction temperature of the mixture around 200^0C. The reaction temperature gradually increased to 400^0C, and the mixture was stirred for 6 hours. The color of the combination shifts from dark grey to greyish green at this point. An additional 6 gm of $KMnO_4$ were added to the mixture and stirred for another 6 h so that the color of the mixture becomes grayish brown. Now, 250 ml of triple distilled water was slowly added to the solution which raises the temperature of the solution to around 960 C at which the mixture was stirred for 30 min. The solution was then cooled down to room temperature. Now, an additional 500 ml triple distilled water and 15 ml 30% H_2O_2 were added to the solution to stop the oxidation. At this stage, the color of the solution becomes yellow ochre signifying the high oxidation level of graphite. Now, the yellow solution was washed two times with 1M HCl (Hydrochloric Acid) solution and repeated washing was done with triple distilled water until a pH of 5 was obtained. This was done by centrifugation of the solution and decantation of the supernatant. A rigorous washing and decantation step is necessary to exfoliate the graphene oxide layers and to remove the unexfoliated graphene oxide layers. The thick yellow brown gel was filtered and dried overnight to get a fine yellow graphene oxide (GO) powder. A stoichiometric amount of GO was then taken in triple distilled water and ultrasonicated for 30 min to get a homogeneous solution.

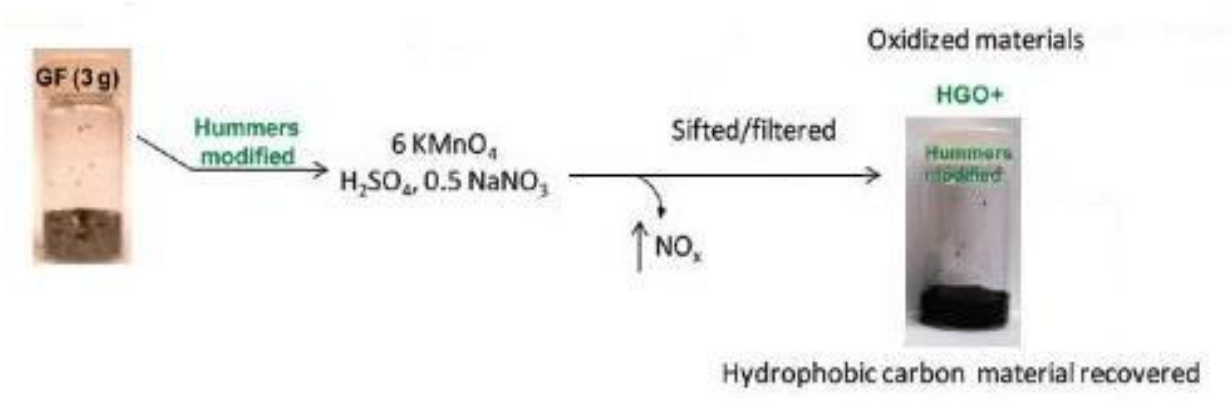

Fig. 2.6. GO Synthesis process[3]

1.4. Reduced Graphene Oxide (RGO) Synthesis

RGO Synthesis: Oxidized material samples were reduced with hydrazine hydrate before being annealed in Ar/H2 at 300 and 900 degrees Celsius. 100 mg of enhanced GO materials are distributed in 100 ml distilled water and agitated for 30 minutes to reduce hydrazine. 1 mL of hydrazine hydrate is then added. After 45 minutes of heating at 950°C in a water bath, a black solid precipitated from the reaction mixture. Filtration isolates the products, which are then washed with distilled water to yield 54 mg of chemically reduced enhanced GO i.e., RGO. NMR spectra show no signal from oxidized carbon after reduction. This signifies that RGO is of very high grade. We estimate that individual RGO flacks have a thickness ranging from 1-3 nm based on AFM measurements[3].

Structural characterization of GO and RGO:

In our experiment we used GO where the level spacing is around 9.0 Å (from XRD spectra). The X-ray photoelectron spectroscopy (XPS) confirms that GO produced by modified Hammer's method is more oxidized than GO produced by Hummer's methods. XPS confirms that improved GO has 63% oxidized carbon and 37% graphitic carbon. From 13C NMR we get the apparent peak of oxidized carbon of GO at around 287 eV. TEM images confirm the structure regularity of GO. UV-Vis spectra supports the regular structure of GO due to greater retention of carbon ring in basal plane. Large extinction coefficient of GO indicates that it has large number of aromatic rings or isolated aromatic domains.
Although the following λ_{max} results from the electronic transition show that these aromatic rings are not extended conjugation, total absorption indicates that GO produced by the modified Hummer's approach retains more aromatic rings than GO produced by Hummer's method[3].

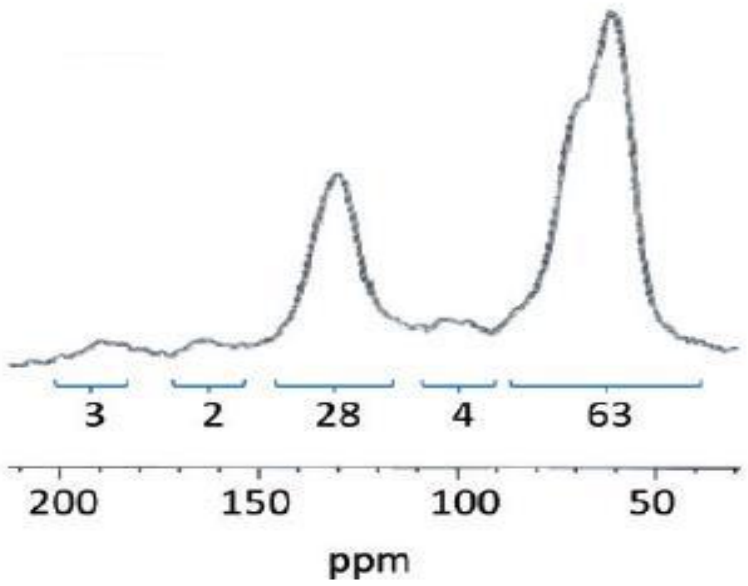

Fig. 2.7. 13C NMR Spectra of GO[3]

2. Experimental Methodology

2.1. High resolution transmission electron microscope (HRTEM)

2.1.1. Introduction:

It's a type of transmission electron microscopy with a modern twist (TEM). For high magnification of nanomaterials, HRTEM is utilized. HRTEM is an excellent imaging technique for nanomaterials at the atomic scale because of its high resolution. The TEM is a technique that gives morphological, compositional, and crystallographic information by using energetic electron contact with the material. HRTEM creates an interference image by using both transmitted and scattered electrons. It's a phase contrast image that can be as small as a crystal's unit cell. HRTEM has been utilized extensively and successfully for investigating crystal structures and lattice defects in a variety of sophisticated materials at the atomic level.
Point defects, stacking faults, dislocations, precipitates grain boundaries, and surface features can all be characterized with it. HRTEM has a 2D spatial resolution of around 0.05 nm. In 3D crystal, different views from various angles are combined to create a 3D map. Electron crystallography is the name for this method.

2.1.2. Working Principle:

TEM i.e., Transmission Electron Microscope has three important sections:

1. Depending on the application, the specimen system can be stationary or move slowly. The mechanical stability of the TEM plays an essential role in defining its resolution.
2. The illumination system is made up of an electron cannon and two or more condenser lenses that focus the electron beam on the sample. The diameter of the beam is determined by the specimen arrangement.
3. At least three lenses are used in the imaging system to provide a magnified image of the sample on a fluorescent screen or a monitor of an electronic camera system. The unique resolution of the microscope is determined by the imaging lens design.
4. An image recording device, e.g., CCD with photodiodes is used to record the image produced.

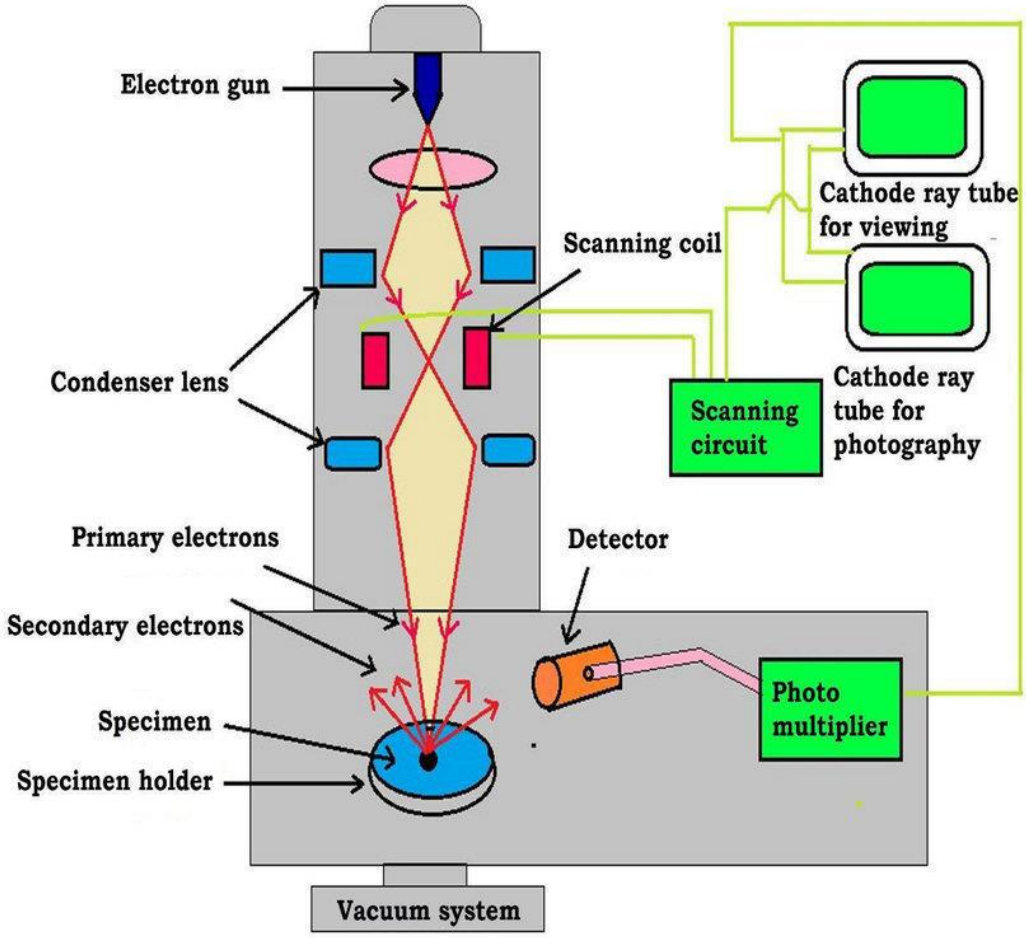

Fig. 2.8. Schematic diagram of HRTEM[14]

2.1.3. Components:

- **<u>Specimen system:</u>**

  Because any drift or vibration would be amplified in the final image, the specimen stage is designed to keep the specimen as still as possible. TEM specimens are always round, having a 3 mm diameter. The specimen must be perpendicular to this disc and thin enough to let electrons pass through and generate the magnified image. The specimen is first placed in a container that can be evacuated before entering the TEM column. The specimen stage is divided into two types: side-entry and top-entry. The specimen is attached to the end of a rod-shaped specimen holder and inserted horizontally through the airlock, which is then triggered by rotating the specimen holder around its long axis. The specimen is clamped to the bottom end of a cylindrical holder with a conical collar in the top-entry stage. A sliding and tilting arm loads the holder into position through an airlock, which is subsequently removed and retracted. The cone of the specimen holder fits snugly into a conical well of the specimen stage inside

the TEM, which may be manipulated in the horizontal (x and y) directions by a precision gear system.

- **Illumination system:**

The energy of the electron beam produced by the electron cannon is adequate to pass through the sample specimen. An electron source, a cathode (due to the high negative potential), and an electron-accelerating chamber make up this cannon. The electrons are emitted through a process known as thermo-ionic emission. A V-shaped filament composed of tungsten wire is spot-welded to straight-wire leads that are installed in a ceramic or glass socket as the electron source. The filament is heated to roughly 2700 K using a direct current (dc), at which point tungsten emits electrons into the surrounding vacuum. The electron gun's filament can be constructed of tungsten or lanthanum hexaboride (LaB6). Although LaB6 source is more expensive than tungsten filament, it has a longer lifespan. The filament is encircled by a control grid with a central aperture positioned on the column's axis; the cathode's apex is positioned at or slightly above or below this aperture. The cathode and control grid are insulated from the rest of the instrument and have a negative potential equal to the required accelerating voltage.

With the help of an electric field parallel to the optic axis, electrons are accelerated to their final kinetic energy E0 after emission from the cathode. A potential difference V0 between the cathode and anode is used to create this field. An anode is a circular metal plate with a central hole through which an accelerated electron beam emerges[6]. Pass through the middle aperture at a constant energy if the high voltage has stabilized sufficiently. The electron gun's control and alignment are vital to its successful operation.

The condenser lens must have at least two electron lenses in order to provide a high-quality magnified image of the sample. A powerful magnetic lens is used as the first condenser lens. It creates a real image by using a virtual electron source. The spot size can be used to adjust the lens current. The weak magnetic lens used as the second condenser lens yields little or no magnification. This lens has a condenser aperture with a variable diameter that allows the angle of illumination of the electron form optic axis to be altered. The use of a small spot size reduces the effects of heating and irradiation on the specimen. In order to move the electron beam (incident on the specimen) in the y and x directions, the illumination system includes two pairs of coils that apply homogeneous magnetic fields in the horizontal (x and y) directions. A second set of coils is used to alter the incident beam's angle with respect to the optic axis.

- **Image producing system:**

  On the viewing screen or on the digital display system, the TEM imaging system creates a magnified image of the specimen. The quality and design of these lenses, particularly the first imaging lens, the objective lens, have a significant impact on the image's spatial resolution. With a short focal length, it's a powerful lens. To avoid picture drift caused by thermal fluctuations, this lens must be kept at room temperature. The TEM also contains precision controls that allow the specimen picture to be accurately focused on the viewing screen by making small fractional adjustments to the objective current. The first condenser lens has a great deal of focusing power. The second condenser lens creates a nearly parallel beam for analytical electron microscopy.

  We can restrict electrons to arrive at the specimen parallel to the axis and must remain unscattered during their passage through the specimen using parallel lighting and properly controlled tilt controls. When an electron is scattered by one or more atoms in the material, it returns to the optic axis at the same angle. The diaphragm around the aperture absorbs electrons scattered at larger angles, so they don't contribute to the final image. We can assure that practically all scattered electrons are absorbed by the diaphragm by reducing the deflection angle. As a result, parts of the material that scatter electrons strongly appear as dark areas in the final image, which is referred to as diffraction contrast. Using an objective stigmator positioned below the objective lens, the TEM operator can eliminate blurring and correct for axial astigmatism in the objective. A diaphragm, which limits the specimen region from which electron diffraction is recorded, can also be used here. Only electrons that fall within the aperture's diameter are transmitted through it. As a result, the diaphragm's introduction offers diffraction data with good spatial and angular resolution.

  Between the objective and the final lens in a TEM system, there are numerous lenses. This intermediate lens is primarily used for two purposes. First, image magnification can be altered in small steps by altering the focal length, which is commonly 103-106. Second, an electron diffraction pattern can be formed on the TEM viewing screen by increasing the intermediate lens excitation. A projector lens is then used to create an image or diffraction pattern across the entire TEM screen. The final-image magnification is the algebraic product of each imaging lens' magnification factors.

- **Image Recording:**

  The electron picture is monochromatic and must be made visible to the naked eye either by letting electrons fall on a fluorescent screen at the foot of the microscope column or by digitally recording the image for display on a computer monitor. Computerized photographs are saved in TIFF or JPEG formats and can be examined or image-processed before being published. Charged coupled diode (CCD) sensors with a million-photodiode array are used in this electronic image recording. There are various advantages to using electronic recording. The recorded image may be seen on a display screen at a high magnification, which makes focusing and astigmatism correction much easier. The image data is saved digitally in computer memory before being transferred to magnetic or optical discs, where prior photographs can be quickly accessed for comparison. The image's digital nature also allows for numerous types of image processing.

2.2. Ultraviolet–Visible Spectroscopy

2.2.1. Introduction to Ultraviolet–visible Spectroscopy

UV–Vis Spectroscopy, sometimes known as UV–Vis Spectroscopy, is a technique for measuring light absorbance in the ultraviolet and visible portions of the electromagnetic spectrum. It makes use of visible and near-infrared light. Incident light can be absorbed, reflected, or transmitted as it strikes materials. Atomic excitation is caused by the absorption of UV-Vis radiation, which refers to the transition of molecules from a low-energy ground state to an excited state[7].

The wavelength of light reaching the detector is measured after a light beam passes through an object. The wavelength is used to determine the chemical structure and quantity of molecules present. As a result, both quantitative and qualitative data can be collected. In the wavelength range of 160 to 3500 nm, information can be collected as transmittance, absorbance, or reflectance of radiation. Electrons are promoted to excited states or anti-bonding orbitals as a result of incident energy absorption. Photon energy must match the energy required by the electron to go to the next higher energy state for this transfer to take place. The essential operating principle of absorption spectroscopy is this mechanism. There could be three different sorts of ground state orbitals involved:

i. Bonding molecular orbital: σ , π
ii. Non-bonding atomic orbital: n
iii. Anti-bonding molecular orbital: σ^* , π^*

Transition which involves excitation of electron from s bonding orbital to σ anti-bonding orbital is called σ to σ^* transition. Likewise, π to π^* represents the excitation of an electron of a lone pair (non-bonding electron pair) to an

antibonding π orbital. Electronic transitions occurring due to absorption of UV and visible light are:

i. σ to σ*,
ii. n to σ*,
iii. n to π*,
iv. π to π*[3].

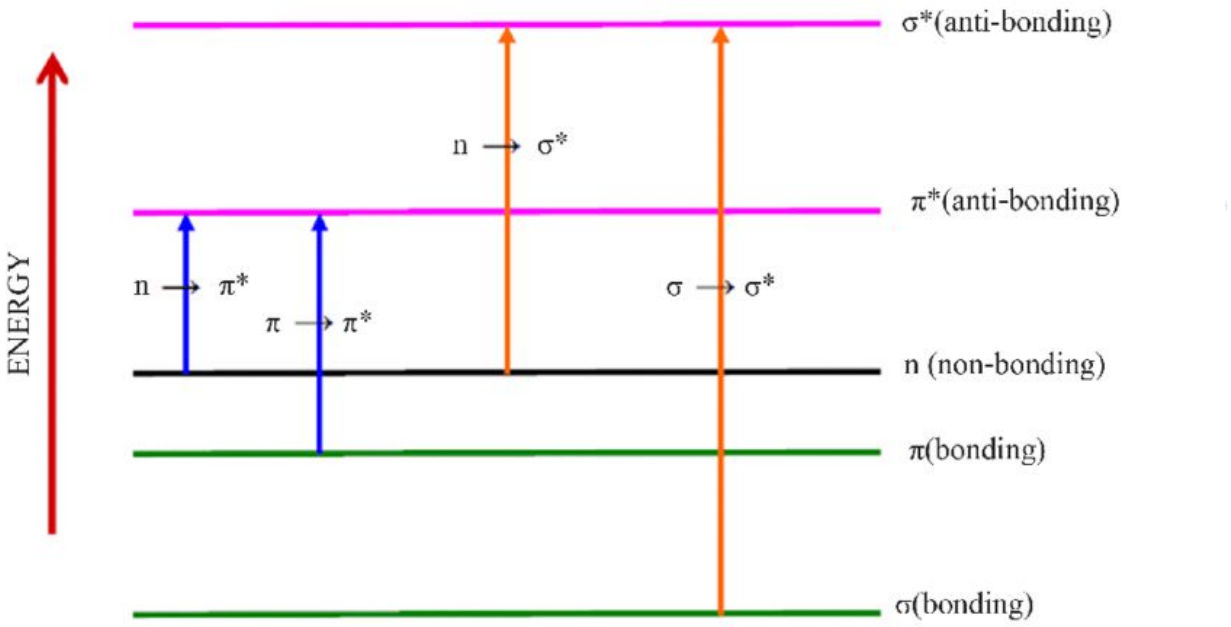

Figure 2.9. Electron transitions in UV-Vis spectroscopy

When a given wavelength and energy of light is focused onto a sample, it absorbs some of the incident wave's energy. A photodetector detects the sample's absorbance and measures the energy of transmitted light from the sample. The wavelength is used to generate the absorption or transmission spectrum of the light absorbed or transmitted by the sample. The Lambert-Beer rule (Figure 2.7.) is a fundamental principle of quantitative analysis that states that a solution's absorbance scales directly with its analyte concentration. The absorbance (unit less) A is defined as the molar absorptivity of the absorbing species (M-1 cm-1), b is the sample holder path length (usually 1 cm), and c is the solution concentration (M)[8].

UV−Vis−NIR spectrometer can monitor absorbance or transmittance in UV – visible wavelength range. The relation between incident light of intensity 'Io' and transmitted light of intensity 'I' is described as follows[8].

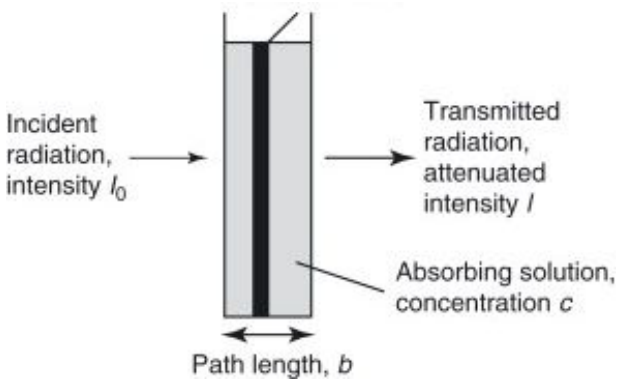

Figure 2.10. Lambert−Beer Rule

Transmittance, $T=\frac{I}{I_0}$; Transmission rate, $T\%=\frac{I}{I_0}\times 100$

Absorbance, A is defined as logarithmic inverse of transmittance, i.e. $A = \log(\frac{1}{T})$

$$\log(\frac{1}{T}) = \log(\frac{I_0}{I}) \quad \ldots(1)$$

we know $I=I_0\, e^{-kcl}$ or, $T=\frac{I}{I_0} = e^{-kcl}$ …(2)

$$A = \log(\frac{1}{T}) = kcl \quad \ldots(3)$$

The constant of proportionality, 'k', is used here. While transmittance is unaffected by sample concentration, absorbance is proportional to both sample concentration (Beer's law) and optical path (Bouguer's law). Furthermore, when the optical path is 1 cm and the concentration of the targeted substance is 1mol/l, k is denoted as $'\varepsilon'$ and is characterized as molar absorption coefficient. The material's molar absorption coefficient is representative of the material under specified conditions. The Lambert Beer rule is based on the assumption that there is no stray, produced, scattered, or reflected light.

2.2.2. Components of Ultraviolet–visible Spectroscopy

The spectrophotometer is the instrument used in ultraviolet-visible spectroscopy. It compares the intensity of light before it goes through a sample and measures the intensity of light before it passes through the sample.

The essential components of a spectrometer are –

- **<u>UV Light Source:</u>**

  Electrically igniting deuterium or hydrogen at low pressures produces a continuous UV spectrum. Both deuterium and hydrogen lamps emit light

with wavelengths ranging from 160 to 375 nm[3].

- **Visible Light Source:**

  The radiation source is usually a Tungsten filament (300–2500 nm), a deuterium arc lamp (190–400 nm), a Xenon arc lamp (160–2,000 nm), or, more recently, light emitting diodes (LED) for visible wavelengths.

- **Monochromator & Cuvettes:**

  A monochromator source is employed, and light is separated into two halves of identical intensity via a half-mirror splitter before reaching the sample. One component (or sample beam) passes through a cuvette containing a clear solvent solution of the material to be studied. The second beam, sometimes known as the reference beam, travels through a comparable cuvette that contains only solvent. Containers for the reference and sample solutions must be transparent to the passing beam.

- **Detectors:**

  The intensity of light transmitted by cuvettes is detected by the detector, which delivers the data to a meter, which records and displays the values. The intensities of light beams are calculated and compared by electronic detectors. Several UV is spectrophotometers contain two detectors – a phototube and a photomultiplier tube – and simultaneously monitor the reference and sample beams. CCDs (Charge-Coupled Devices) are like diode array detectors.

- **Recording devices:**

  Most of the time, the amplifier is connected to a computer via a pen recorder. The computer saves all the information and generates the spectrum of the desired molecule. The following functions can be recalled or continuously monitored by a microcomputer with completely automated equipment, depending on the sophistication of the software:

  i. Base-line correction
  ii. Conversion of analog to digital (a/d) data
  iii. Conversion of extinction values to concentrations[8].

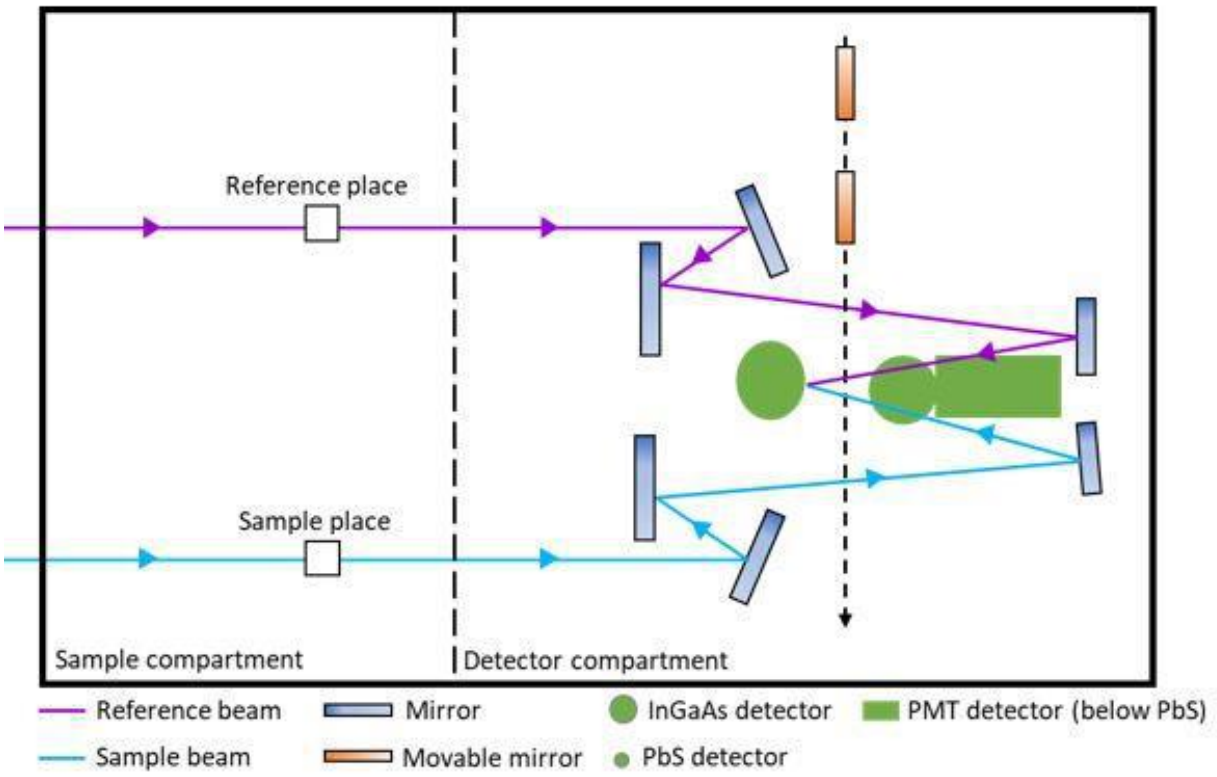

Figure 2.11. UV−Vis−NIR Spectrometer[8]

2.2.3. Applications of Ultraviolet–visible Spectroscopy

- **Qualitative & Quantitative analysis:** UV-Vis absorption spectroscopy can be used to identify substances that absorb UV light. The absorption spectrum is compared to the spectra of recognized chemicals for identification. Aromatic compounds and aromatic olefins are commonly studied using UV-Vis absorption spectroscopy[9]. UV-Vis Spectroscopic measurements can also be used to determine the quantity of a sample.
- **Structure elucidation of organic compounds:** UV-Vis spectroscopy is important in elucidating the structure of organic molecules, determining the presence or absence of unsaturation, and determining the presence of hetero atoms. The location and combination of peaks can be used to determine if the chemical is saturated or unsaturated, whether hetero atoms are present or not, and so on.
- **Impurities Detection:** One of the most effective ways for determining contaminants in organic molecules is UV-Vis absorption spectroscopy. Due to contaminants in the sample, additional peaks can be seen, which can be compared to those of normal raw material. Impurities can be determined by measuring absorbance at a given wavelength as well[9].

2.2.4. Instrument Specifications

a) Name: JASCO UV-VIS Absorption Spectrophotometer
b) Model: V-630

Figure 2.12. JASCO UV-VIS Absorption Spectrophotometer

2.3. Fluorescence Spectroscopy

2.3.1. Introduction

Lasers have long played a vital part in spectroscopy, which has made a significant contribution to the current state of atomic and molecular chemistry. In chemistry and physics, fluorescence spectroscopy and time-resolved fluorescence are generally used as research methods. Fluorescence is the virtually instantaneous absorption of light energy by molecules at one wavelength and subsequent remission at another, usually longer wavelength. Fluorescent chemicals have two distinct spectra: an excitation spectrum (the wavelength and amount of light absorbed) and an emission spectrum (the wavelength and amount of light emitted). Fluorometry is a highly specific analytical technique because of this premise.

Fluorescence is measured using fluorometry. A fluorometer, sometimes known as a fluorimeter, is a device that measures fluorescence. A fluorometer produces the wavelength of light needed to ignite the analyte of interest, selectively transmits the wavelength emitted, and then measures the intensity of the emitted light. When compared to other analytical techniques, fluorometry is chosen for its exceptional sensitivity, high specificity, simplicity, and low cost. Fluorometry is more sensitive than absorbance measurements in most cases. It is an important analytical tool for both quantitative and qualitative research[10].

Photon emission mechanisms such as fluorescence and phosphorescence occur during molecular relaxation from electronic excited states. Transitions between electronic and vibrational states of polyatomic fluorescent molecules are involved in these photonic processes (fluorophores). Fluorophores are the most important component of fluorescence spectroscopy. The components of molecules that cause them to glow are known as fluorophores. Fluorophores are mostly molecules with aromatic rings, such as Tyrosine, Tryptophan, Fluorescein, and so on.

Fluorescence: Prompt fluorescence: $S1 \rightarrow S0 + h\nu$
The release of electromagnetic energy is immediate or from the singlet state.

Delayed fluorescence: $S1 \rightarrow T1 \rightarrow S1 \rightarrow S0 + h\nu$
This result comes from two intersystem crossings, at first from singlet to triplet, and then again from triplet to singlet.

Phosphorescence: $T1 \rightarrow S0 + h\nu$
Delayed release of electromagnetic energy from the triplet state.

2.3.2. Spectrofluorometer

A spectrofluorometer is a device that uses the fluorescence properties of certain substances to provide information about their concentration and chemical environment in a sample. The emission is monitored at a single wavelength, or a scan is done to record the intensity versus wavelength, commonly known as an emission spectrum, when a specific excitation wavelength is chosen.

High-intensity light sources are typically used in spectrofluorometers to blast a sample with as many photons as feasible. This allows the greatest number of molecules to be in an excited state at any given time. Normally, the fluorescence is collected at a 90-degree angle to the optical axis set by the excitation light beam in all the devices. Instead of measuring the difference in intensity of two signals, which is measured in a spectrometer, a spectrofluorometer measures a signal over a zero background. The light source, monochromator, and light detector are the three main components of a spectrofluorometer.

Light Source: A spectrofluorometer uses a high-pressure xenon arc lamp as its light source. This lamp's bulb contains high-pressure xenon, which is stimulated to a higher level by an electrical arc created by current flowing through the electrodes. The spectrum of light emitted ranges from roughly 250 nm to 1100 nm.

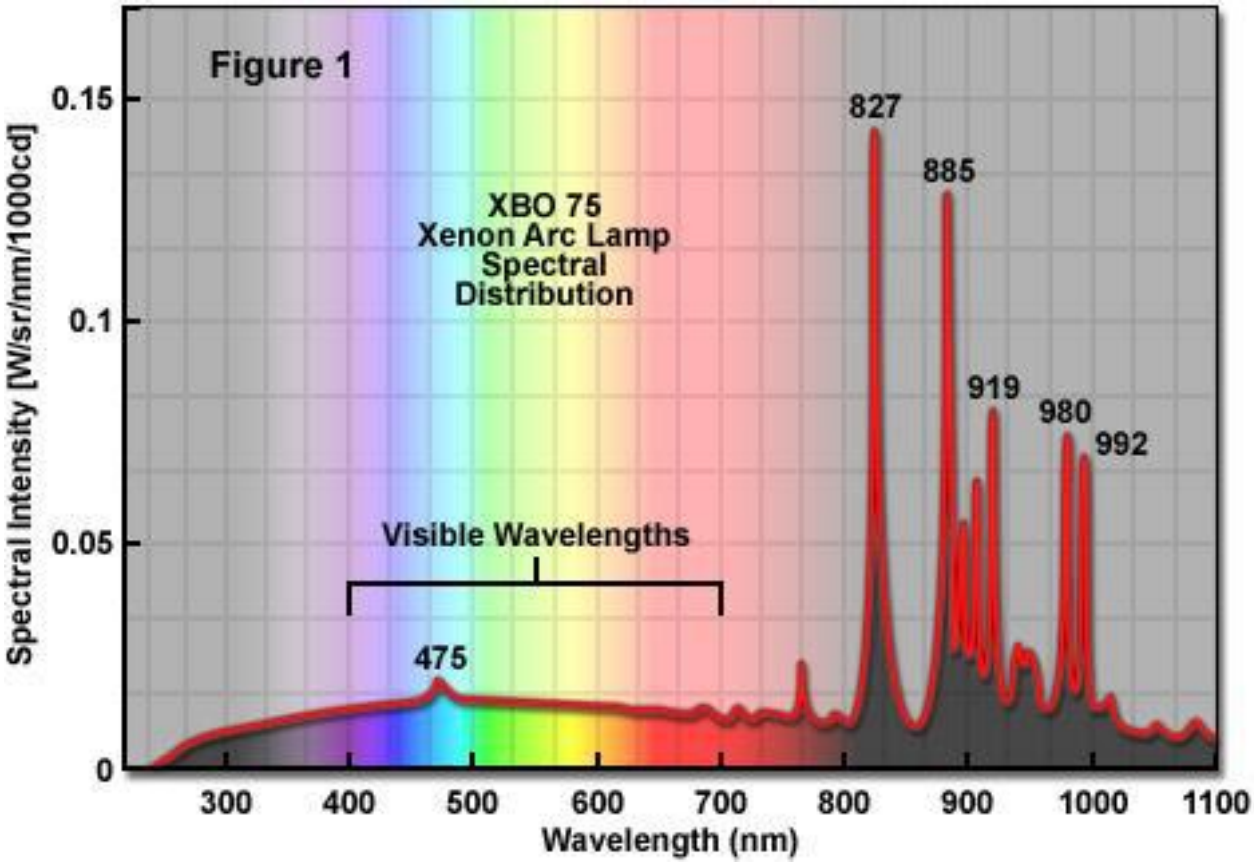

Figure 2.13. Spectral distribution for the 300W xenon arc lamp[11]

When utilizing a xenon arc lamp, monochromators are used to pick the wavelength for irradiating the sample; in the collection channel of a spectrofluorometer, they are used to record the range of wavelengths produced by a fluorophore. A diffraction grating with slits at the entrance and output make up the simplest monochromator. When light strikes the grating at an angle, it diffracts into a succession of angles, the first of which is usually chosen for measurement. When a monochromator is adjusted to deliver radiation at wavelength λ, it also delivers radiation at wavelength 2λ. The second order's strength is typically roughly a tenth of the first order's; yet this is enough to pollute the emission spectrum. With a judicial selection of filters, the second order can be removed. The amount of stray light, or radiation present at any wavelength other than the targeted wavelength, is a characteristic of every monochromator. For reducing stray light, various solutions are possible, the first of which is a judicious grating selection. Ruled grating and holographic grating are the two types of grating. To construct a monochromator, gratings can be arranged in a variety of ways, the two most prominent being the Czerny-Turner and the Seya-Namioka.

A photomultiplier tube (PMT) or photodiode is a light detector that converts light into an electrical signal. The PMT can be used in the wavelength range of 230 nm to 830 nm. It is clear that the sensitivity is not the same even within the working wavelength range, and the results must be corrected.

Polarizers are used in spectrofluorometers to measure anisotropy. The superposition of the wavelength transmission of the various parts of the instrument defines the operational zone of the instrument. Even when measuring fluorescence parameters inside this zone, the variance in transmission must be considered. Photomultiplier tubes are used to detect the fluorescence, which is then quantified using the proper electronic instruments. Typically, the output is presented in a graphical format and saved digitally[11].

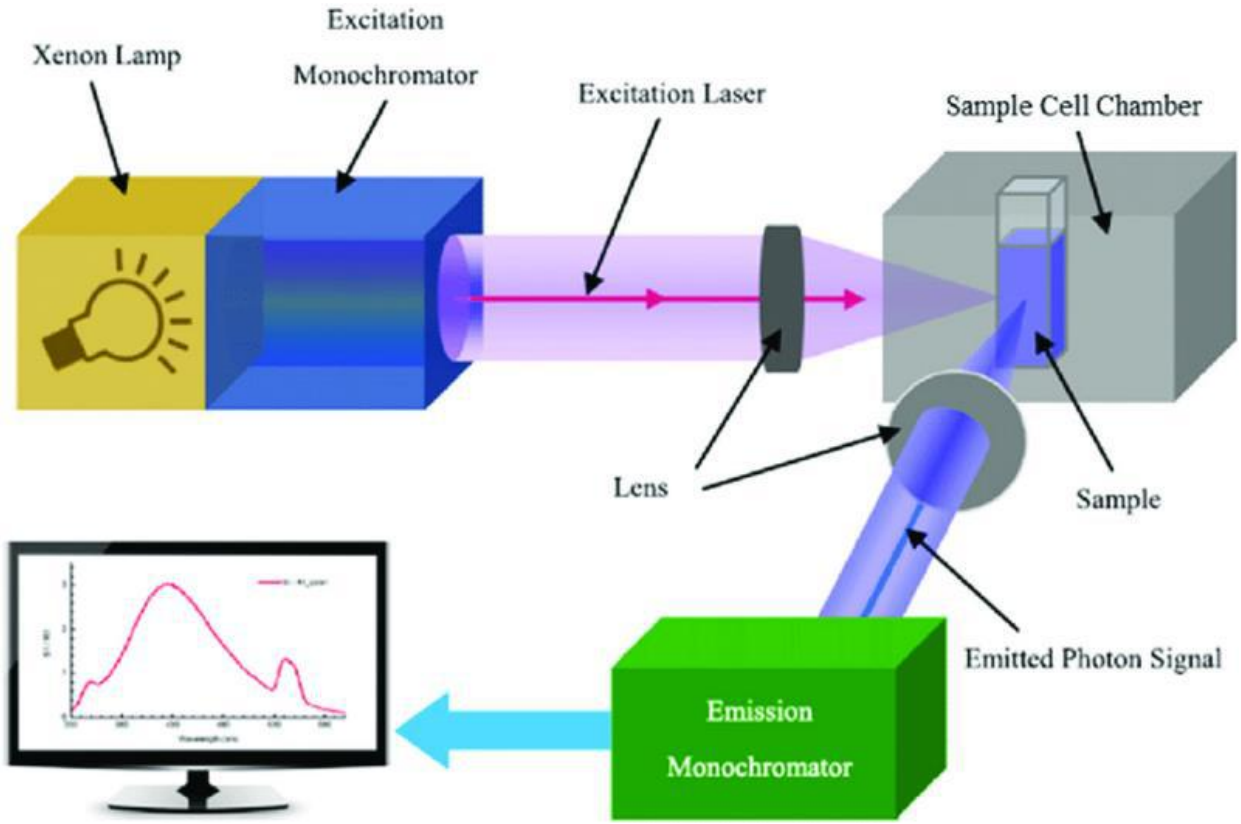

Figure 2.14. Schematic Diagram of Arrangements in a Spectrofluorometer[12]

2.3.3. Applications of Fluorescence Spectroscopy

- **<u>LIF Spectroscopy in cancer diagnosis:</u>** Laser spectroscopic techniques have the potential for in-situ, near real-time diagnosis, and the use of non-ionizing radiation assures that the diagnosis can be repeated without harm. In two techniques, laser induced fluorescence (LIF) has been used to diagnose cancer. One strategy is to give a medication like hematoporphyrin derivative (HpD) to the patient, which is selectively retained by the tumor. When the medicine is photo stimulated with the right wavelength of light, it fluoresces in the tumor. The tumor is detected and imaged using this

fluorescence. Intersystem crossover also leads to the population of the triplet state as a result of photo excitation. The molecule in the excited triplet state can either react directly with biomolecules or produce singlet oxygen, which is harmful to the host tissue. Photodynamic treatment of tumors takes advantage of the resultant damage of the host tissue[10].

- **Glucose Determination:** Blood glucose levels (fasting, pp) are a very good predictor of human health. An abnormally high level of glucose can reveal a lot about disorders like diabetes or hypoglycemia. Fluor photometry is frequently utilized because of its ease of use and great sensitivity.
- **Bioscience:** Fluorescence spectroscopy can be used to sequence DNA. A DNA sample is put into a fluorescence spectrometer with an extrinsic fluorophore to acquire a reading of the sample's concentration.
- **Agriculture:** Spectroscopic techniques are frequently used to identify various crop kinds. Citrus seedling varieties can be identified using the laser-induced fluorescence emission approach.
- **Study of Marine Petroleum Pollutants:** Fluorescence spectroscopy is a useful technique for detecting oil slicks on the water's surface, determining petroleum pollutants in saltwater, determining specific petroleum derivative compounds, and identifying pollution sources[10].

2.3.4. Instrument Specifications

i. Instrument Name: JASCO Spectrofluorometer
ii. Instrument Model: 8200

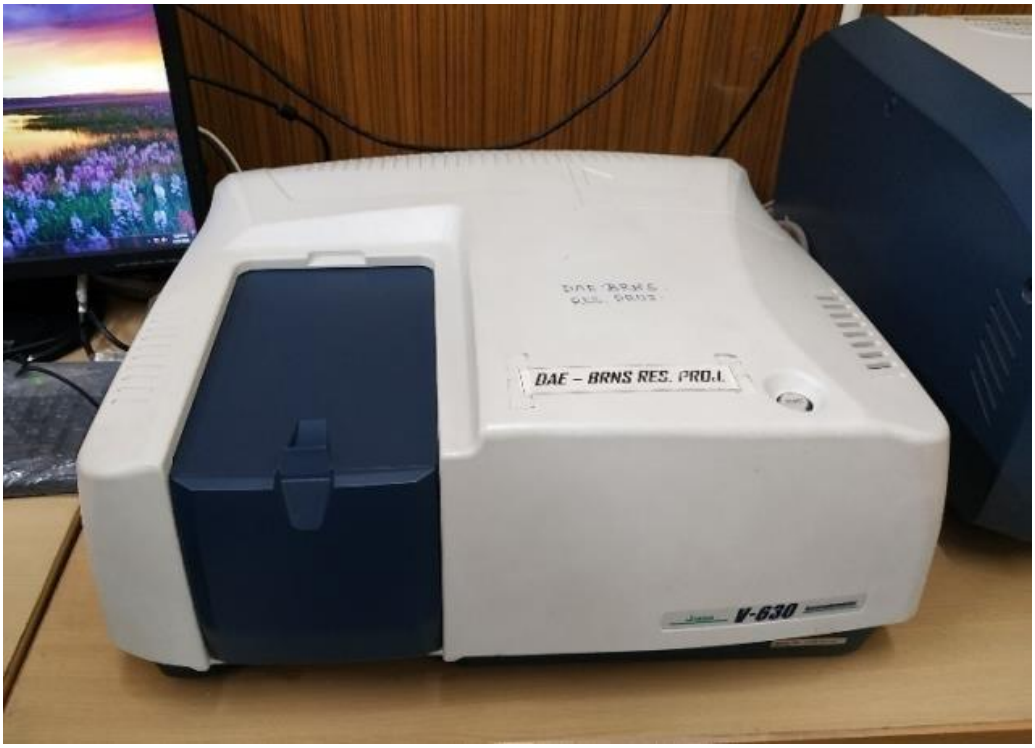

Figure 2.15. JASCO Spectrofluorometer

2.4. Nuclear Magnetic Resonance (NMR) Spectroscopy

2.4.1. Introduction

The spectroscopic technique of nuclear magnetic resonance spectroscopy is used to study local magnetic fields surrounding atomic nuclei. Certain nuclei resonate at a specific frequency in the radio frequency band of the electromagnetic spectrum when exposed to a strong magnetic field. Slight fluctuations in this resonance frequency provide extensive information about the atom's molecular structure. According to the NMR principle, many nuclei have spin and all nuclei are electrically charged. When an external magnetic field is applied, energy can be transferred from the base energy to a higher energy level[10].

i. Nucleis are electrically charged and many of them have spin.
ii. Upon applying external magnetic field, energy transfer is possible from minimum base energy to higher energy levels.
iii. Energy transfer takes place at a frequency that resonates with radio frequency.
iv. Energy is emitted at the same wavelength when the spin comes back to its base level.
v. As a result, the processing of the NMR spectrum for the concerned nucleus is yielded by measuring the signal that matches this transfer[13].

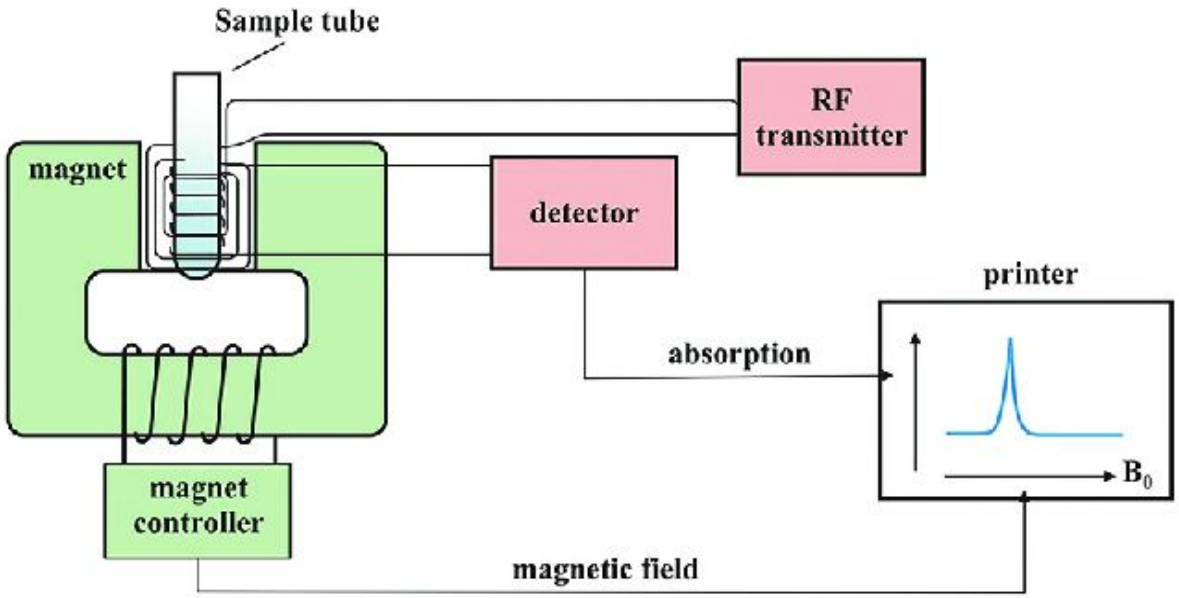

Figure 2.16. Diagram of an NMR Spectrometer[13]

2.4.2. NMR Spectroscopy Hardware

Hardware in NMR spectroscopy consists of nine major parts. In the following, they have been briefly discussed:

- **Sample tube**: It is a glass tube which is 8.5 cm long and 0.3 cm in diameter.
- **Magnetic coils:** Magnetic coil generates magnetic field whenever current flows through it.
- **Permanent magnet**: It helps in providing a homogenous magnetic field at 60 – 100 MHz.
- **Sweep generator:** Modifies the strength of the magnetic field which is already applied.
- **Radiofrequency Transmitter:** It produces a powerful but short pulse of the radio waves.
- **Radiofrequency Receiver:** It helps in detecting receiver radio frequencies.
- **RF Detector:** It helps in determining unabsorbed radio frequencies.
- **Recorder:** It records the NMR signals which are received by the RF detector.
- **Display system:** A computer that displays the records the data[13].

2.4.3. Applications of NMR Spectroscopy

- NMR spectroscopy is a spectroscopic technique used by chemists and biochemists to study the characteristics of organic molecules, while it can be applied to any sample with spin-containing nuclei.
- NMR can be used to analyze mixtures containing known substances quantitatively. NMR can be used to compare unknown chemicals to spectral libraries or to derive their basic structure directly.
- NMR can be used to assess molecule conformation in solutions as well as to examine physical features at the molecular level such as conformational exchange, phase shifts, solubility, and diffusion after the basic structure is known[13].

2.5. Time Resolved Spectroscopy

Time Resolved Spectroscopy is a type of spectroscopy that is used to track interactions between molecules and short-term motions. It is a helpful approach in biomolecular structure characterization and dynamics because it can quantify changes in the picosecond or nanosecond time range.

2.5.1. Time Correlated Single Photon Counting (TCSPC)

TCSPC[15] is based on the detection of single photons in a periodic light signal, measurement of the individual photon detection times, and reconstruction of the waveform from the individual time measurements. The method takes advantage of

the fact that the light intensity for low-level, high-repetition-rate signals is typically so low that the likelihood of detecting one photon in a single signal period is substantially lower than one. As a result, the detection of multiple photons can be ignored, and the method depicted in Figure 2.13. can be employed instead.

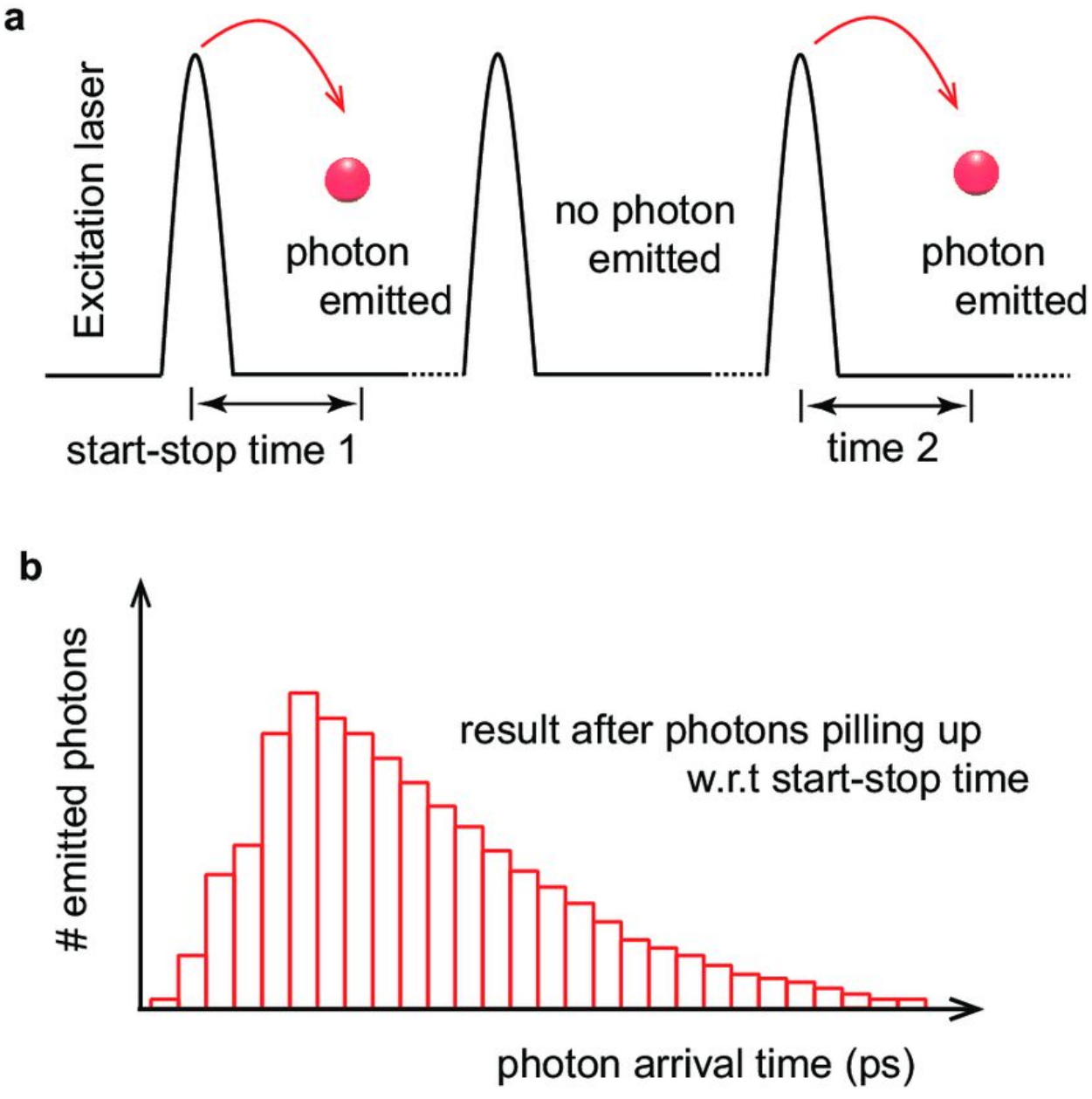

Figure 2.17. a) TCSPC Measurement Technique[16]

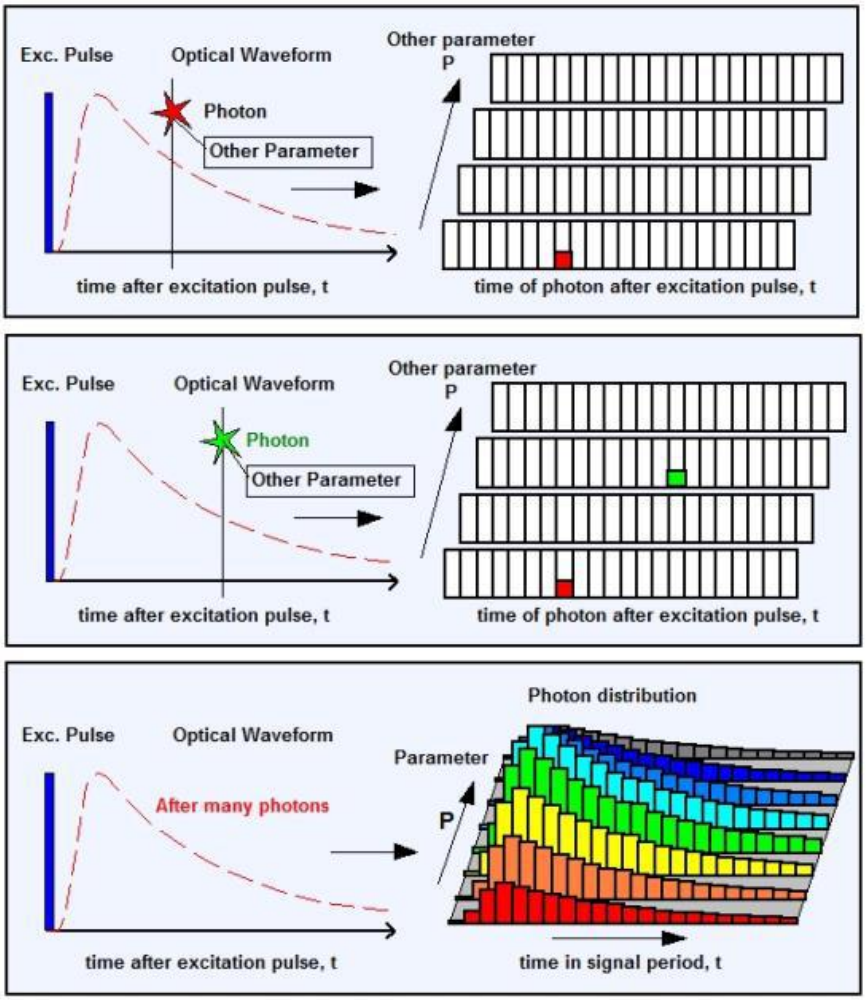

Figure 2.17. b) Multi-Dimensional TCSPC[15]

Due to the detection of individual photons, the detector signal consists of a train of randomly distributed pulses. Many signal intervals are devoid of photons, whereas others contain a single photon pulse. Periods with multiple photons are extremely rare. The time of the matching detector pulse is measured when a photon is detected. The events are stored in memory by inserting a '1' in a memory location according to the detection time. The histogram of detection timings, i.e., the waveform of the optical pulse, grows up in the memory after many photons. Even though this approach appears to be hard at first glance, it has a number of significant advantages:

I. TCSPC's temporal resolution is limited by the transit time spread, not the width of the detector's output pulse.
II. Because TCSPC has a near-perfect counting efficiency, it achieves the best signal-to-noise ratio for a given number of photons detected.
III. TCSPC can record the signals from several detectors simultaneously.
IV. TCSPC can be employed in confocal and two-photon laser scanning microscopes as a high-resolution high-efficiency lifetime imaging (FLIM) technology when paired with a fast-scanning technique.
V. TCSPC can collect fluorescence lifespan and fluorescence correlation data

at the same time.

VI. TCSPC devices with cutting-edge technology achieve count rates in the MHz range and acquisition times of a few milliseconds[15].

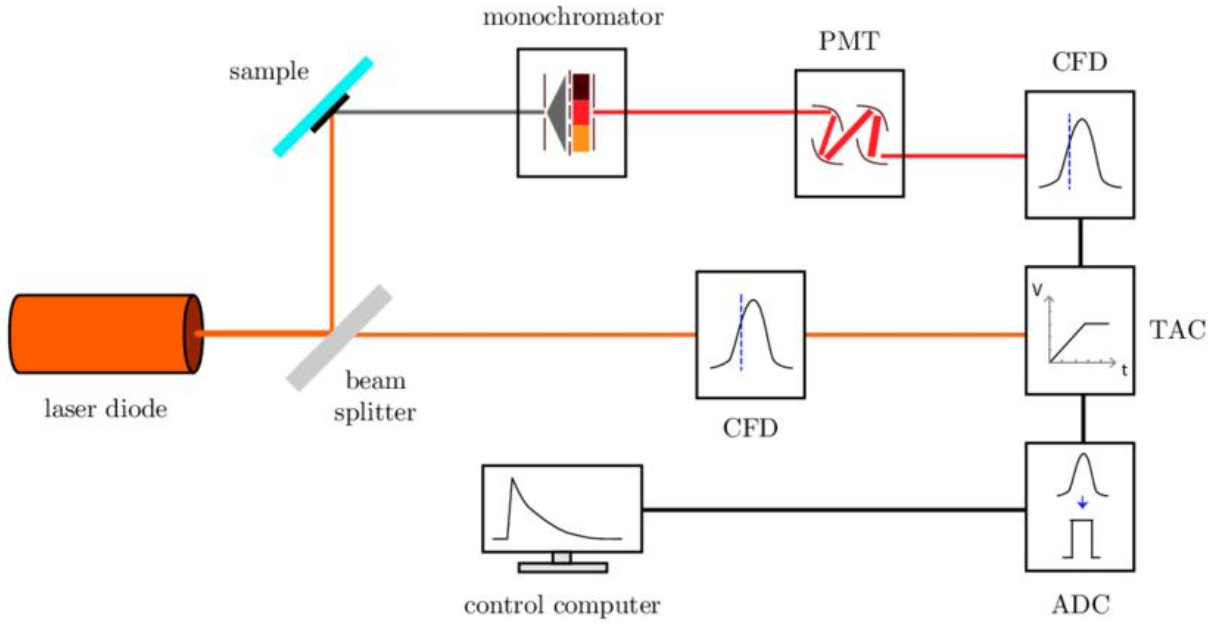

Figure 2.18. Block diagram of TCSPC using Laser Diode[17].

Here, CFD = Constant Fraction Discriminator, TAC = Time to Amplitude Converter, ADC = Analog to Digital Converter

2.5.2. Applications of Time Correlated Single Photon Counting (TCSPC)

- ✓ Fluorescence microscopy[18].
- ✓ TCSPC also has many applications in diverse areas of Science & Technology.
- ✓ Wide-field photon counting detectors are used in optical communications systems, and recent breakthroughs in superconducting detectors and SPAD array technology can be credited to the rapidly expanding applications in these fields.

2.6. Transient Absorption Spectral Analysis

2.6.1. Introduction

The transient absorption spectral measurements of the dyad-GQD (and GO) were made by using the third harmonic of Nd: YAG laser as excitation source (355 nm) at the different delay times of the excitation and analyzing or probing pulses. It is to be pointed out that the peaking of the transient absorption spectra observed at around 540 nm region could be assigned to the fluorene anion of the contact ion-pair. [19] The direct evidence of occurrence of photo induced electron transfer (PET) process is provided from the observations of transient donor cationic and acceptor anionic species. Data obtained from the transient absorption decays at the ambient temperature can also be used to calculate KCR (charge recombination rates) values. From the decays the ion-pair lifetimes (τ_{ip}) along with the corresponding charge recombination rates (KCR) (approximately KCR~1/ τ_{ip}) were computed.

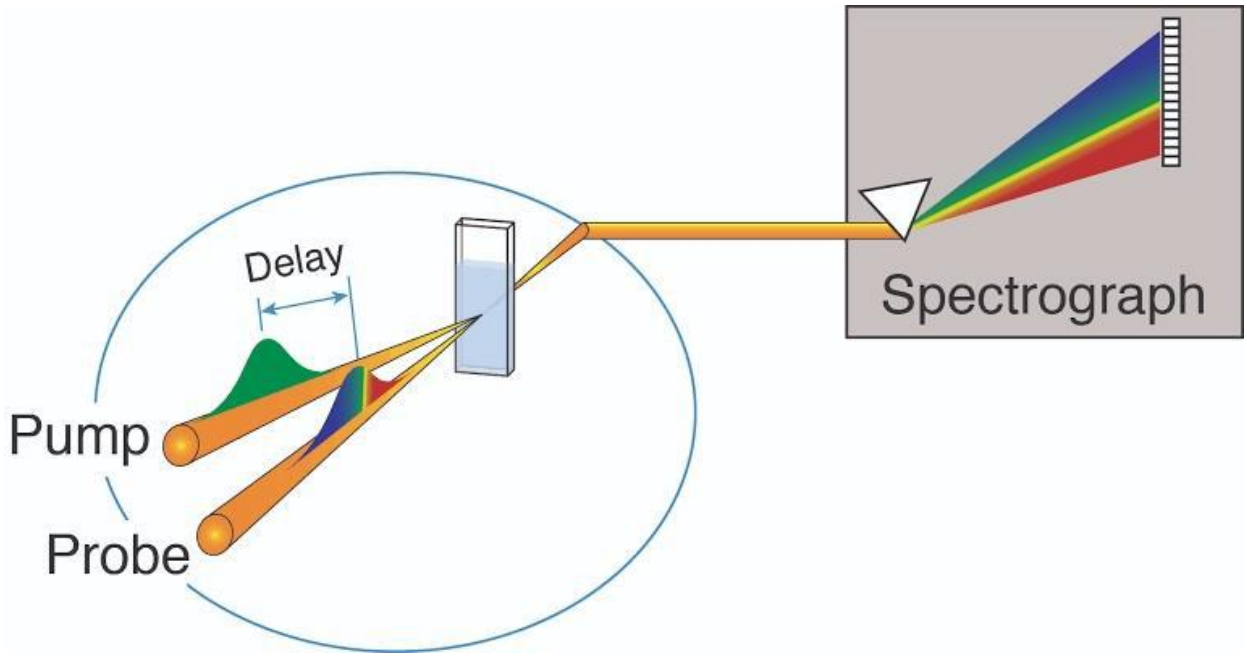

Figure 2.19. Transient Absorption Spectra Analysis[19]

2.6.2 Applications

- **Spectro electrochemistry:** In this process it collects transient absorption spectra on a semiconductor surface submerged in electrolyte solution under an applied potential, sheds light on how the interfacial electronic structure affects the transport of photogenerated charges.
- **Microscopy:** In order to study the effects of film morphology on local excited state dynamics and image directly charge transport in solution-processed organic and hybrid organic-inorganic lead-halide perovskite semiconducting films, ultrafast transient absorption microscopy was used.

This technique measures excited state dynamics with sub-micron spatial resolution.

- **Thermal Signatures:** Transient absorption spectra in organic and metal oxide semiconductor films can reveal significant heat contributions[20].

References

1. K. K. Park, H. Jung, T. Lee, S. K. Kang, “Synthesis and structure of benzotriazolyl fluoresces”, Bull. Korean Chem. Soc.,vol- 31, 984, 2010.
2. Sujuan Zhu ORCID logo*ab, Xuexue Bai a, Ting Wang a, Qiang Shi a, Jing Zhu a and Bing Wang, “One-step synthesis of fluorescent graphene quantum dots as an effective fluorescence probe for vanillin detection”, RSC Adv., 2021, 11, 9121-9129. DOI: 10.1039/D0RA10825A (Paper)
3. D.C. Marcano, D.V. Kosynkin, J.M. Berlin, A. Sinitskii, Z. Sun, A. Slesarev, L.B. Alemany, W. Lu and J.M. Tour, “Improved synthesis of graphene oxide”, Am. Chem. Soc., vol-4, 8, 2010.
4. A. Mallick, A.S. Mahapatra, A. Mitra, J.M. Greneche, R.S. Ningthoujam and P.K. Chakrabarti, “Magnetic properties and bio-medical applications in hyperthermia of lithium zinc ferrite nanoparticle integrated with reduced graphene oxide”, Journal of Applied Physics, 123, 055103, 2018.
5. https://www.britannica.com/technology/transmission-electron-microscope
6. R. F. Egerton, “Physical principles of electron microscopy”, springer, 2005.
7. Wikimedia Foundation. 2022. Ultraviolet–visible spectroscopy. Wikipedia. https://en.wikipedia.org/wiki/Ultraviolet_visible_spectroscopy [accessed 15 Jun, 2022]
8. https://www.eag.com/wp-content/uploads/2019/08/UV-Vis-Optical-System-in-Lambda-1050.jpg
9. PharmaTutor Edu Labs. 2020. Applications of Absorption Spectroscopy (UV, Visible). PharmaTutor Pharmacy Infopedia. https://www.pharmatutor.org/pharma-analysis/analytical-aspects-of-uv-visible-spectroscopy/applications.html [accessed 15 Jun, 2022]
10. E.D. Becker, “High resolution NMR: theory and chemical application”, Third edition, Academic press, 2000.
11. Michael W. Davidson, “Fundamentals of Xenon Arc Lamps”
12. https://upload.wikimedia.org/wikipedia/commons/thumb/0/0f/Schematic-diagram-of-the-arrangement-of-optical-components-in-a-typical_Spectrofluorometer.png
13. Nuclear Magnetic Resonance Spectroscopy for Medical and Dental Applications: A Comprehensive Review - Scientific Figure on ResearchGate. Available from: https://www.researchgate.net/figure/Schematic-presentation-of-a-typical-nuclear-magnetic-resonance-spectrometer-showing-the_fig1_333657432 [accessed 20 Jun, 2022]
14. SYNTHESIS OF SILVER NANOPARTICLES USING SILK FIBROIN : CHARACTERIZATION AND POTENTIAL ANTIBACTERIAL PROPERTIES. https://www.researchgate.net/figure/Schematic-diagram-of-HR-TEM_fig23_341277064 [accessed 21 Jun, 2022]
15. TCSPC Laser Scanning Microscopy - Upgrading laser scanning microscopes with the SPC730 TCSPC lifetime imaging module. Becker & Hickl GmbH, www.becker-hickl.com [accessed 19 Jun, 2022]

16. Nanophotonic antennas for enhanced single-molecule fluorescence detection and nanospectroscopy in living cell membranes - Scientific Figure on ResearchGate. Available from: https://www.researchgate.net/figure/TCSPC-technique-for-fluorescence-lifetime-analysis-a-TCSPC-technique-is-a-fast_fig8_321568911 [accessed 20 Jun, 2022]
17. Exploring and Exploiting Charge-Carrier Confinement in Semiconductor Nanostructures - Scientific Figure on ResearchGate. Available from: https://www.researchgate.net/figure/Simplification-of-the-time-correlated-single-photon-counting-TCSPC-method-used-to_fig19_314236894 [accessed 20 Jun, 2022]
18. Liisa M Hirvonen and Klaus Suhling, Wide-field TCSPC: methods and applications, Meas. Sci. Technol. 28 (2017) 012003
19. Elles Research Group, https://ellesgroup.ku.edu/ta_spectroscopy.
20. Journal of Materials Chemistry. C, https://doi.org/10.1039/C8TC02977F.

Chapter :3

Developments of artificial light energy converters by using Time resolved spectroscopy

- **Introduction**
- **Experimental Details**
- **Results and Discussion**
- **Conclusions**
- **Acknowledgement**
- **References**

Abstract

On comparing the dyad-Graphene quantum dot (GQD) with the pristine dyad and dyad-graphene oxide (GO) systems, the former looks better light energy converter due to relatively more capability of retention of trans-conformers even on photoexcitation. Additional electron transfer (ET) reaction in case of dyad-GQD nanocomposite occurs due to involvement of two ET reactions of the donor (amino) part of the dyad with fluorene as well as GQD which also acts as electron acceptor. The concurrent occurrences of the two reactions facilitate the formation of relatively stable charge-separated species, as confirmed from both the transient absorption spectra, as well as observed larger fractional contributions, f (Table 1) of fluorescence lifetimes in comparison to pristine dyad as well as dyad-GO nanocomposite systems.

1. Introduction

Recent researches on photo switchable short chain dyads[1-10] reveal great applications in molecular electronics, designing of molecular components of photovoltaic cells and artificial light energy converters, energy storage devices etc. In the present investigation, a novel synthesized dyad, organic (E)-4-(((9H-fluorene-2yl)imino)methyl)-N,N-dimethylaniline (NNDMBF) has been chosen where N,N-dimethyl amino donor (NNDMB) is being attached with the acceptor fluorene (F) (Figure 1 (a)) . Our primary aim is to do comparative analysis to look at the suitability for designing efficient artificial light energy converter when the dyad is in its pristine form and when combined with graphene quantum dots (GQD). Further the efficiency of the dyad would be compared when the quantum dot would be replaced from GQD to carbon quantum dot (CQD)[1].

2. Experimental Details

2.1. Materials

The synthesis and characterization of the present short chain dyad NNDMBF are described elsewhere[11]. The synthesis and characteristics of GQD have been described elsewhere[12].

UV-vis absorption spectra by JASCO spectrophotometer (model V-630) and steady state fluorescence and excitation spectra by JASCO spectrofluorometer of model 8200 have been measured.

Fluorescence lifetimes were determined by using a time correlated single-photon-counting (TCSPC) technique with the model FLUOROLOG TCSPC HORIBA JOBIN YVON using nanosecond diode lasers of 375 nm and 440 nm (Horiba scientific, DD-375L) as excitation source profiles. The decay kinetics are monitored at emission wavelengths of 480 nm. 520 nm and 550 nm. The quality of fit is assessed over the entire decay, including the rising edge, and tested with a plot of weighted residuals and other statistical parameters e.g., the reduced χ^2 and the Durbin-Watson (DW) parameters. All the solutions prepared for room temperature measurements were deoxygenated by purging with an argon gas stream for about 30 mins.

Femtosecond broadband Transient Absorption measuring system was based on a femtosecond Ti: Sapphire amplifier (wavelength ~ 800 nm and pulse width < 35 fs). The output from the amplifier (Spitfire Ace, Spectra physics) was divided into two components to generate pump and probe pulses. Pump pulses (at 610 and 532 nm) were obtained from the nonlinear optical parametric amplifier (TOPAS). The probe beam was a white-light continuum (WLC), which was generated by focusing a small fraction of 800 nm light (from Spitefire Ace) on a sapphire crystal. To obtain a stable and continuous white-light probe, the 800 nm beam was adjusted using an iris and neutral density filter. The probe beam was split into two beams, named the reference and the sample beams. These two beams were detected separately so that the unsolicited noises can be eliminated. The detection of the probe beam was carried out in both conditions: with probe and without probe with the help of a mechanical chopper of frequency 500 Hz. The time delay between pump and probe pulses was controlled with an optical delay line driven by a stepper motor. TA spectra were recorded by dispersing the beam with a grating spectrograph (ActonSpectra Pro SP 2358) followed by a CCD array. The WLC probe confronted group velocity dispersion (GVD), which was compensated with the help of a chirp correction program (Pascher Instrument). Light pulses of a particular wavelength from another TOPAS were used as a probe during the measurement of TA kinetics. Two photodiodes having variable gain were used to record TA .

3. Results and Discussion

3.1. UV-vis Absorption and Steady State Fluorescence Measurements

Studies on the theoretical computations on ground state optimized geometry of the dyad NNDMBF (Figure 3.1. a) and 1 b)), by using B3 -LYP/6-311 g (d,p) level of theory on HOMO-LUMO surfaces it indicates that there may be the two types of conformers Cis- and Trans- , in which the latter form is found to be more stable in the ground state. The trans-form of the dyad NNDMBF appears to be relatively planar.

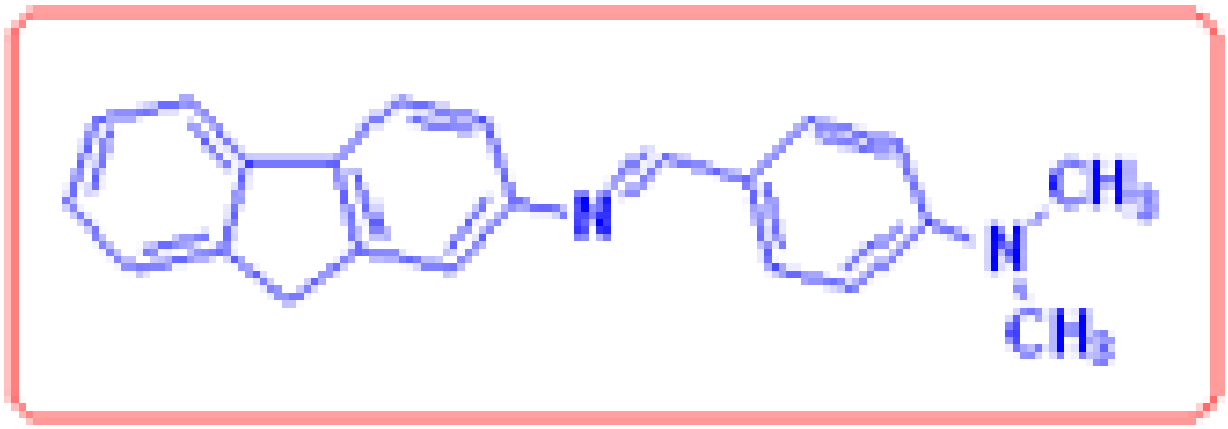

Figure 3.1. a). Molecular structure of the dyad NNDMBF

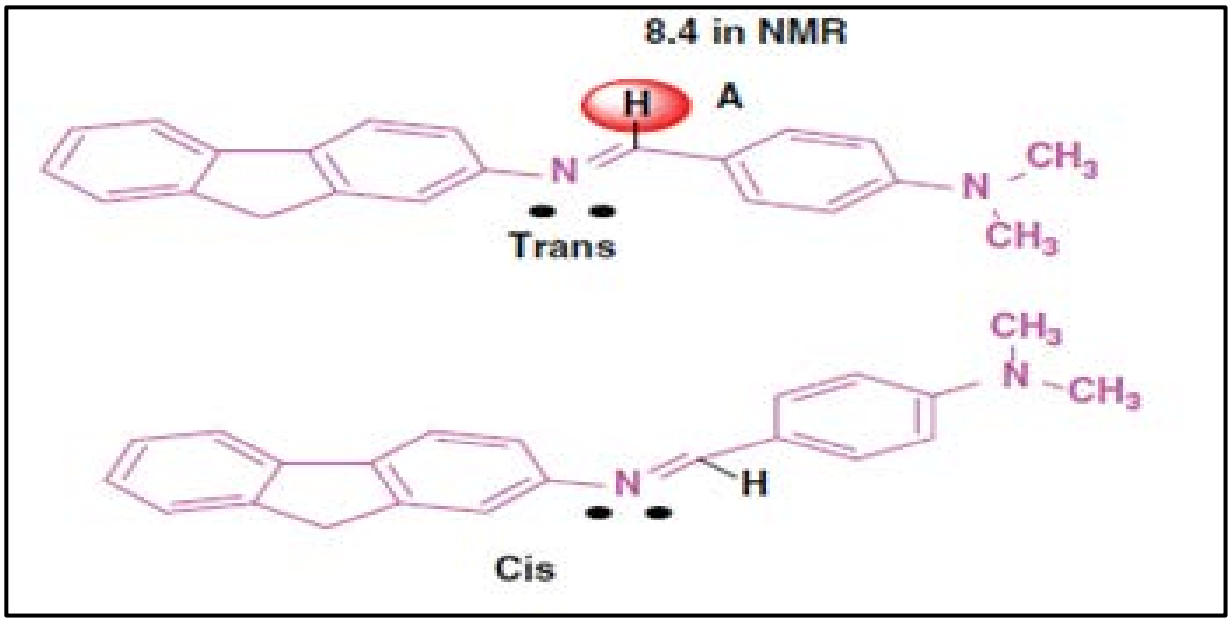

Figure 3.1. b). Cis- and Trans-structure of the dyad

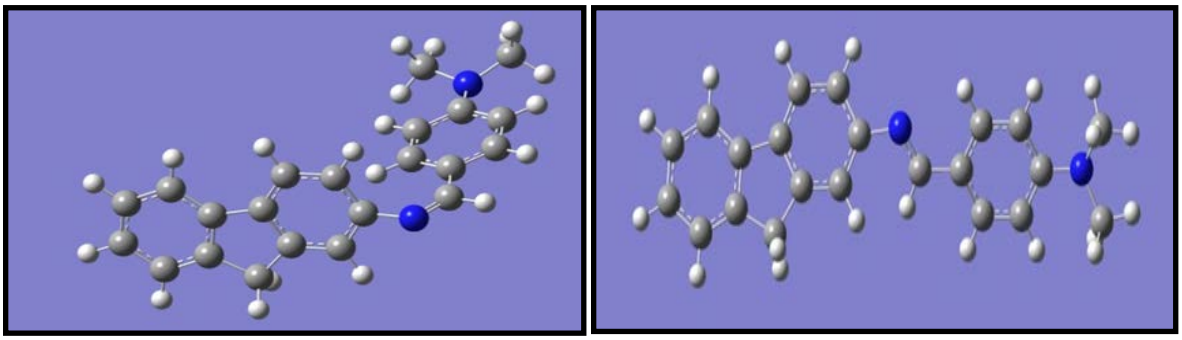

Figure 3.2. a). Cis form of dyad NNDMBF in vacuum; b). Trans form of dyad NNDMBF in vacuum

Trans-form of the dyad appears to be more planar than the cis-one (Figure 3.2.).

UV-vis absorption spectra of the pristine dyad (p-dyad) in ACN solvent exhibits a broad long wavelength band at around 365 nm region (curve 0 of Figure 3.3.). The charge transfer nature of this broad band has been confirmed from solvent polarity effect.

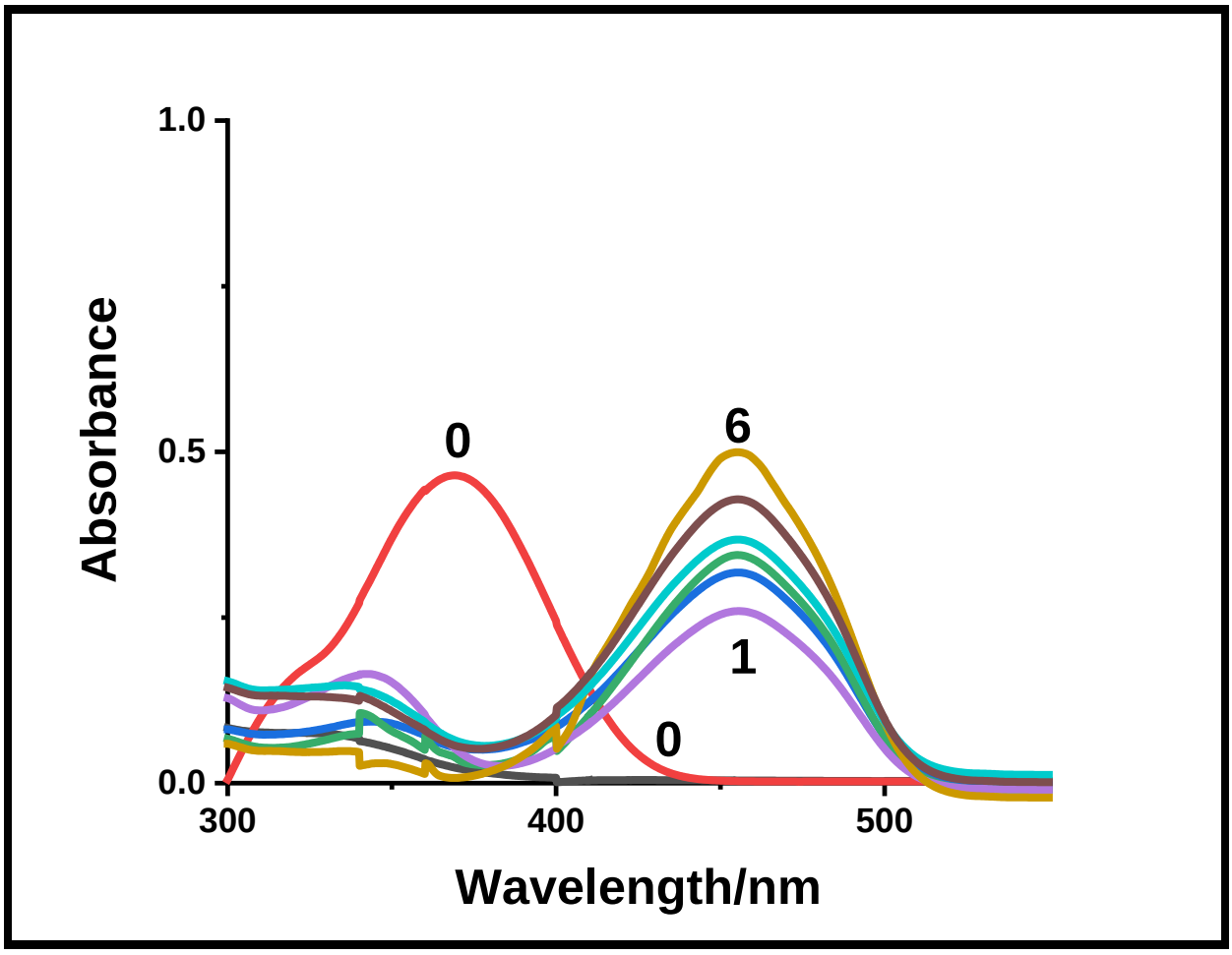

Figure 3.3. UV-vis absorption spectra of the dyad NNDMBF in ACN at the ambient temperature in presence GQD of concentrations (µg/ml) in 0:0; 1:0.1 ; 2:0.2 3: 0.4 ; 4: 0.6 ; 5: 0.8; 6: 1.0

With addition of GQD the 365 nm band diminishes gradually with the concomitant development of another band near 450 nm region (curves 1-6, Figure 3.3.) . Following the observations made earlier it appears that when the dyad adsorbs the surface of GQD, the band associated with the cis- conformation develops, peaking at about 440 nm, through interconversion (trans to cis) process in the ground state.

On exciting the CT absorption band of the dyad NNDMBF-GQD system at 365 nm region, CT fluorescence band envelop develops at around 420 to 470 nm region (Figure 3.4. a)) along with a very weak shoulder –like band at 550 nm. The 425 nm as well as 550 nm band become gradually enhanced with increase of concentrations of GQD.

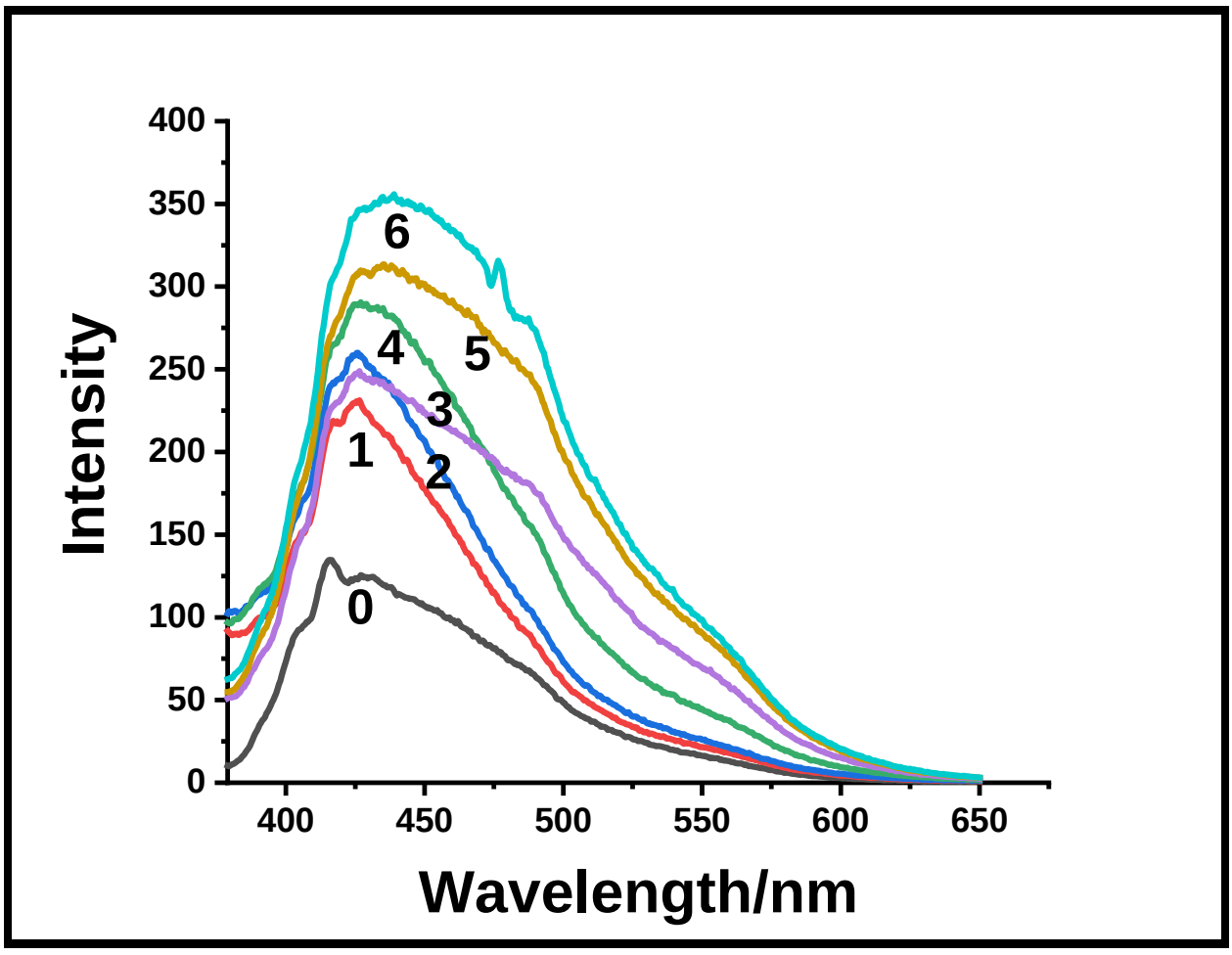

Figure 3.4. a). Fluorescence CT emission spectra (exc~ 370 nm) of dyad NNDMBF at the ambient temperature in presence of GQDnps of conc. (µg/ml) in 0: 0; 1: 0.1; 2: 0.2;3: 0.4;4: 0.6; 5: 0.8; 6: 1.0 (Exc. wavelength~ 365 nm)

However, the increment in 550 nm region appears to be relatively slower. The above findings demonstrate that even with the 365 nm excitation (region of mostly trans-isomers) the emitting region of cis isomer at 550 nm appear to be formed in

the excited state. This observation demonstrates that in the ground state photo switchable conversion of the trans-dyad to the cis form facilitates when combined with grapheme quantum dots (GQD). This shows in presence of GQDs, the photo switchable character of the dyad reduces in the excited state.

On the other hand, when the excitation was made at 450 nm wavelength (the region of cis isomer of UV-vis absorption spectra) of CT absorption band of the dyad-GQD system, the CT fluorescence emission mostly originates from 550 nm region (Figure 3.4. b)) indicating in this region mostly excited cis-isomeric species of the dyad prevails.

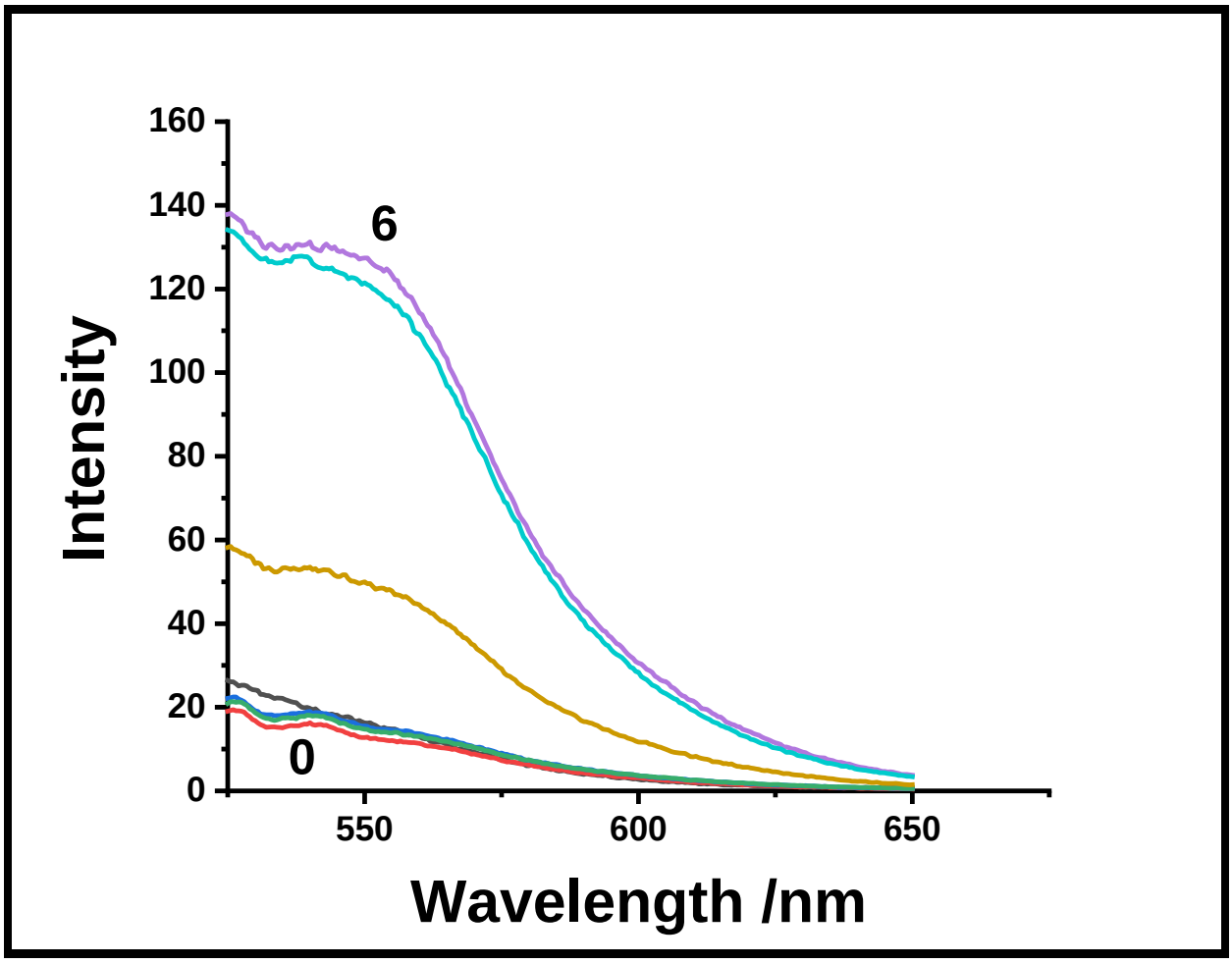

Figure 3.4. (b). Fluorescence CT emission spectra (exc~ 450 nm) of dyad NNDMBF in presence of GQD of conc. (µg/ml) in 0:0; 1: 0.1; 2:0.2; 3: 0.4; 4:0.6; 5: 0.8; 6: 1.0 at the ambient temperature

The fluorescence excitation spectra of the pristine dyad and its nanocomposite forms with GQD were measured by monitoring at 480 nm, 520 nm and 550 nm wavelengths (Figure 3.5. a)–c)). Figure 5 of excitation spectra clearly demonstrates that the steady state intensities of two excited conformers, trans-and cis-, could be varied by changing the excitation wavelength from 375nm (region of mostly trans-isomer) to 440 nm regime, the domain of primarily cis-conformers.

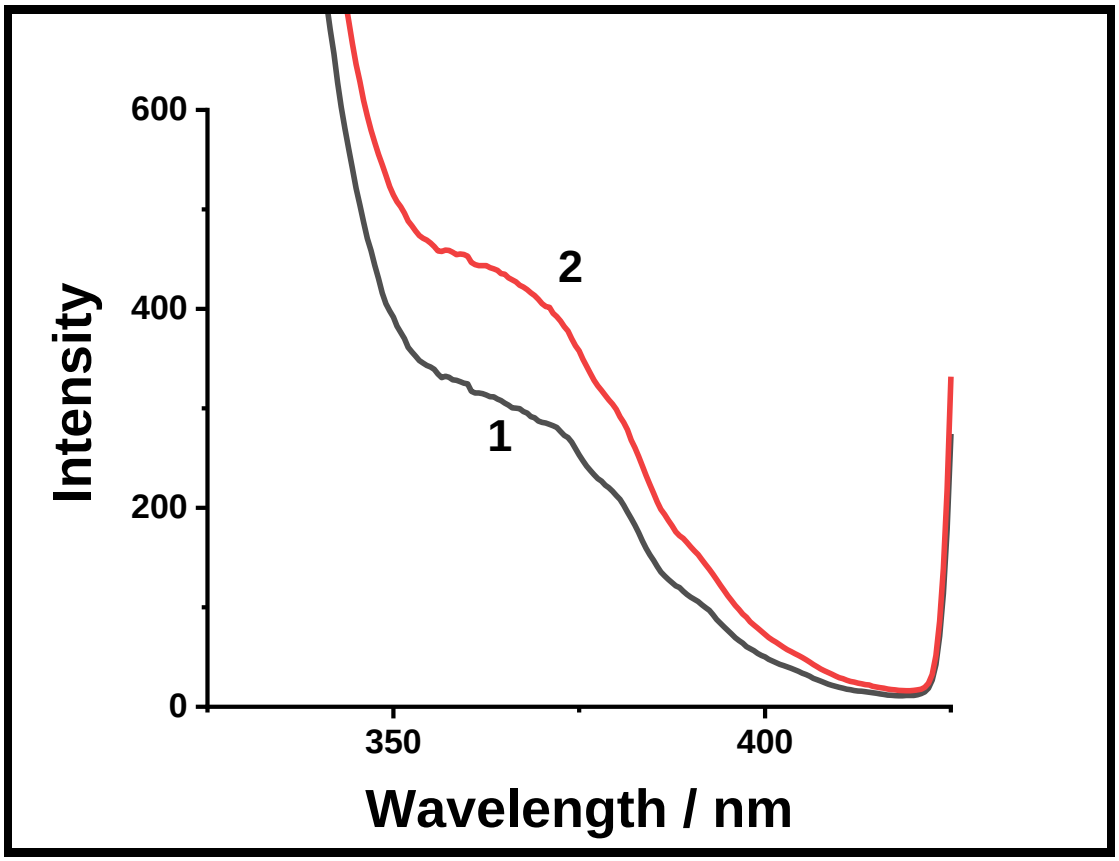

Figure 3.5. a)

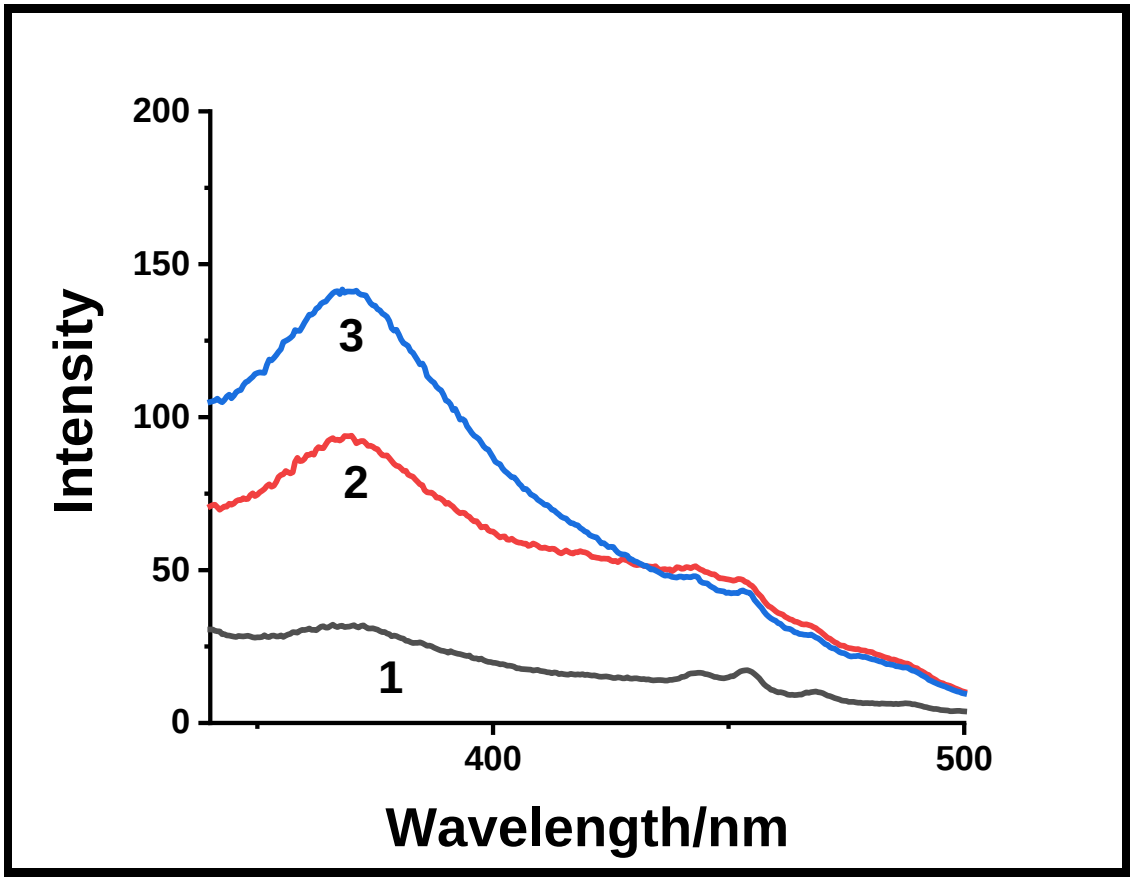

Figure 3.5. b)

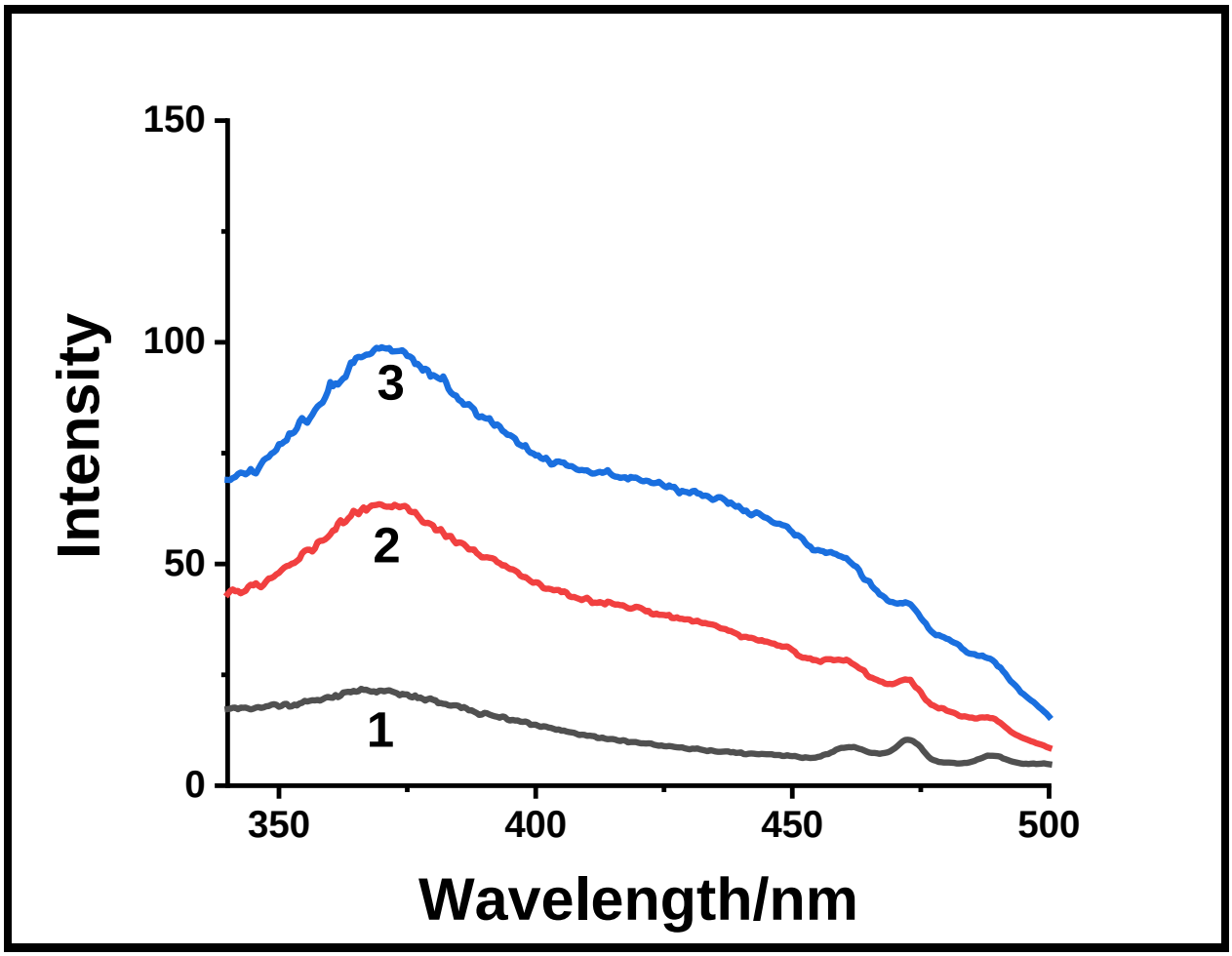

Figure 3.5. c)

Figure 3.5. Fluorescence excitation spectra of the dyad-GQD nanocomposite system in (a). mon wavelength ~ 480 nm, GQD conc(µg/ml) in 1:0; 2: 0.4;(b). mon wavelength ~ 520 nm, GQD conc(µg/ml) in 1: 0.1; 2: 0.2;3: 0.4 (c). mon wavelength ~ 550 nm, GQD conc(µg/ml) in 1: 0.1; 2: 0.2;3: 0.4

3.2. Fluorescence lifetime measurements by TCSPC method

Measurements of the fluorescence lifetimes of the dyad NNDMBF were made by using the time correlated single photon counting (TCSPC) technique. By monitoring the different positions of the steady state fluorescence spectra, the possibility of formations of different conformers, apart from trans- one, in the excited state due to photoexcitation has been examined. These findings further provide us the idea that the present short-chain dyad NNDMBF possesses photo-switchable character, especially in its pristine form.

When excitation was made at 375 nm (by using diode laser) in case of the pristine dyad NNDMBF, it was found that at the monitoring wavelength 480 nm (the peak region), majority emission originates from a species having lifetime of 25 ps. (Table 1).

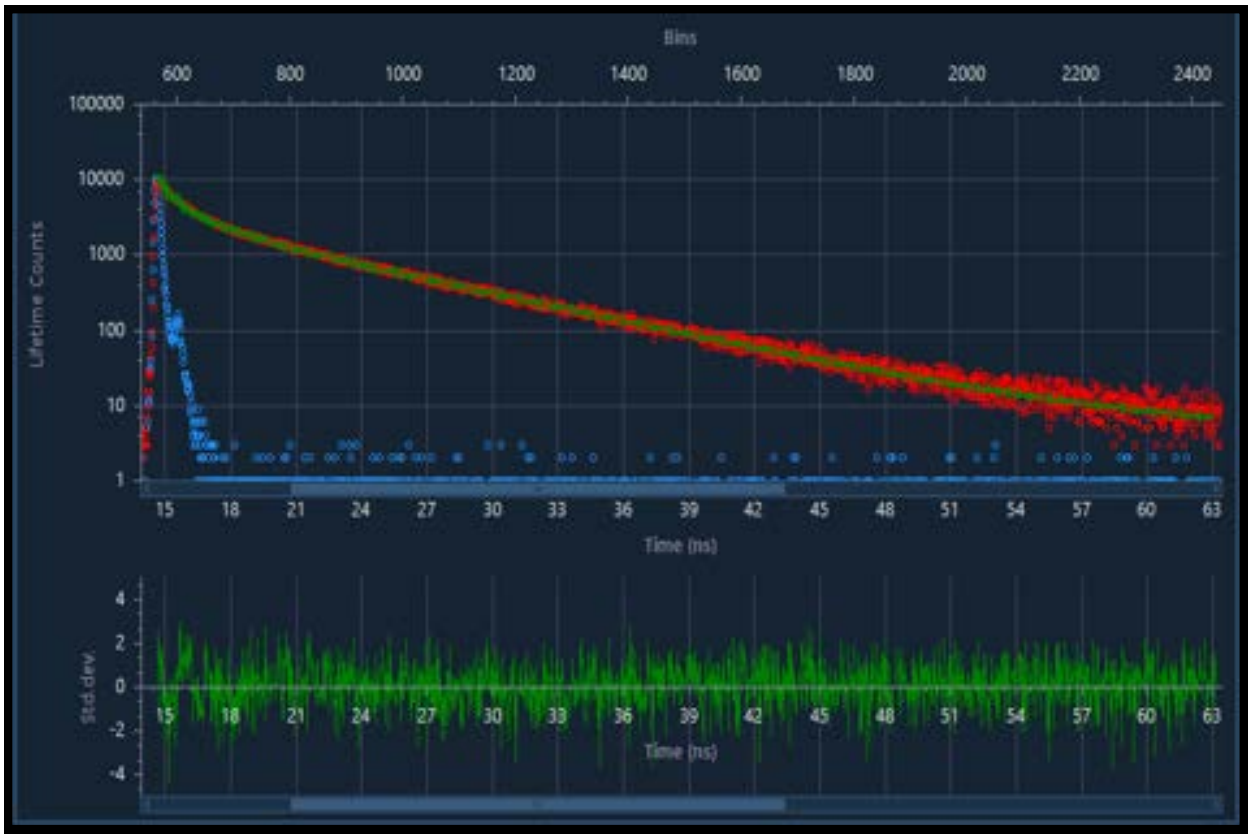

Figure 3.6. Fluorescence decay of the dyad –GQD system in ACN ex =375 nm, em = 480 nm, the fast (blue) decaying component represents impulse response (diode laser). The residual is also shown. (χ^2 ~ 1.12)

On monitoring at the 550 nm region again only faster component of lifetime of 25 picoseconds (ps) order was observed (Table 1).We measured the fluorescence lifetimes of the dyad in presence of GQD(nanocomposite systems)by using the excitation wavelength at 375 nm (Figure 3.6.), the region of mostly trans-isomer. By monitoring at the different positions of the steady state fluorescence band on the longer wavelength side of the excitation wavelength 375 nm, primarily two lifetimes, both in the range of picoseconds, one in the range of 50 ps and the other in the 20 ps domain(Table 1) were observed.

Hence the above findings demonstrate that when the trans-type of dyad in its pristine form is excited by using 375 nm wavelength, most ground state trans isomers convert to the cis-type isomers having ~ 25 ps lifetime component. Thus, the dyad NNDMBF appears to behave as photo switchable dyad. However, in the case of nanocomposite dyad., when the dyad combines with GQD i.e.., quantum dots , 50 ps component, appearing to possess trans-type structure, are found to be present along with the 25 ps component which corresponds to cis isomer. Thus , by developing nanocomposite systems with GQDs, photoconversion (from trans to cis) could be impeded considerably (72 % , Table 1).

Table 1: Fluorescence Lifetime data of the short chain dyad NNDMBF in absence (pristine) and presence of GQD at the different excitation and emission wavelengths at the ambient temperature. Values in parentheses besides lifetimes correspond to fractional contributions (f) of the particular species in the total steady state fluorescence emission intensity

Samples	λ_{exc} (nm)	λ_{em}(nm)	τ_1 / (f_1)	τ_2 (f_2)	χ^2
Dyad in ACN	375 440	480 550 550	1.5ns(0.06) - -	25ps (0.94) 22 ps (1.0) -	1.13 1.12 ---
Dyad + GQD(1μg/ml)	375 440	480 520 550 550	54 ps(0.72) 50 ps (0.67) 56ps(0.63) 56ps (0.10)	25ps(0.28) 25 ps(0.33) 22 ps (0.37) 26ps (0.90)	1.11 1.13 1.13 1;07
Dyad + CQD[1]	375 440*	480 550 550	6.4 ns(0.84) 6.0ns (0.77)	. 256ps(0.16) 260ps (0.23)	1.156 1.077
. Dyad + GO (1x10^{-6} M)	375 440	480 550 550	3.61(0.21) 3.44 (0.17) 3.01 (0.09)	91 ps(0.79) 82 ps(0.83) 100 ps (0.91)	1.080 1.09 1.16

Comparison of the results of GQD is done with those of carbon quantum dots (CQD) and GO. Thus, the experimental observations made from the fluorescence lifetime measurements of the pristine dyad reveal that though trans-isomer primarily dominates in the ground state but on photoexcitation, most of the trans components convert (photoconversion) to the cis form in the excited level. However, this photoconversion is somewhat impeded when this form absorbs the GQDs.

From the above results and following the observations made earlier[1] it could be hinted that relatively stable trans-conformer in the excited state in case of the nanocomposite dyad NNDMBF-GQD in comparison to the pristine form may arise from the surface trap effects[13].

The phenomenon should be clearly understood if one compares dyad-GQD with dyad-CQD systems where the situations were more prominent[14], a larger fraction of the atoms in the latter case being on the surface may form electronic states which may act as traps[15] for electrons or holes . These trap states may hinder the photoconversion of trans- to cis- isomeric forms of the dyad.

This conformation of elongated nature will help to impede energy wasting charge recombination processes and thus nanocomposites may serve as better candidates for designing artificial light energy converter relative to the pristine form.

3.2.1. GQD acts as an electron acceptor within dyad-GQD nanocomposite system

Ghosh et al[16] reported the negative values of the free energy change of electron transfer process within aniline derivatives and GQDs. This observation suggests that photoinduced electron transfer (PET) processes from aniline derivatives to GQDs is feasible and could be responsible for the luminescence quenching of GQDs. The Photoinduced ET has been confirmed by detecting radical cations for certain aniline derivatives, using a nanosecond laser flash photolysis set up.

The direct evidence of occurrence of photoinduced electron transfer (PET) process is provided from the observations of transient donor cationic and acceptor anionic species from the measurements of transient absorption spectra at the different delay times between exciting and analyzing or probing pulses. The excited singlet CT state of the dyad, $^{1}(D^{\delta+}\text{-sp-}A^{\delta-})^{*}$, initially formed by laser photoexcitation of the ground CT, will suffer nonradiative relaxation to form full electron transfer (ET) species, $^{1}(D^{+}\text{-sp-}A^{-})^{*}$in the excited singlet state.

3.2.2. Transient absorption spectra from laser flash photolysis measurements

The femtosecond transient absorption spectral measurements of the dyad-GQD were made by using a femtosecond Ti: Sapphire amplifier as excitation source (360 nm) at the different delay times of the excitation and probing pulses. It is to be pointed out that the peaking of the transient absorption spectra observed at around 540 nm region could be assigned to the fluorene anion of the contact ion-pair, as confirmed earlier by Ganguly and Durocher[17]. The direct evidence of the occurrence of photoinduced electron transfer (PET) process is provided from the observations of transient donor cationic and acceptor anionic species. The transient spectra peaking at around 420 nm of the pristine and nanocomposite dyad NNDMBF in ACN correspond to donor cationic species ($NNDMB^{+}$)(Figure 3.7. a)-c)).This was confirmed from the production of the oxidized species of NNDMB (NNDMB +) artificially by constant current charger (model DB 300 DB Electronics, India).

This electron transfer (ET) possibility could be tested for the present system, Dyad-GQD by using Rehm-Weller relation[17,18]:

$-\Delta G^{0} = E^{ox}(D/D^{+}) - E^{RED}(A^{-}/A) - E_{0\,0}^{*}$

where the symbols have their usual meanings.

The potential parameters were determined ($E^{OX}1/2$ (D/D^{+}))~ +1.85 V, $E^{RED}1/2(A^{-}/A)$ ~−0.72 V) andE_{00} *is chosen at 3.35 eV (370 nm). The driving energy, ΔG^{0}or exergonicity was computed to be −0.78 eV. This shows there is a possibility from thermodynamic point of view of the occurrence of electron transfer reactions within the dyad in the excited singlet state. Now, since the back ET for formation of the ground state is also largely possible from charge recombination mechanism as evidenced from negative value (−2.57 eV) of ΔG^{b} (G), estimated from the relation,

$$\Delta G^{b}(G) = -E^{OX}_{1/2}(D/D^{+}) + E^{RED}_{1/2}(A^{-}/A) \text{ ("G" for ground state)}$$

it appears that the formation of ground state dyad through charge recombination would be largely facilitated in case of pristine dyads(which have only cis structure in the excited state). The situation would be less favored in case of trans-structure of the excited dyad (due to elongated form, the redox partners will be far apart). Thus, it seemingly indicates that the yield of charge separated states would be lower in case of pristine dyad and due to stability, the charge separated yield will become larger in case of the nanocomposite dyads where the dyad combines with GQDs. Interestingly in case of dyad-GQD nanocomposite system, the band near 400 nm , which corresponds to cationic species of the donor part (amino) of the dyad, remain nearly undiminished with increase of delay times(Figure 3.7. b)). Whereas the 550 nm region of the acceptor fluorine anionic part significantly diminishes showing the possible occurrences of charge recombination reactions. As the donor part of the dyad NNDMBF has high probability to undergo efficient PET reactions with both the acceptor F as well as GQD, which is also known to act as electron acceptor, the trans structure of the dyad may undergo additional PET reactions relative to the situation in pristine form. The significant fluorescence lifetime quenching of the trans conformer occurs from ns to ps. Thus, it appears that due to involvement of PET reactions of the dyad with GQD (acceptor GQD interacts with the amino donor part of the dyad NNDMBF) the shape of the trans structure may be changed altering or quenching the fluorescence lifetimes from ns to ps order. This additional nonradiative photoinduced ET reactions may facilitate the formations of stable charge-separated species and consequently be helpful to build efficient artificial light energy converters. In case of graphene oxide (GO) nanocomposite dyad (Figure 3.7. c)) the situation differs from GQD but is similar to pristine dyad (Figure 3.7. a)) where both the cationic donor and anionic acceptor lower down in intensity with increase of delay times due to charge recombination processes within the redox partners of the dyad. This shows that though GQD acts as efficient acceptor with the amino donor of the dyad NNDMBF but GO possesses no such role.

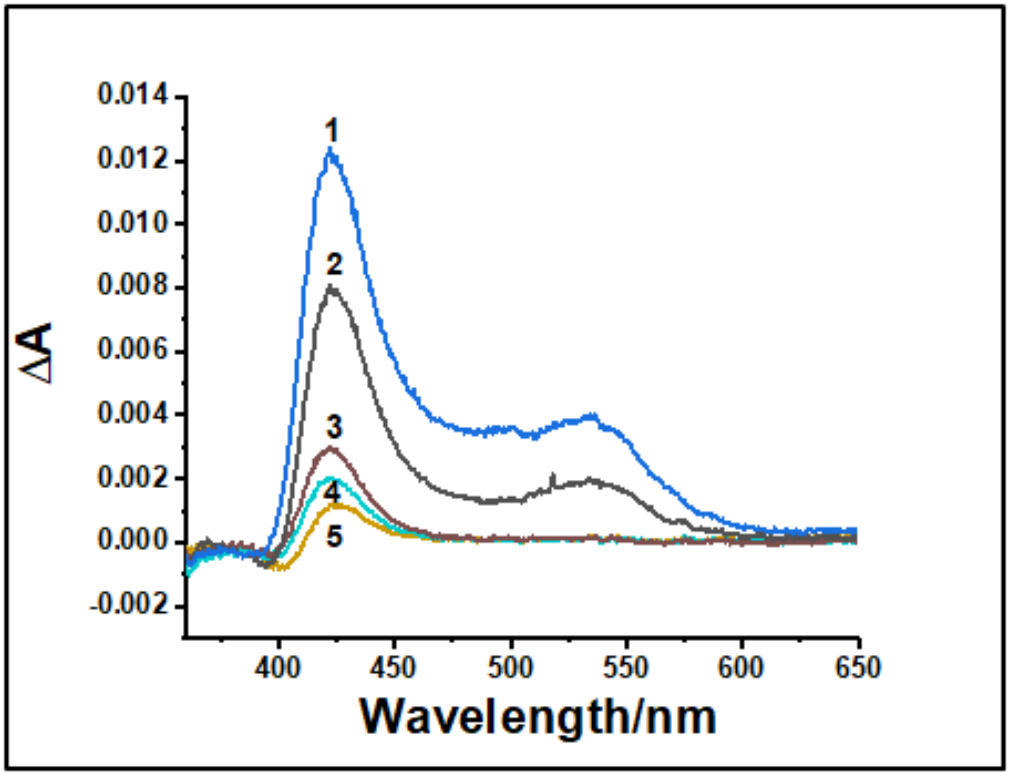

Figure 3.7. a). Transient absorption spectra of the pristine dyad in ACN at the different delay times shown in: 1, 0.3ps; 2, 0.5ps; 3, 3ps; 4, 6ps; 5, 10 ps

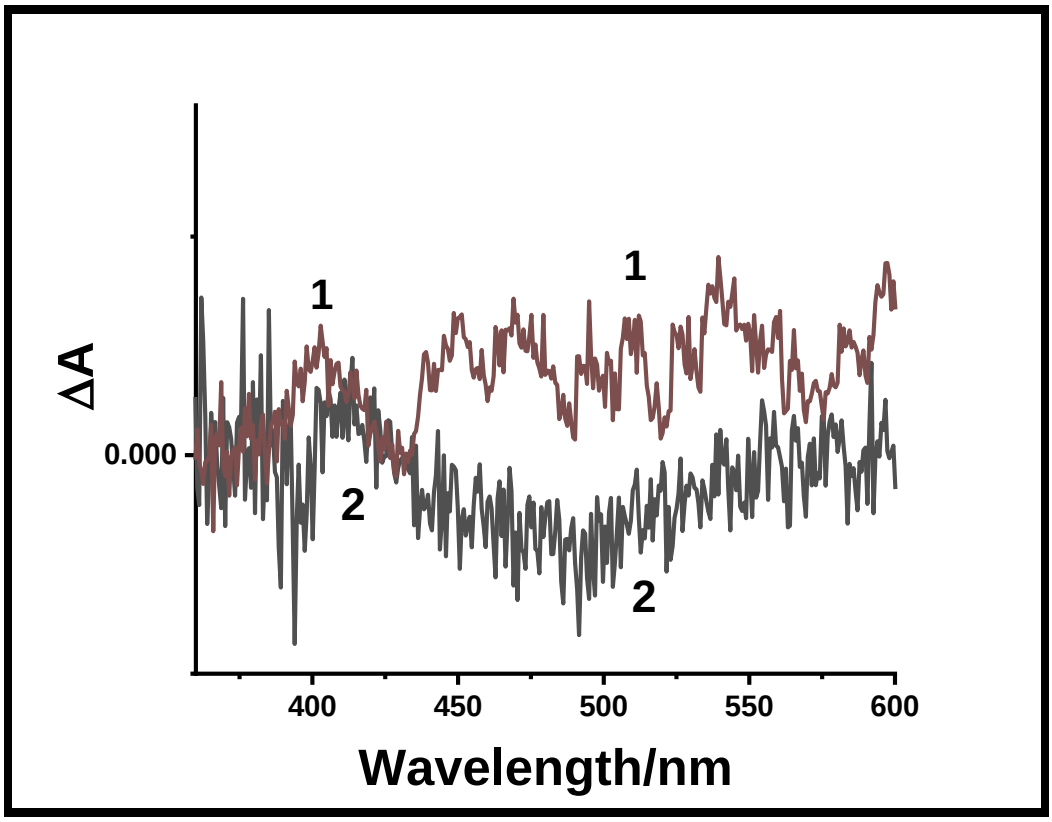

Figure 3.7. b). Transient absorption spectra of the dyad-GQD nanocomposite in ACN at the delay times shown in: 1, 0.2ps; 2, 500ps

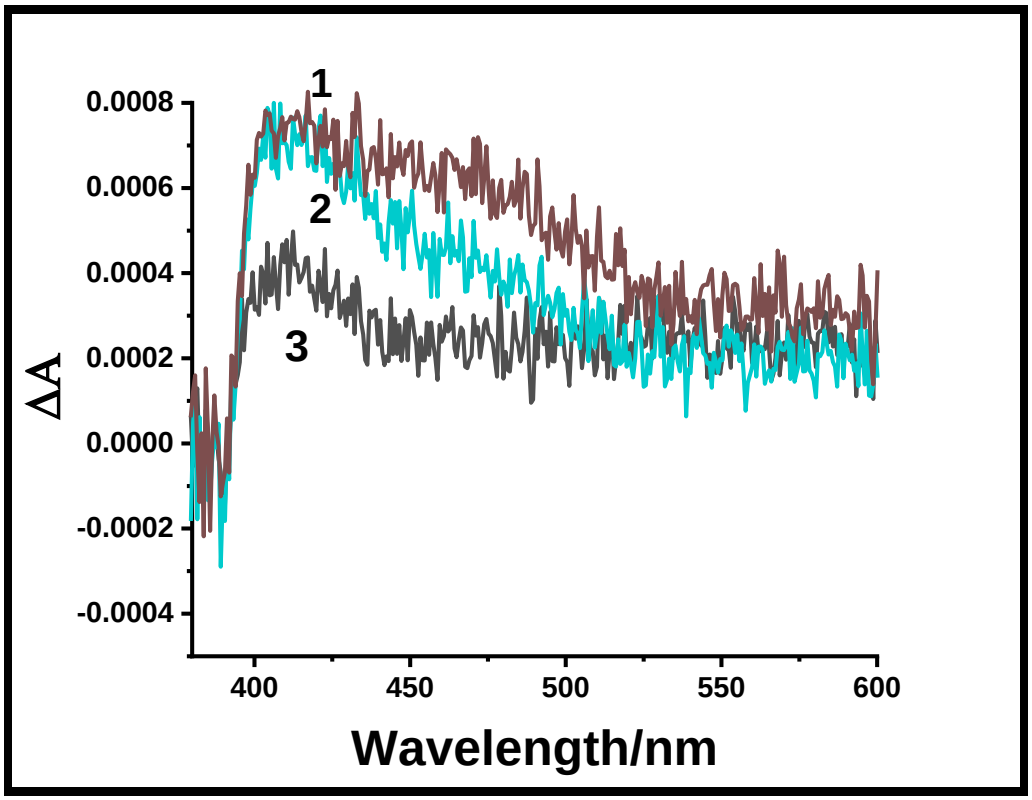

Figure 3.7. c). Transient absorption spectra of the dyad-GO nanocomposite system in ACN at the different delay times shown in: 1, 3ps; 2, 6ps; 3,500ps

Thus, additional ET reactions in case of dyad-GQD nanocomposite (Scheme 1) seemingly

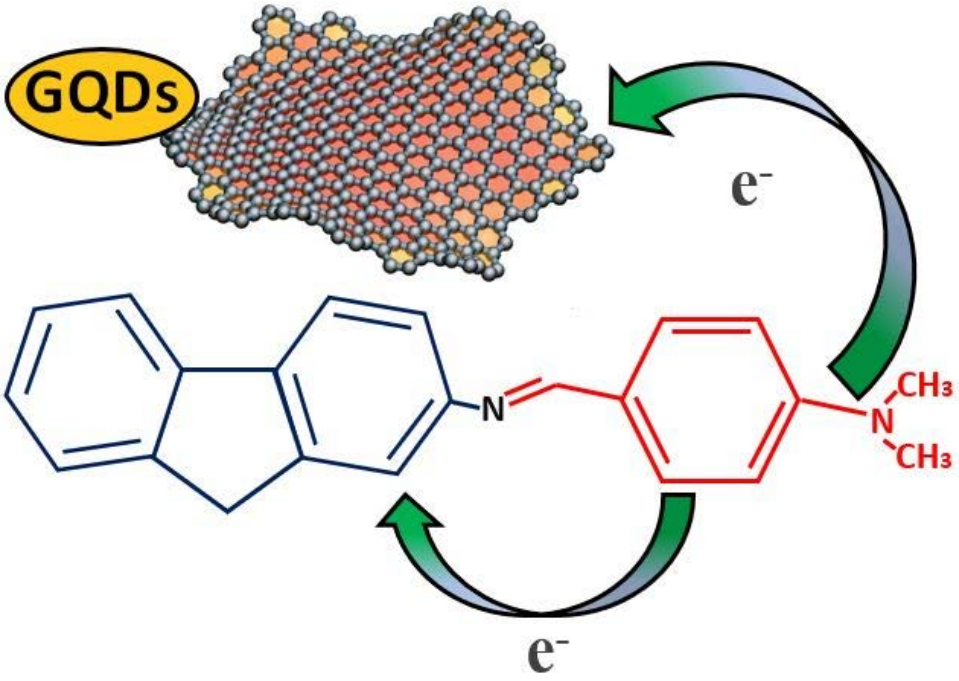

Scheme 1 indicates the possibility of forming relatively stable charge-separated species (Figure 7 (b)), as evidenced from both the transient spectra, and observed larger fractional contributions, f (Table 1) in comparison to pristine dyad as well

as dyad-GO nanocomposite systems. Transient absorption decay measurements (Figure 8 (a) and (b)) monitoring at 420 nm (donor cationic region) further substantiates the fact of formation of stable charge –separated yield. The yield φ_R of the charge-separated species is given by the expression $\varphi_R = k_{CS}\tau_{ip}$ where ion-pair lifetime, $\tau_{ip} = (k_{CR} + k_{CS})^{-1}$, k_{CS} and k_{CR} being the charge-separated and energy wasting charge-recombination rates. φ_R is obtained experimentally by taking the ratio of the absorbance due to charge-separated species (approximately constant absorbance at long delay times) and the initial value estimated by extrapolating the ion absorbance to t = 0 in Figure 3.8.. Table 2 shows the values of all the parameters (φ_R, τ_{ip}, k_{CS} and k_{CR}) for the pristine dyad and dyad-GQD.

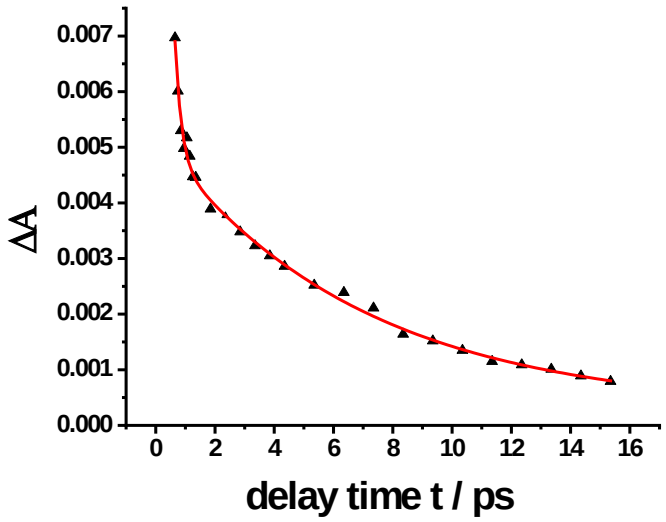

Figure 3.8. a). Transient absorption decay of the pristine dyad at the ambient temperature (r^2 ~0.99) (monitoring at 420 nm (donor cationic region))

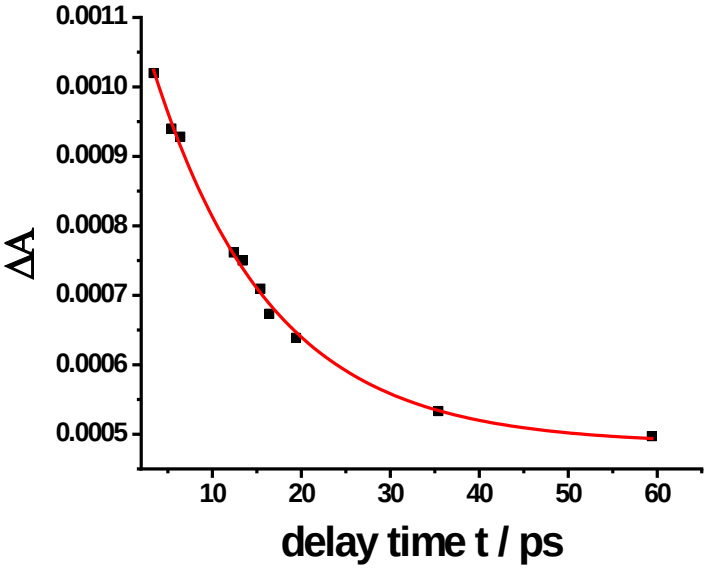

Figure 3.8. b). Transient absorption decay of dyad-GQD system at the ambient temperature (r^2 ~0.99) (monitoring at 420 nm (donor cationic region))

Table 2: Values of Ion-Pair Lifetime τ_{ip} and Yield (φ_R)of charge-separated species along with rates of charge-separation (k_{CS}) and charge recombination (k_{CR}) processes of the two systems of pristine dyad (pd) and GQD-dyad (gqd-d) systems in ACN solvent at the ambient temperature systems.

Systems	φ_R	τ_{ip} /ps	k_{CS} /s^{-1}	k_{CR} / s^{-1}
P -dyad	0.02	7.5	$3x\ 10^9$	1.3×10^{11}
GQD-dyad	0.4	13.3	$3x10^{10}$	$4.5x10^{10}$

Their values have been compared. On comparison it shows that φ_R of dyad-GQD system is 20 times larger than that of the pristine dyad, On the other hand k_{CR} is observed to be nearly one order larger in case of the pristine dyad. Moreover, the charge-separated rate (k_{CS}) of this pristine dyad is one order less than the corresponding quantity found for dyad-GQD nanocomposite. These results are in accord to our expectation as in the cases of the pristine dyad due to excitation trans ground forms mostly convert into cis form where charge recombination should be major role. This will result very small (0.02) charge-separated yield for pristine form only. Large φ_R value (0.4, Table 2) observed in case of dyad –GQD demonstrates the formation of stable charge –separated species indicating very slow charge-recombination rate processes. All these observations made from transient absorption measurements seemingly indicates that nonradiative ET reactions of the donor part of the dyad both with fluorene and GQD acceptor may be responsible to stabilize the charge-separated state more efficiently than the pristine dyad. Thus, the dyad combined with GQD appears to be the better candidate than its pristine form to building up efficient light energy converters where energy wasting charge recombination process plays minor role.

Thus, the experimental observations made from the fluorescence lifetime measurements of the pristine dyad reveal that though trans-isomer primarily dominates in the ground state but on photoexcitation, most of the trans components convert (photoconversion) to the cis form in the excited level. However, this photoconversion is somewhat impeded when the dyad adsorbs the graphene quantum dots (GQDs) or GO (RGO) or CQDs.

From the above results and following the observations made earlier it could be hinted that relatively stable trans-conformer in the excited state in case of the nanocomposite dyad NNDMBF-GQD in comparison to the pristine form may arise from the surface trap effects[1].

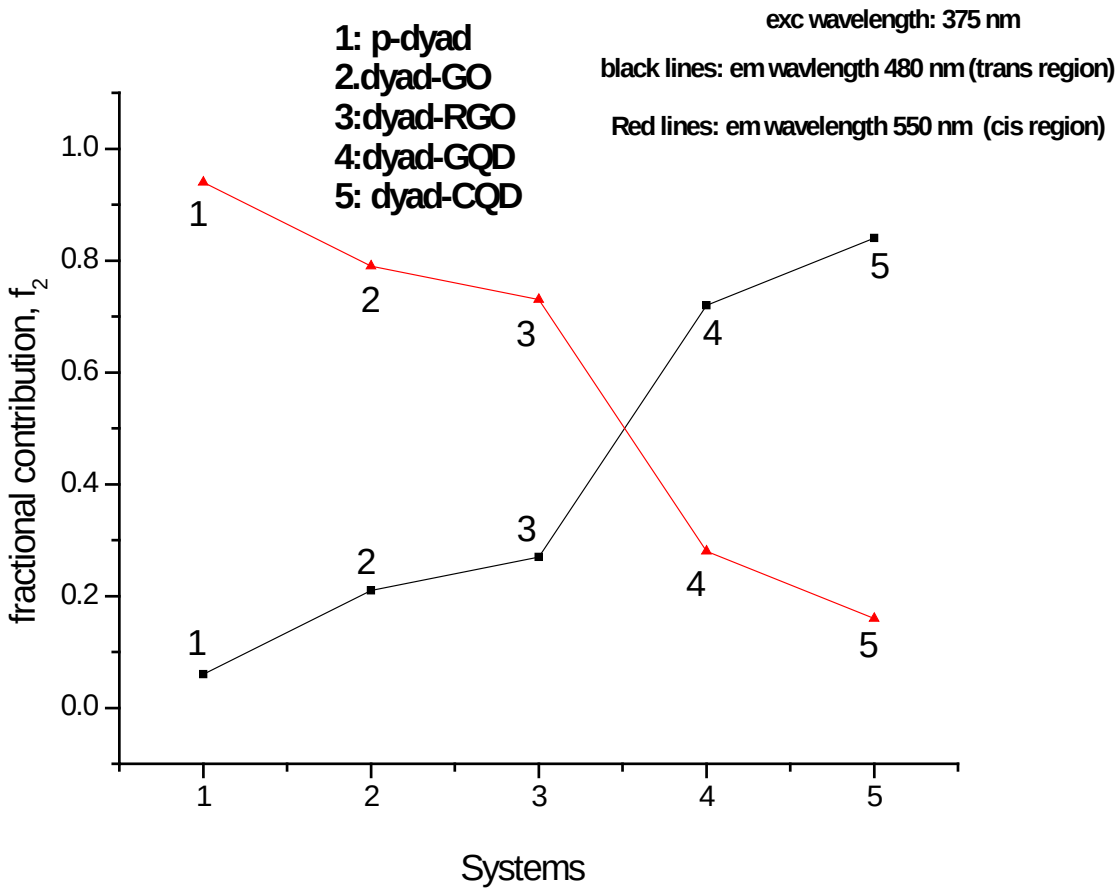

Figure 3.9. Changes of f values (for both elongated and folded conformers) of the different syatems: 1: p-dyad; 2 dyad-GO; 3 dyad-RGO; 4.dyad-GQD; 5 dyad-CQD

The theoretical predictions along with the steady state and time resolved spectral measurements clearly reveal that in the ground state trans-isomer of the dyad prevails but on photoexcitation cis-isomeric species of the dyad predominates. This cis form having folded in nature generates from the relatively planar trans conformer through interconversion processes. In presence of GQD, the photoconversion is somewhat hindered resulting the presence of excited trans-isomers along with the cis ones. The different f values of the lifetimes associated with elongated (trans-conformer), and folded (cis-) conformations have been reproduced in the Figure 3.9. (exc wavelength ~ 370 nm) for pristine dyad and several other nanocomposite systems including GQDs and CQDs. This figure clearly shows that charge separated species (trans conformers) abruptly increases if the nanocomposite dyads contain quantum dots (GQD or CQD). This observation was in accord to our expectation.

4. Conclusions

On comparing the dyad-GQD with the pristine dyad (p-dyad) or GO, the former looks better light energy converter due to greater retention capability of trans-conformers even on photoexcitation. This trans conformation being of elongated nature impedes energy destructive charge recombination processes within these redox components and may serve as better candidate for artificial light energy conversion systems relative to its pristine form which on photoexcitation converts mostly into folded structure cis form, where charge recombination prevails. This conformation of elongated nature will help to impede energy wasting charge recombination processes and thus nanocomposites may serve as better candidates for designing artificial light energy converter relative to the pristine form. Involvement of PET reactions of the dyad with GQD (acceptor GQD interacts with the amino donor part of the dyad NNDMBF) appears to change the shape of the trans structure from its extended nature to somewhat new type of conformation altering or quenching the fluorescence lifetimes from ns (observed for trans form of the dyad - CQD nanocomposite system) to ps order. This additional nonradiative ET reactions of the donor part of the dyad both with fluorene and GQD acceptor may be responsible to stabilize the charge-separated state more efficiently than the pristine dyad.

Acknowledgment

We are thankful to Dr A Saha of UGC-DAE Consortium for Scientific Research, Kolkata Center, III/LB-B Bidhannagar, Kolkata 700 098, India for helping in time resolved experiments. We are grateful to Prof Suman K Pal of IIT, Mandi for extending their facility of Femtosecond broadband Transient Absorption measurements. Thanks are due to Dr Asish Soni of the same institute for helping us in the measurements of Transient absorption spectra.

References

[1] I. Mitra, S. Paul, M. Bardhan, S.Das, M.Saha, A.Saha and T. Ganguly *ChemPhys Letts* 726, 1, 2019

[2] G. Dutta (Pal), S. Paul, M. Bardhan, A. De, and T. Ganguly, *SpectrochimicaActa Part A*180, 168, 2017

[3] G. Dutta (Pal), P. Chakraborty , S. Yadav, A. De, M. Bardhan, P. Kumbhakar,S. Biswas, H.S. DeSarkar, and T. Ganguly,*J Nanosci Nanotechnol*16, 7411, 2016

[4] G. Pal, A. Paul, S. Yadav,M.; Bardhan, A.. De, J. Chowdhury, A. Jana, and T. Ganguly,*J NanosciNanotechnol*15, 5775, 2015

[5] G. Zaragoza-Galán, J. Ortíz-Palacios , B.X. Valderrama , A.A. Camacho-Dávila , D. Chávez-Flores , V.H. Ramos-Sánchez , and E. Rivera, *Molecules* 19, 352, 2014

[6] S. Bhattacharya, T.K. Pradhan, A. De, S.RoyChowdhury, A.K.De, and T. Ganguly, , *J PhysChem A* 110, 5665, 2006

[7] E. Allard, J.Cousseau, J. Ordúna, J. Garín, H. Luo, Y. Araki, and O.Ito, ***Phys. Chem. Chem. Phys.***,4, 5944, 2002

[8] S.Fukuzumi, K. Ohkubo, H. Imahori, J. Shao, Z.Ou, G. Zheng, Y. Chen, R.K. Pandey, M. Fujitsuka, O.Ito, and K.M. Kadish, *J Am Chem Soc* 123, 10676, 2001

[9] S Paul, S Mondal, I.Mitra, D Halder, S Das, M Saha, M Chakraborty ,P K Chakrabarti, B B Show, T Ganguly *J Mol Structure* 1274, 134548, 2023

[10] A Karatay, D Erdener, C Gürcan, E A Yildiz, ... A Elmali *J Photochem Photobiol A: Chemistry* 426, 113741, 2022

[11] S. Paul, I. Mitra, R. Dutta, M. Bardhan,M. Bose, S. Das, M. Saha and T. Ganguly, *J Nanosci Nanotechnol* 18,7873, 2018

[12] J P Naik, P Sutradhar, M Saha. J Nanostruct Chem 7, 85, 2017

[13] C T Smith, M A Leontiadou, R Page, P.O.Brien, D.J.Binks *AdvSci* 2, 1500088, 2015

[14] Y. Wang, A Hu *J Mater Chem* C2, 6921, 2014

[15] H. Zou, C. Dong, S. Li, C. Im, M. Jin, S. Yao, T. Cui, W. Tian, Y. Liu, H. Zhang, *J. Phys. Chem. C* 122, 9312, 2018

[16] T Ghosh, S Chatterjee, E Prasad *J Phys Chem A* doi:10.1021/acs.jpca.5b08522

[17] T Ganguly, D K Sharma. S Gauthier,D Gravel, G Durocher *J Phys Chem* 96, 3757, 1992

[18] D Rehm, A Weller Bur Bunsen-Ges Phy Chem 73, 834, 1969

Chapter :4

Overall Conclusions

1. Overall Conclusions

On comparing the dyad-GQD with the pristine dyad, the former looks better light energy converters due to greater ability of retention of trans-conformers even on photoexcitation. This trans conformation being of elongated nature, where the redox partners the donor and the acceptor within the dyad would be far apart, will help to impede energy destructive charge recombination processes within these redox components and may serve as better candidate for artificial light energy conversion systems relative to its pristine form which on photoexcitation converts mostly into folded structure cis form from its ground extended trans-structure. The theoretical predictions along with the steady state and time resolved spectral measurements clearly reveal that in the ground state trans-isomer of the dyad NNDMBF prevails but on photoexcitation cis-isomeric species of the dyad predominates. This cis form having folded in nature generates from the relatively planar trans conformer through interconversion processes. In presence of GQD, the photoconversion is somewhat hindered resulting the presence of excited trans-isomers along with the cis ones. The hindrance effect for photoconversion is not as efficient as observed in the case of carbon quantum dots (CQDs) where more than 80% of the ground state trans-conformers were able to retain their identity of trans-configuration even on photoexcitation. Thus dyad-CQD systems appear to be better artificial light energy conversion devices relative to the dyad-GQD nanocomposites. Nevertheless, developments of artificial energy conversion devices with GO or GQD could not be avoided. Being very strong due to its electrostatic forces resulting from delocalized electrons flowing through positively charged carbon atoms, Graphenes are the excellent candidates which may be used to form chemically and physically stable artificial devices. However, if the light energy conversion efficiencies of the dyad-GQD is compared with the pristine dyad system, the former looks better light energy converter due to relative stability or ability of retention of trans-conformers even on photoexcitation, as evidenced from the observed value of fractional contributions, f (Table 1, Chapter3) and transient absorption spectra. This conformation of elongated nature will help to impede energy wasting charge recombination processes and thus nanocomposites may serve as better candidates for designing artificial light energy converter relative to the pristine form.

Additional ET reactions in the case of dyad-GQD nanocomposite occur due to involvement of two ET reactions of the donor (amino) part of the dyad with fluorene as well as GQD which also acts as electron acceptor. The simultaneously occurrences of the two reactions facilitate the formation of relatively stable charge-separated species, as evidenced from both the transient spectra, and observed larger fractional contributions, f (Table 1) of fluorescence lifetimes in comparison to pristine as well as dyad-GO nanocomposite systems.